E.T.S. of Industrial Engineering,

IT and Telecommunications

Design Analysis and 3D Printing of a Medium-Sized Metal Component:

A Case Study on Topological Optimization

International Bachelor's Degree

in Industrial Engineering

Bachelor's Thesis

Author: Adrian Ardaiz Rodríguez

Supervisors: Fernando Veiga Suárez

Virginia Uralde Jiménez

Pamplona, September 1, 2023

upna

Universidad Pública de Navarra

Nafarroako Unibertsitate Publikoa

Pamplona, Spain. To date August 25, 2023.

Adrian Ardaiz Rodríguez: 

Abstract

Additive Manufacturing technologies have revolutionized the manufacturing industry by enabling the fabrication of complex geometries with unprecedented design freedom. This Bachelor's Degree Thesis explores how topological optimization can be used in metal pieces as a mean to enhance their structural performance such that, maintaining the piece required properties, diminishes its material used, hence reducing weight and price. This technique holds a tremendous potential to reduce material consumption when designing components.

By employing software and simulation tools such as *SolidWorks* and *Ultimaker Cura*, as well as hardware as the *Prusa i3 MK3S+* 3D printer, the research seeks to identify the most efficient material arrangement of the pieces. It is of utmost importance to maintain the mechanical properties while considering the constraints of additive manufacturing.

The final scope of this research is supporting 2 projects of different companies in which both a piece of equipment needs to be optimized. On the one hand, a part of an injection blow mold for the manufacture of a container for the pharmaceutical industry is studied. On the other hand, a gear belonging to *Enpa*, a gear manufacturing company.

The thesis encompasses a thorough review of existing literature on additive manufacturing in this sector. A case study of tensile test specimens is carried out to analyze the practical results of a piece being optimized topologically. Through this experimental validation, the thesis demonstrates the potential benefits of implementing topological optimization.

In conclusion, the findings suggest that the successful simulations carried out with both metal components, gear and pharmaceutical, could be extrapolated into practice which would imply a significant reduction in weight and material usage.

Acknowledgements

Thanks to UPNA for the great facilities it provided me for this project. Special mention to the library and the OpenSpace, a great facility yet to be discovered by many students, that without its 3D printers, this would never have been possible.

Obviously immensely grateful for the great tutor that have guided me all along this journey, Fernando Veiga, with the help of Virginia Uralde. Thank you very much for your support, for always being there for everything I need.

Table of contents

1 Introduction

To be able to understand the scope and potential of the project, it is carried out a comprehension from a broad point of view of the matter: **Additive Manufacturing** (AM). The study begins by examining the main technologies that constitute AM. Subsequently, the focus is shifted to the potential of **printing metals** with this technology, exploring the advantages, material diversity, and cutting-edge technologies. Additionally, it is introduced the field of **topological optimization**, where the advantages offered by AM technology meet computational methods to optimize structures for superior performance and efficiency.

AM is the industrial production name for 3D printing, a computer-controlled process that using computer-aided design (CAD) creates three-dimensional objects with precise geometric shapes by depositing materials, usually in layers. This contrasts with traditional manufacturing processes that often require machining or other techniques to remove surplus material. It has revolutionized the way objects are designed, prototyped and produced.

The term 3D printing encompasses several manufacturing technologies that build parts layer-by-layer. Each varies in the way they form plastic and metal parts and can differ in material selection, surface finish, durability, and manufacturing speed and cost. **AM technologies** can be broadly divided into 7 categories:

- **Fused Deposition Modeling** (FDM) / **Fused Filament Fabrication** (FFF), a plastic filament is melted and deposited on the build platform of the 3D printer to form the object layer by layer. It is the most common 3D printing technique.

- **Selective Laser Sintering** (SLS), a laser beam is used to sinter powdered material (plastic, ceramic, metal…). The energy of the laser bonds the tiny grains of powdered material together to form a solid structure.

- **Selective Laser Melting** (SLM) / **Direct Metal Laser Sintering** (DMLS), is quite similar to SLS, the difference is that in SLM, the powdered material is melted and not sintered. The high-power laser used in SLM 3D printers fuses the particles of powder together to form a solid object. **This AM process is mainly used for the direct manufacturing of end-use metal parts for industrial applications in the aerospace or medical industries.**

- Electron Beam Melting (EBM), based on the same principle as the SLM, in this case, the energy generated by an electron beam. It produces high-quality metal components with excellent mechanical properties.
- Stereolithography (SLA), based on the photopolymerization process, utilizes a high-power laser to cure photosensitive resin (in a holding tank) layer by layer, creating objects with great precision and smooth surface finish.
- Digital Light Processing (DLP), similar to SLA but instead of a laser, it uses digital light projection to cure the resin so it is able to solidify entire layers at once.
- Binder Jetting, whereas photopolymerization selectively cures resin in a holding tank, material jetting uses printheads to dispense resin while simultaneously curing it.

AM has numerous advantages. Not only accelerates the process of manufacturing compared to traditional processes, but also it enables the production of complex geometries such as voids that would be very difficult if not impossible with traditional methods. This freedom enables to optimize components for specific applications, resulting in better performance. Besides this usually results in a reduction of material waste which promotes sustainability and cost-effectiveness. Ideal for rapid prototyping, the digital process means that design alterations can be done quickly and efficiently during the manufacturing process. This capability accelerates product development cycles, reducing the time to market and project costs. In addition, parts that previously required assembly from multiple pieces can be fabricated as a single object which can provide improved strength and durability. AM can also be used to fabricate unique objects or replacement pieces where the original parts are no longer produced.

However, one of the most significant highlights of AM lies in its use of metals, unleashing a new era of opportunities. With metal combined with AM, engineers can create lightweight yet robust components, revolutionizing industries like aerospace and automotive. Furthermore, AM enables the customization and personalization, especially useful in the medical field, where prosthetics can be tailored to the specific needs of each patient.

Among the various materials printed with AM technologies, metals hold a prominent position due to their mechanical strength, thermal conductivity and corrosion resistance. 3D printing from metal is

one of the most desirable and also the most difficult-to-use additive technologies. Combining the advantages of both the AM technologies and the properties of metals, it can create a synergy that allows the production of lightweight and durable parts with very complex shapes and internal structures designed for specific applications.

A wide variety of metal and metal alloys, including gold, silver, stainless steel, titanium or aluminium, are used for AM. These can be made to create a variety of different metal parts, ranging from jewellery to aerospace components.

As seen the **two main AM technologies used when printing metals** are EBM and DMLS. The characteristics of each one are described below, but it is worth mentioning that both have been key in the development of AM technology, unlocking new possibilities in this field and that they continue to expand their applications and impact across various industries.

Direct Metal Laser Sintering, which is a type of SLM, employs a high-powered laser as the energy source to melt and fuse the metal powder. The laser selectively scans and sinters the metal powder layer by layer to build the desired component. The process takes place in a controlled atmosphere or under inert gas to prevent oxidation. DMLS is known for its high accuracy, surface finish and capability to produce complex geometries.

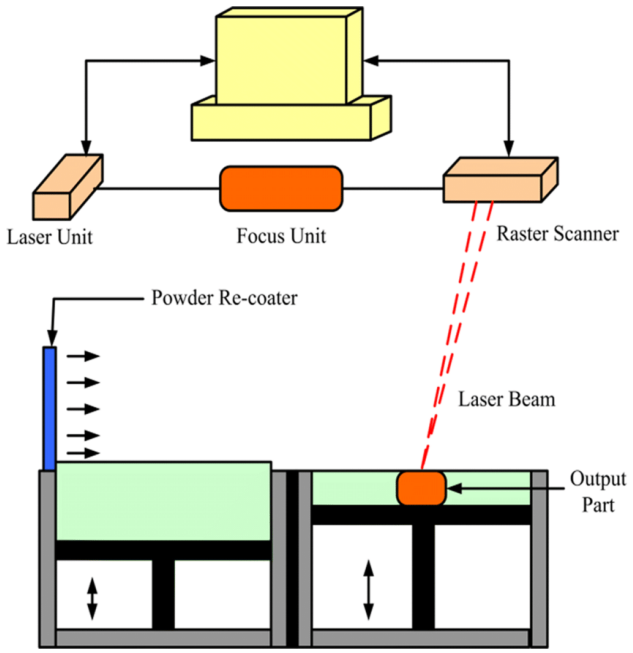

Figure 1. Schematic Diagram of DLMS process

It's often used to reduce metal, multi-part assemblies into a single component or lightweight parts with internal channels or hollowed-out features. DMLS is viable for both prototyping and production since parts are as dense as those produced with traditional metal manufacturing methods like machining or casting. Creating metal components with complex geometries also makes it suitable for medical applications where a part design must mimic an organic structure.

Electron Beam Melting is an advanced AM technology that uses an electron beam as an energy source to melt and fuse metal powder together. In EBM, the electron beam scans across the metal powder bed, selectively melting and sintering powder particles to create a solid layer. The process takes place in a high-vacuum environment or under a controlled atmosphere to prevent oxidation during fabrication. EBM is particularly used for processing high melting point metals like titanium.

This technology has some advantages with respect to others. Its faster printing speeds make it suitable for large and complex parts. Due to the minimal residual stress and reduced risk of cracking it yields excellent mechanical properties. Finally, it has a lower risk of contamination, as the process is performed in a vacuum or controlled environment.

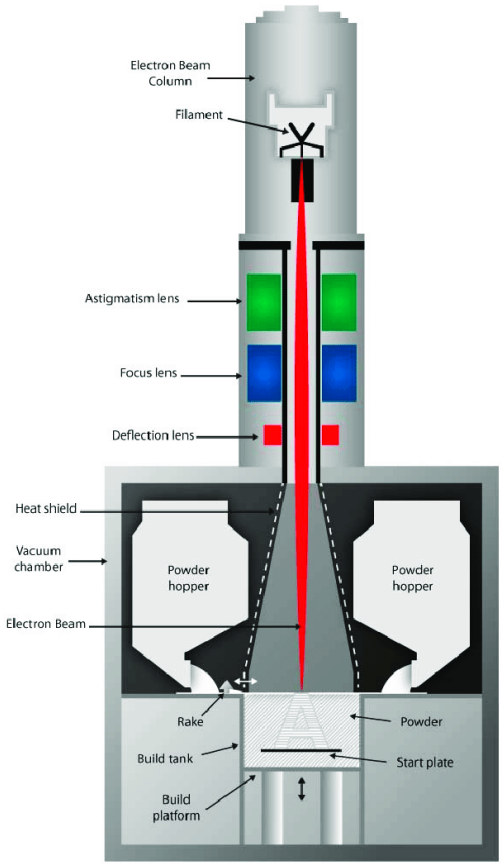

Figure 2. Schematic Diagram of EBM process

AM intrinsically reduces the waste of material and reduces the overall costs, however, in this research, these advantages are taken a step forward with **topological optimization** (TO).

TO is a process that aims to find the optimal material distribution within a given 3D geometrical design space for a defined set of rules set by the designer. The goal is to maximize performance by mathematically modelling and optimizing for **factors such as external forces, load conditions**, **boundary conditions**, **constraints,** and **material properties** within the design constraints. In practice, this translates to removing unnecessary material while maintaining structural integrity and the desired performance of the component. Applying this concept to 3D printing in metals adds another layer of complexity and potential for innovation.

Conventional TO uses finite element analysis to evaluate the design performance and produce structures to satisfy objectives such as stiffness-to-weight ratio, strain energy-to-weight ratio, reduced material volume-to-safety factor ratio or natural frequency-to-weight ratio.
TO generated form designs are often difficult to manufacture using traditional manufacturing methods, that is where AM comes in, enabling the printing of almost any design.

The **steps of how a component is topologically optimized** can be summarized as follows:

1. Problem definition: define goals and constraints, such as performance metrics and design limitations. At this stage, preserved areas or fixed locations are also specified.
2. Simulation and Optimization: the algorithm iteratively adjusts the material distribution within the design space to achieve the optimal configuration.
3. Validation and Visualization: validate the optimized design through additional analysis, ensuring it meets the specified performance criteria.

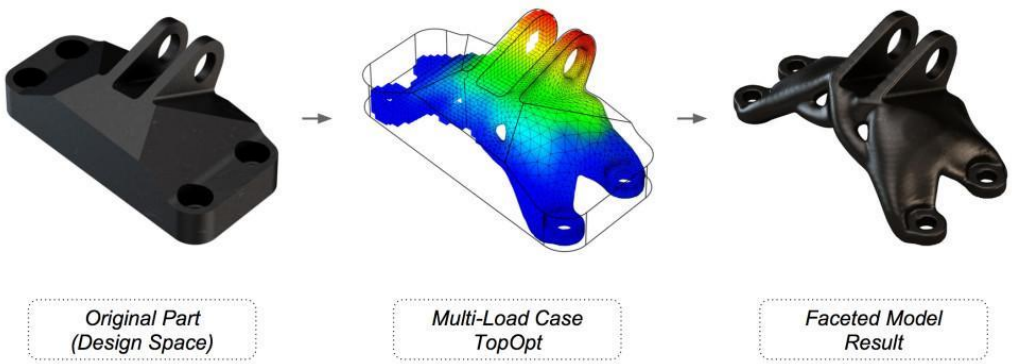

Figure 3. Topology Optimization Design steps

The advantages of topology optimization extend beyond material reduction. TO can drastically reduce product development timelines which translates to reduced costs. The automated process generally leads to better-performing parts in much less time than would be needed for traditional design methods. The best design for a given part isn't always intuitive, and it's possible that a design team would have never come up with it without the help of a computer. TO algorithms don't have the biases that humans do, so they tend to disregard aesthetics and common design rules in favour of improved performance. Besides, because these parts are lighter, they also tend to reduce energy demand in their end-use applications.

By combining TO algorithms with metal 3D printing, engineers can create complex geometries that are tailored for specific applications, resulting in improved mechanical properties and reduced material waste. This powerful combination not only leads to resource-efficient and sustainable solutions but also opens new frontiers for innovative designs.

1.1 Standards

The utilization of established standards is integral to ensure the accuracy for precise engineering. Among the most widely known and recognized is the International Organization for Standardization (ISO), which sets global benchmarks for various industries. By following these standards, the research is collected in a frame that ensures precision and enhances the credibility of the results.

This investigation englobes two critical facets: the standardized nomenclature within the realm of 3D printing, and the recognized protocols governing tensile traction tests.

- ISO 6892-1:2019. Metallic materials. Tensile testing. Part 1: Method of test at room temperature
- ISO 17296-3:2014. Additive manufacturing. General principles. Part 3: Main characteristics and corresponding test methods
- ISO/ASTM 52900:2021. Additive manufacturing. General principles. Fundamentals and vocabulary
- ISO/ASTM 52902:2019. Additive Manufacturing. Test artifacts. Geometric capability assessment of additive manufacturing systems
- ISO/ASTM 52909:2022. Additive manufacturing. Finished part properties. Orientation and location dependence of mechanical properties for metal powder bed fusion
- ISO/ASTM 52910:2018. Additive manufacturing. Design. Requirements, guidelines and recommendations
- ISO/ASTM 52936-1:2023. Additive manufacturing of polymers – Qualification principles - Part 1: General principles and preparation of test specimens
- ISO/ASTM 52941:2020. Additive Manufacturing. System performance and reliability. Acceptance tests for laser metal powder-bed fusion machines for metallic materials for aerospace application
- ISO/ASTM/DTR 52912:2021. Fabricación aditiva. Ensayos no destructivos. Implantación intencionada de defectos en piezas metálicas
- ISO/ASTM/TS 52930:2021. Fabricación aditiva. Principios de cualificación. Instalación, operación y rendimiento

1.2 Terminology & Acronyms

Many terms written in this work are specific of this field. So that the reader is able to understand the entire text a brief description of the fundamental principles in additive manufacturing can be found in the standard *ISO/ASTM 52900:2022*.

To enhance readability and simplicity, acronyms will frequently be employed for various additive manufacturing processes and techniques. The first occurrence of each acronym will be accompanied by its expanded form, and thereafter, the acronyms will be used consistently throughout the text.

AM	Additive Manufacturing
TO	Topological Optimization
PLA	Polylactic Acid
CAD	Computer-Aided Design
FDM	Fused Deposition Modeling
FFF	Fused Filament Fabrication
SLS	Selective Laser Sintering
SLM	Selective Laser Melting
DMLS	Direct Metal Laser Sintering
EBAM	Electron Beam Melting
SLA	Stereolithography
DLP	Digital Light Processing
PBF	Powder Bed Fusion
FEM	Finite Element Method
FEA	Finite Element Analysis
AI	Artificial Intelligence
CFF	Continuous Fiber Fabrication
UV	Ultraviolet
LPBF	Laser Powder Bed Fusion
DED	Direct Energy Deposition
LMD	Laser Metal Deposition

2 Object

This thesis aims to investigate the potential of TO combined with AM using SolidWorks for two distinct applications: a metal gear for an industrial company and a pharmaceutical mold component. The study will focus on optimizing the material distribution of each component to achieve lighter designs while complying with their structural requirements.

Furthermore, the research will explore the feasibility and the compatibility of these two technologies together, TO with AM, by conducting tensile tests on real specimens printed with a 3D printer. The same tests will be conducted on topologically optimized specimens to verify the efficacy of the process.

The study aims to contribute to the advancement of innovative and resource-efficient engineering solutions, benefiting various industries with enhanced performance and cost-effectiveness in their components.

3 State-of-the-art

3.1 Topological optimization

The origins of TO can be traced back to the 1950s when engineers started using mathematical methods, such as the Finite Element Method (FEM), to solve structural problems. In the 1980s the concept of TO started to take shape with the development of methods such as the Solid Isotropic Material with Penalization (SIMP). This method penalized intermediate densities in the design to achieve discrete material distribution.

Back in the 1990s is when the idea of leveraging computing power to speed the development of structures that are optimized for characteristics such as mass and stiffness first emerged in the world of academia. Companies like Altair Engineering played a key role in making TO accessible to a wider audience with the commercialization of their OptiStruck software. With the advance in computational capabilities, researchers and engineers explored new methods, including evolutionary algorithms, level-set-based optimization and topological derivatives.

During the 2000s TO continued to gain traction and adoption. The integration of topological optimization with the Finite Element Analysis (FEA) software from companies like ANSYS and COMSOL made the optimization process more accessible and user-friendly for engineers. This decade also saw increased research on optimizing composite materials and the consideration of manufacturing constraints in the optimization process

It was not until the 2010s when TO was integrated with AM technologies. Since then, it experienced a period of rapid growth and diversification, leading to structures with intricate geometries, lightweight which resulted in higher performance.

Today TO is an established discipline with a wide range of applications across various industries. Some notable software companies are SolidWorks, Siemens, and Altair Engineering, which continue to innovate and enhance this technology.

Researchers and companies are exploring multi-material optimization, and multi-physics scenarios, incorporating artificial intelligence (AI) and machine learning techniques to continue to push the boundaries of technology, shaping the future of engineering and design.

Some of the key methods and algorithms used in TO are:

- Finite Element Method, is a numerical method used to solve partial differential equations governing the mechanical behaviour of structures. FEM is essential for conducting simulations and evaluating the mechanical response of the optimized designs.
- Solid Isotropic Material with Penalization, is a widely used method in TO. Allows engineers to obtain a binary material layout, fully solid or void regions.
- Evolutionary Algorithms, inspired by biological evolution, are employed to iteratively search for optimal designs. Genetic algorithms, particle swarm optimization, and differential evolution are examples of evolutionary algorithms commonly used for TO.
- Level Set Methods, are employed to represent the interface between solid and void regions as an implicit function. These methods enable the TO algorithm to efficiently handle changes in topology during the optimization process.
- Density-Based methods, are variations of SIMP that use continuous material density values instead of binary solid-void representation. This method provides more accurate and smoother material distributions, often leading to better performance in the designs.
- Topology Derivatives, or sensitivity analysis, are used to calculate the sensitivity of the objective function with respect to the material distribution. These derivatives guide the optimization algorithm in determining where material should be added or removed to improve performance.
- Homogenization methods, are employed to represent the macroscopic properties of a structure with varying material properties at a fine scale.
- AI and Machine Learning are increasingly being integrated into TO. Reinforcement learning, neural networks, and surrogate modelling are some examples of AI-based approaches used in TO.
- TO with Manufacturing Constraints, advanced algorithms that consider constraints such as minimum feature size, overhang angles, and support requirements during the process.
- Multi-objective optimization, optimizes designs for multiple conflicting objectives, such as stiffness and weight reduction, allowing engineers to explore the trade-offs and find the optimal solution.
- Uncertainty Quantification, considers uncertain parameters in the optimization process, resulting in robust designs that perform well under varying conditions.

3.2 Topological optimization in metal components

At the forefront of engineering innovation, the symbiosis of TO with 3D printing using metals has freed a new era of design possibilities. In recent years the scientific research surrounding AM on structural steel design has experienced rapid growth, focusing efforts mainly in the aerospace, automotive and medical industries [12]. Aviation and medicine are the fields where TO has been more widely used together with metal AM, in comparison with the automotive industry.

Metal AM has attracted increasing attention because it realizes geometrically complex, fully functional metallic structures that are hard to produce by traditional processes Just like in plastic 3D printing, metal allows for the creation of complex geometries, but with improved strength-to-weight ratios, due to the superior mechanical properties of metals. Optimized designs can achieve even higher levels of performance and durability. For this same reason, metal is the quintessential material in industrial applications. Employing TO in steel construction is a future trend, driven by the significant benefits it offers, not only as an optimization tool, but as well for its sustainability, and waste and weight reduction. However, significant advances are still needed in this field [13].

Future trends of research. Generative design, powered by artificial intelligence, is unlocking novel solutions. Multi-material and multi-physics optimization techniques are enabling designs that incorporate diverse material properties and address complex real-world scenarios. Moreover, optimization algorithms are now adept at accommodating intricate 3D printing constraints.

Applying TO to metal 3D printing encounters several challenges that are worth considering:

- Nowadays SIMP is still the leading method for TO nowadays [13]. Nevertheless, its reliance on penalization factors can lead to struggles with complex geometries, discrete variables, and multi-objective problems. Besides, since metals have different behaviour compared to plastics, these optimization algorithms should account for factors like metal anisotropy and thermal behaviour. Research trends suggest an escalating importance of Level-Set Methods and Genetic Algorithms, which offer smoother boundary evolution, better handling of topological changes and in general address the SIMP's limitations and offer more versatile and efficient solutions for TO.

- Manufacturability and process complexity. While metal 3D printing is versatile, certain geometries and overhangs might still present manufacturing challenges. The optimized designs need to be feasible for the printing process, which can have specific constraints. This problem requires careful consideration due to factors like support structures, post-processing, and material waste.

-Support structures. They are critical in the printing of some components by avoiding cracks or other failures. However, they only add an additional complexity to the printing process, but may increase significantly the overall costs. In this line of study is sought an effective support structure that relies on a successful printing without any processing errors, while minimizing the material used to produce those supports.

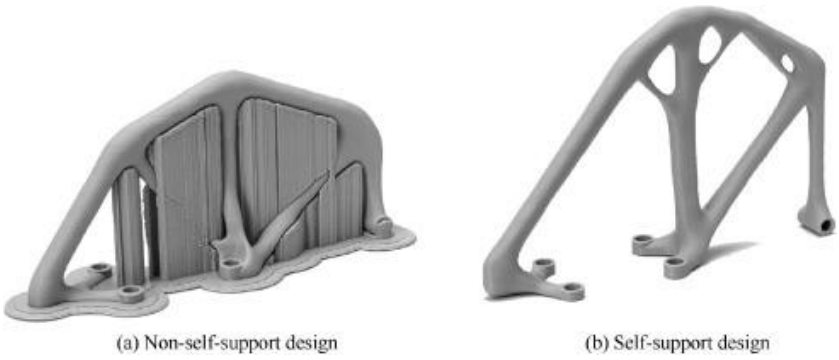

Figure 4. Support structures optimization, available in [1]

- The intrinsic costs of AM technologies surpass those of traditional manufacturing methods. Added to the more specialized and at the same time less developed technologies required by metal 3D printing, it makes it as well more expensive compared to plastic 3D printing. Complex topologies may demand longer printing times, need support structures and incur material wastage, all contributing to increased production costs.

These manufacturing methods are reserved for very highly sensitive parts where performance is an imperative. Another interesting way to reduce the high cost is reconsidering the manufacturing material as suggested in [15]. Thanks to the way 3D printers operate, the possibility of using cheaper and lighter materials opens up, which previously could not be manufactured due to their properties.

Balancing the advantages of TO with the realities of metal 3D printing involves a trade-off essential for seeking an optimal balance between performance enhancement and financial considerations.

-Heat transfer and thermal stress. Metals have higher thermal conductivity compared to plastics, which can lead to challenges in heat dissipation during the printing process. Thermal stress and

distortion must be managed to ensure accurate and reliable prints. This problem can be dealt with a component mentioned above, support structures. Even though eliminating support material is beneficial and necessary, they can be very useful in terms of heat dissipation to counter residual stress and distortion. Their inclusion may alleviate the locally accumulated heat.

- Simulation and validation, are crucial tasks when optimizing metal designs due to the materials' unique behaviour. Artificial Intelligence and Machine Learning models are future trends. The conventional TO process usually requires several iterations to arrive at an optimal design which can be computationally expensive. Machine learning models can be used to drastically reduce this time, since they can learn from historical data and simulation results, facilitating the discovery of optimal designs more rapidly. AI is expected to tackle the challenge of multi-objective optimization, where different goals conflict to find a balanced solution. This holds an enormous potential in situations where there is a lot of uncertainty or complexity such as high-dimensional design spaces.

All in all, incorporating TO with metal 3D printing has been and continues to be an ongoing significant area of research and development. This symbiosis holds the potential to revolutionize the way metal components are designed, leading to more efficient, lightweight, and high-performance structures.

4 Methodology

4.1 Study of the technology

The research presented in this work has been conducted utilizing the extensive facilities and resources provided by the UPNA, which have been instrumental in enabling the execution of this research.

It should be remembered the main goal of the project is the TO of a metal gear and a metal mold, for which a metal 3D printer would be necessary. A metal 3D printer is a very sophisticated machine which unluckily has not been among the resources of the project. Due to the absence of any, **the investigation pertaining to metal components is carried out exclusively through simulations**. Despite this limitation, the utilization of available resources has allowed for a comprehensive exploration of the research objectives. With the purpose of showing experimentally the viability of TO a Tensile Traction Test is carried out, see *7. Tensile Traction Test.*

The primary goal of the methodology was to leverage the capabilities of TO in combination with 3D printing. The main tools to be used are: **SolidWorks**, **UltiMaker Cura**, and the **Prusa i3MK3S+** 3D printer.

4.1.1 Topology Study in SolidWorks Simulation

SolidWorks is a powerful CAD software widely used in various industries for creating 3D models, simulations, and technical drawings. SolidWorks offers a range of tools for modelling, analysis and documentation, making it an essential tool for product development and engineering projects.

Figure 5. SolidWorks software logo

In this case, this software has been mainly used for its powerful Simulation modulus which allows for virtual testing and analysis the behaviour of designs under various conditions before physically producing them. It allows to carry out different studies such as Static Analysis, Thermal Analysis… and the one of interest for this project: **Topology study.**

The theoretical foundations of TO have been defined previously, see *1. Introduction*. Furthermore, TO can be either a subtractive or an additive algorithm. In SolidWorks they “felt the subtractive method was most attractive to our customers. It’s good with existing geometry you want to refine,” said Stephen Endersby, director of product portfolio management. Hence, this software fits perfectly with the object of this project.

SolidWorks **algorithm** utilizes FEA principles to optimize a design. Beginning with an initial model and defined loads, constraints, and material properties, the algorithm discretizes the design into finite elements. Stiffness matrices are calculated for each element, forming a system of equations that determines deformation under loads. Through sensitivity analysis, less significant elements are selectively removed or thinned out, while new elements can be added. Density filtering smoothens transitions between dense and sparse regions. Iterative optimization continues until convergence criteria are met, resulting in a final design that minimizes material usage while maintaining structural performance.

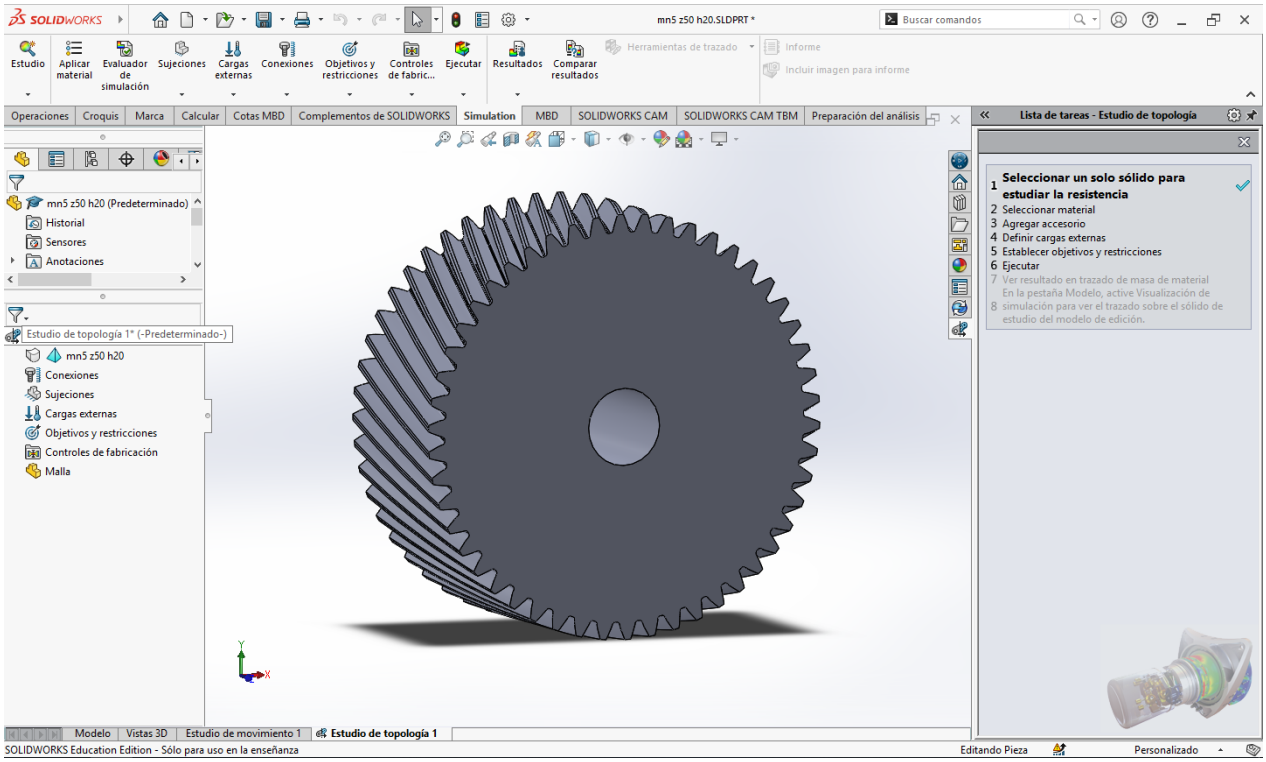

Figure 6. SolidWorks interface

4.1.2 UltiMaker Cura 5.4.0

UltiMaker Cura is an open-source slicing software specifically designed for 3D printing. Slicing is the process of converting a 3D model (usually in STL format) into a G-code file, which are the instructions that the printer can read.

Figure 7. UltiMaker Cura logo

The great advantage of this software is its user-friendly interface, both intuitive and simple for new users and highly customizable for experts. The process starts by importing a digital model in various formats (usually STL), and then the user can customize the piece until the result is the desired one. This process entails configuring an array of printing parameters, including layer height, print speed, and infill density, thus tailoring the printing process to the specific needs of the project.

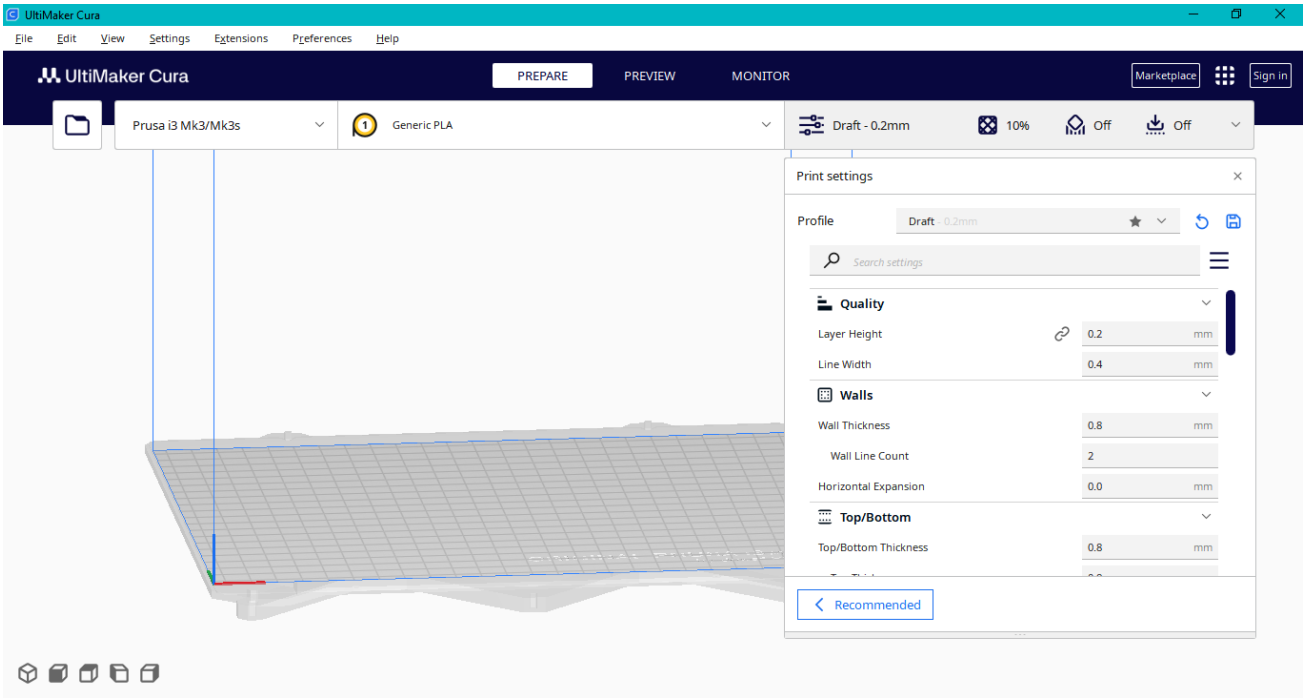

Figure 8. UltiMaker Cura interface

Furthermore, Cura offers a preview of the print, allowing users to observe the layer-by-layer progression of their creation before committing to the physical printing process. This facilitates the identification of potential issues and can be a determining factor when printing metal designs where the economic cost is important and in case of failure the outcome could be fatal. Hence, it promotes a sense of assurance and control over the final outcome.

4.1.3 Prusa i3 MK3S+

The OpenSpace of UPNA count with six Prusa i3 MK3S+ printers for students to use. Thanks to the rapid prototyping offered by 3D printers and the rest of characteristics, see *1. Introduction*, it is a primary tool for the research.

When printing with a 3D printer, users are responsible for tasks such as loading the filament. This printer has the ability to work with several different materials such as PLA, PET/PETG, ABS, Nylon…

Due to its popularity and great prototyping characteristics, the material used in this work is **Polylactic Acid (PLA)**. PLA is known for its biodegradability, which means it can break down naturally over time when exposed to the environment. Besides it has a low warp in comparison to other materials and it is considered to be one of the easiest materials to print. In this study a 1.75mm diameter PLA is used, which is the most widespread, see Figure 9.

Figure 9. Filamento 3D PLA- Diámetro 1.75mm-Bobina 1kg- Color Negro

Another crucial task is leveling the print bed. Ensuring the print bed is properly levelled is crucial for successful adhesion. In the case of the Prusa i3 MK3S+, one of its strengths is the printer's automatic bed levelling system.

Figure 10. Prusa i3 MK3S+ 3D printer

4.2 Steps of workflow

4.2.1 Problem definition and initial designs

Traditionally pieces tended to be designed just to fulfill the task for which they were intended. As the world of engineering continually seeks for innovation, it always questions how to improve these designs, either so that they work better, use less material, or the production cost is lower. This pursuit often entails a significant challenge: **how to strike the perfect balance between structural integrity and material efficiency.** This is where TO emerges as a transformative solution.

In this first stage, one could come up with a new necessity, hence designing the model with the help of TO from scratch. On the other hand, which is the case of this study, an already existing piece is the subject of study. By strategically removing material where it is surplus, it is aimed that the piece continues to accomplish its task satisfactorily while being manufactured with less material which reduces both its weight and in many cases its production costs.

4.2.2 TO in SolidWorks

SolidWorks automatically determines the optimal distribution of material once the user has specified some boundary conditions for the model. The specific steps carried out to encompass the study are detailed below:

1. Create or **import the 3D CAD model** of the design to be optimized.
2. Access the Simulation workspace and select **Topology Study**
3. Define the **material properties**
4. Define the **preserved geometry areas**, and critical areas to remain unchanged
5. Define **loads and constraints**
6. Generate and refine the **mesh**, a finer mesh will create a more accurate study, but will take longer to mesh, the opposite is true for a coarse mesh
7. Choose **optimization objective**, in this case, minimize mass
8. **Run** topology optimization, the software will iteratively remove material to get a refined design that minimizes material usage without compromising performance
9. **Evaluate the results**, but change the levels to identify the key areas of FEA as highlighted to be critical
10. **Export** optimized geometry to STL format

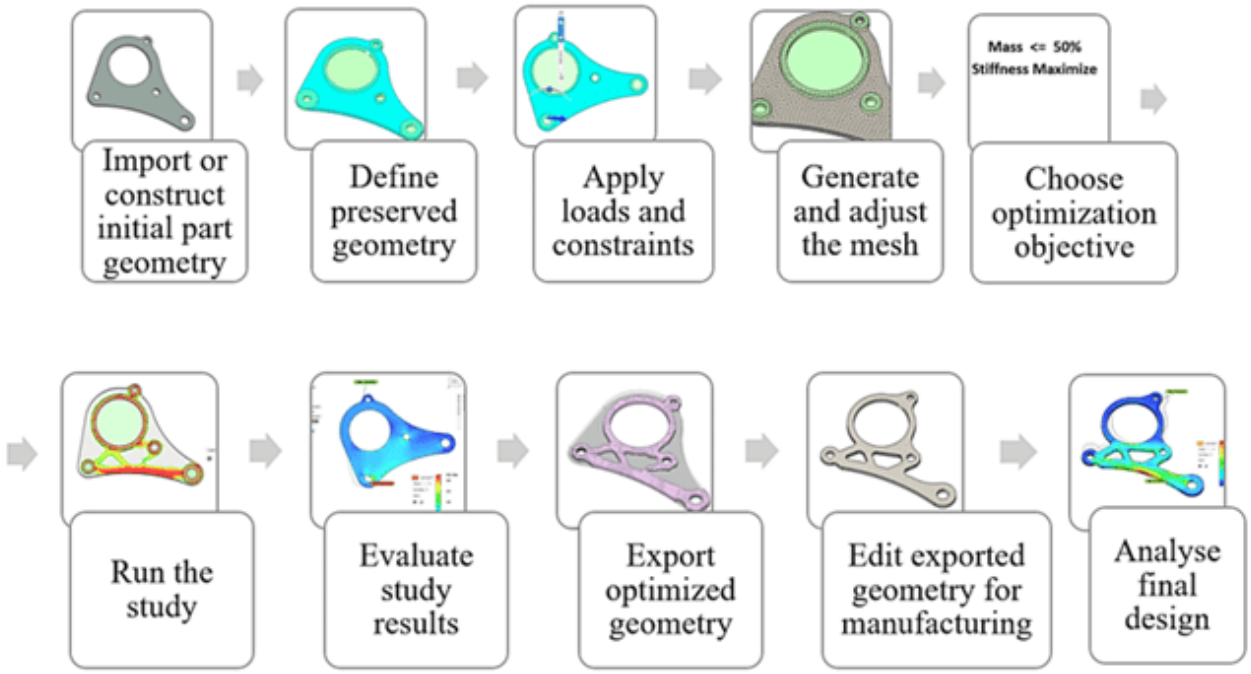

Figure 11. Topology study steps

4.2.3 Export and preprocessing

TO results might require further engineering judgement and refinement to consider practical constraints and manufacturability. However, for the scope of this project, the direct results from the simulation are taken as valid.

4.2.4 Slicing and printing setup in Cura

1. Prepare your SolidWorks model in STL format, see *6.2.1 Topology study in Solid Works Simulation*
2. Select the printer to be used, in this case, Prusa i3 MK3S+
3. Import the STL file
4. Configure the print settings, such as layer height, infill density, print speed…

   In the current research, it is of utmost importance to select an infill density of 100%, since the model is already optimized.
5. Generate supports (if needed), in case the model has overhangs or complex geometries, the support ensures successful printing. They can be automatically generated by the software.
6. Slice the model, UltiMaker Cura processes the model and generates a G-code file that contains the printer's instructions layer by layer.
7. Export the G-code to the SD card of the 3D printer

4.2.5 Printing with Prusa i3 MK3S+

Since it is a fully assembled printer, in order to start the printing, the user only has to insert the SD card with the G-code of the model, select the file, and put the machine to work. Previously it has to be ensured that there is enough PLA, or else a refill should be replaced. While the print is underway, users should monitor the initial layers to ensure proper adhesion and quality.

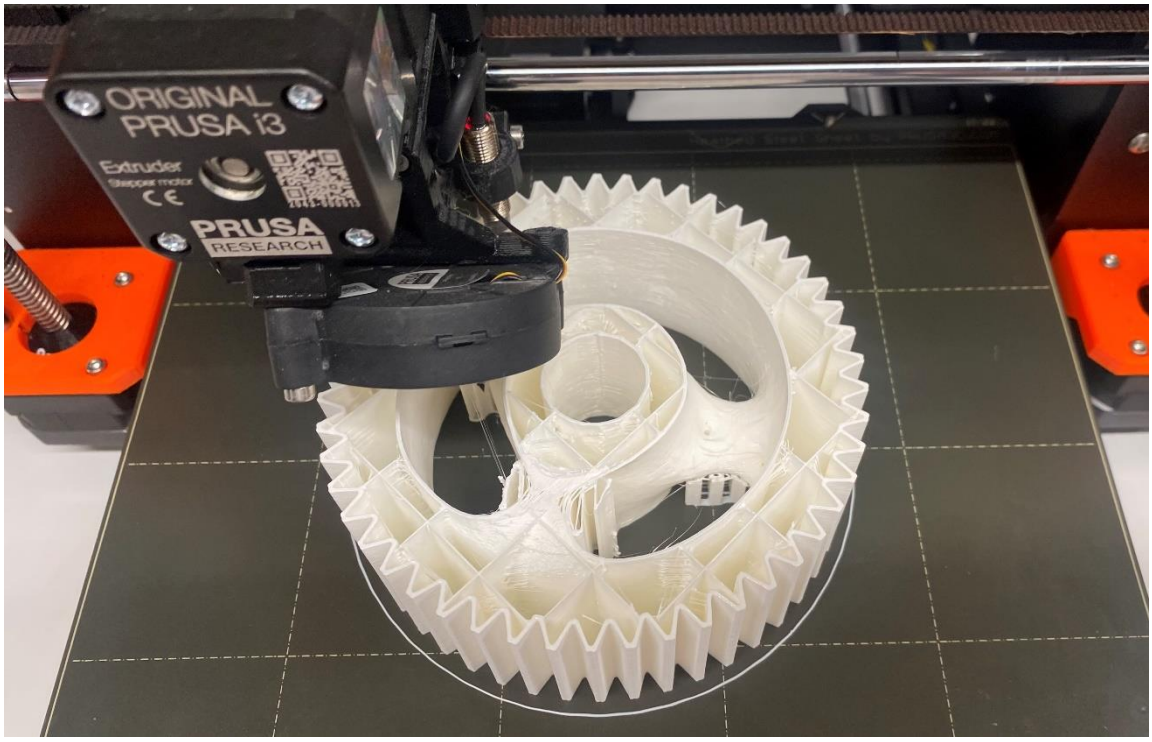

Figure 12. Optimized gear printing process

5 Experimental specimens

In a first attempt to work with TO, it is used a simple piece for study: a **specimen for traction test**. The primary goal is to validate the effectiveness of TO in reducing weight while maintaining mechanical performance. The specimens are printed in a 3D printer with PLA, designed to be tested in the laboratory in order to compare the behaviour of 3 different distributions of material:

- 100% solid specimen
- Topologically optimized specimen
- Equivalent specimen: ordinarily optimized specimen with a % reduce in mass equal to that of the TO specimen

Figure 13. Specimen

Tensile testing is a basic mechanical measurement to assess the mechanical properties of materials by subjecting them to controlled forces along their longitudinal axis until they fracture. The test specimen is securely mounted within a testing machine which applies a steadily increasing axial force. As the force is applied, the specimen elongates, and this deformation is measured using calibrated instruments. These values are used to calculate a stress-strain curve.

In the tensile test, a specimen with specific dimensions and geometry is prepared according to standardized guidelines such as ASTM and ISO standards.

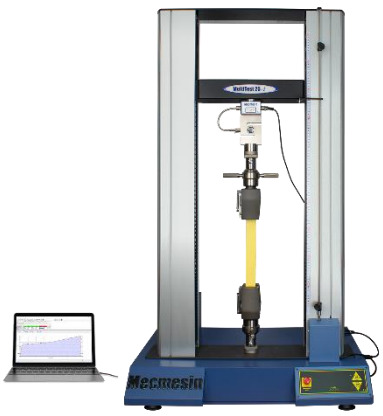

Figure 14. Tensile Traction Test machine

5.1 Design of the specimen

The specimen is designed according to the norm ISO 527-2:2012 and supported by [9]. This article sets the basis for the tensile test study for specimens manufactured by means of a 3D printer, in order to match the properties of the extruded material to be as similar as possible as if solid.

While 4 specimens are proposed, see Figure 15, in this case study only one of them is selected, the ISO 527-2 specimen, see Figure 16.

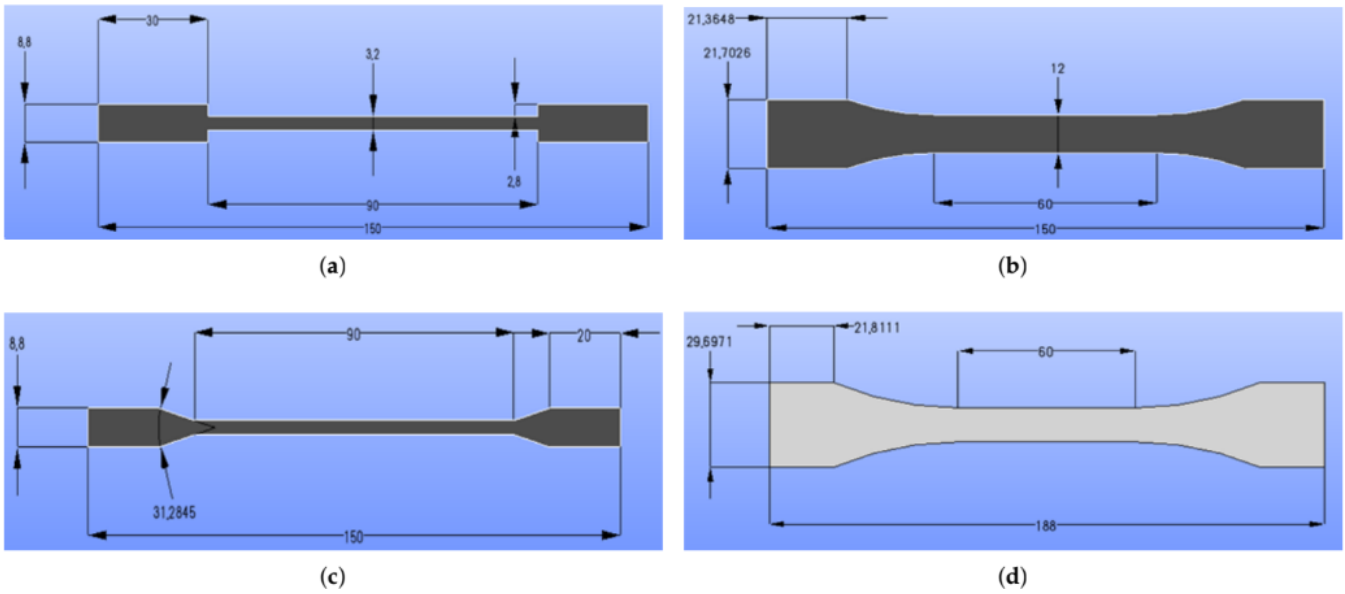

Figure 13. Tensile test specimen geometries and their specifications in mm: (a) ASTM D3039; (b) ISO527-2; (c) ASTM D3039 angle and (d) ISO-modified.

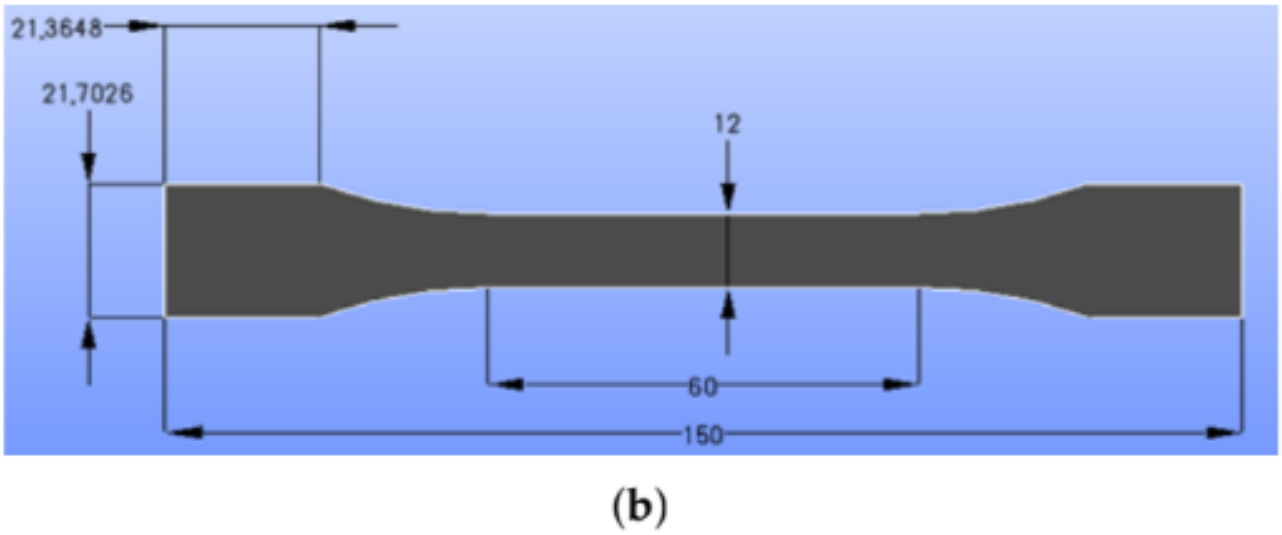

Figure 14. Specimen ISO 527-2

The election of this specimen is founded on its behaviour indicated in [27], which shows it as the one that best suits this study. The dimensions of ISO 527-2 are shown in Table 1.

Table 1. Specimen specifications

Description	ASTM D3039	ASTM D3039 Angle	ISO527-2	ISO-Modified
Tab length in mm	30	20	21.4	21.8
Tab thickness in mm	2.8	2.8	-	-
Thickness in mm	3.2	3.2	6	6
Length in mm	150	150	150	188
Width in mm	15	15	21.7	29.7
Gauge length in mm	90	90	60	60
Angle	-	31.28°	R60	R105

The specimen to be tested is designed using SolidWorks software. It is a very simple design that simply requires a profile drawn by means of lines and circles, and afterwards, the thickness is extruded.

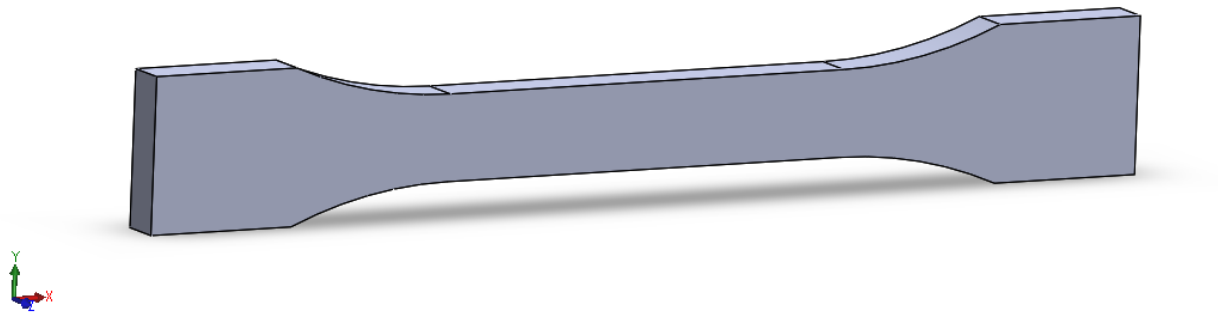

Figure 15. ISO 527-2 specimen designed in SolidWorks

In order to fully characterize the specimen using this software, it is needed to define the material, which is not found by default. The specific characteristics of the material are found in [26] and then input as shown in Figure 18.

SolidWorks allows to measure some physical properties of the objects such as area, density, volume, and center of mass. The specimen has not been physically manufactured at this point, so this tool is used to compute the total mass, necessary to compute percentages relative to the optimization.

The design of the specimen has a total mass of 17.60 grams, see Appendix 4.

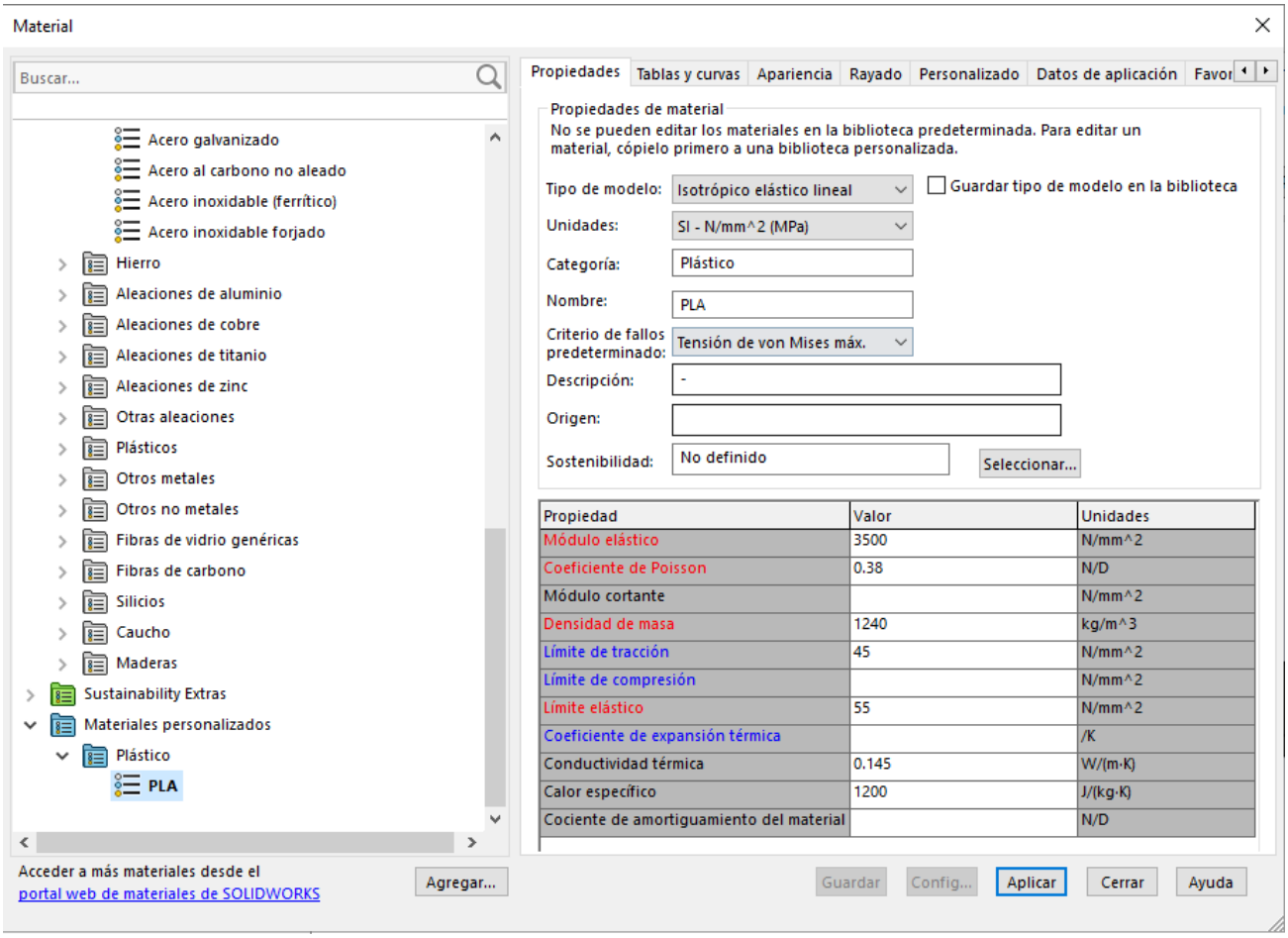

Figure 16. PLA definition

5.2 Topological Optimization of the specimen

The sequence steps for the study can be found in *7.2.2 TO in SolidWorks.*

The final goal of the specimens is to compare the properties of the 100% solid specimen with the TO optimized. For that, first is needed the properties of the 100% solid which are found with software by means of a **tensile test.** A numerical value is obtained which will be a constraint in the topology study, Hence the specimen is supposed to maintain the properties such that to stand that force but with less amount of material.

As seen in Figure 18 the traction limit of PLA is defined to be 45N/mm2. Knowing the part where the specimen breaks is the narrow center, which has dimensions of 12mm*6mm, the theoretical maximum stress the specimen resists is:

$$45\frac{N}{mm^2} * 12mm * 6mm = 3240\ N$$

The tensile test is simply defined with a fixed support and a force, which is rounded to be 3000N, see Figure 19.

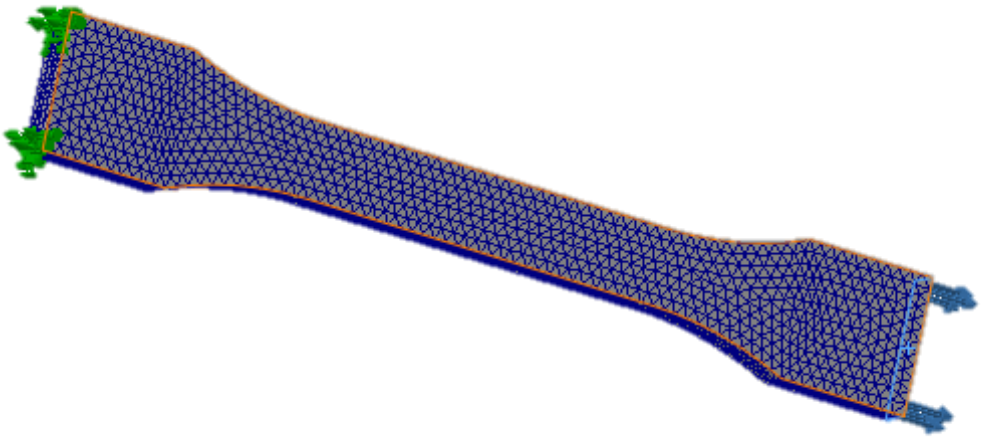

Figure 17. ISO 527-2 specimen tensile test constraints and mesh

The results of the tensile test are found in Figure 20, and the Max Von Misses Stress is 44 MPa. Theoretically, since the 3240 N are not reached the specimen should not get to fracture, as it has been verified in the study.

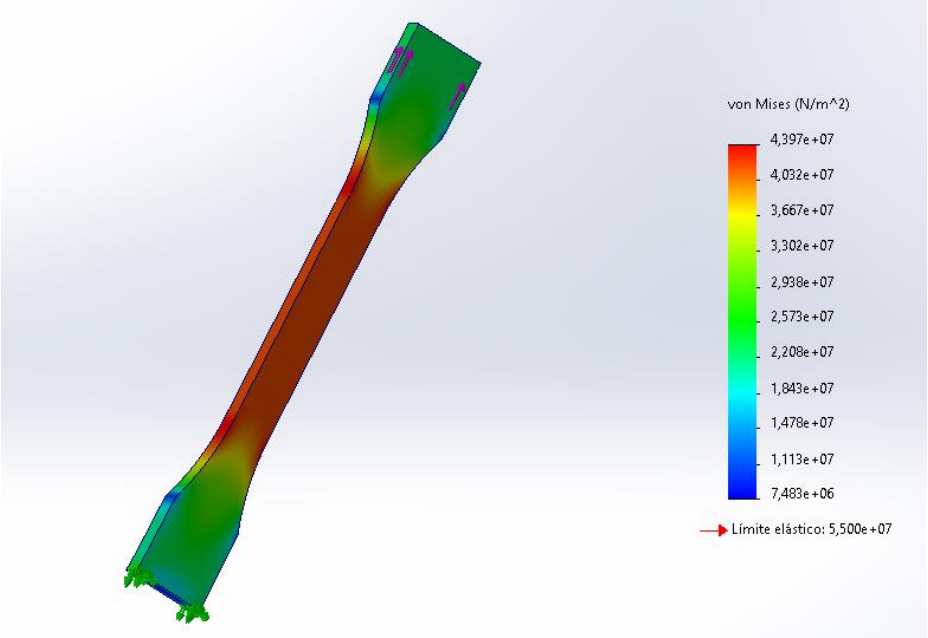

Figure 18. ISO 527-2 tensile test results

The next step is to carry out the actual Topology study. The sequence steps for the study can be found in *7.3.2 TO in SolidWorks.* In the following figures are shown the preserved areas, fixed parts, and loads, respectively.

The testing machine is designed to attach the specimen on both extremes, specially designed for the task, so that the specimen breaks in the center. Hence, both extremes cannot be considered part of the optimization and they are specified as preserved areas as shown in Figure 21.

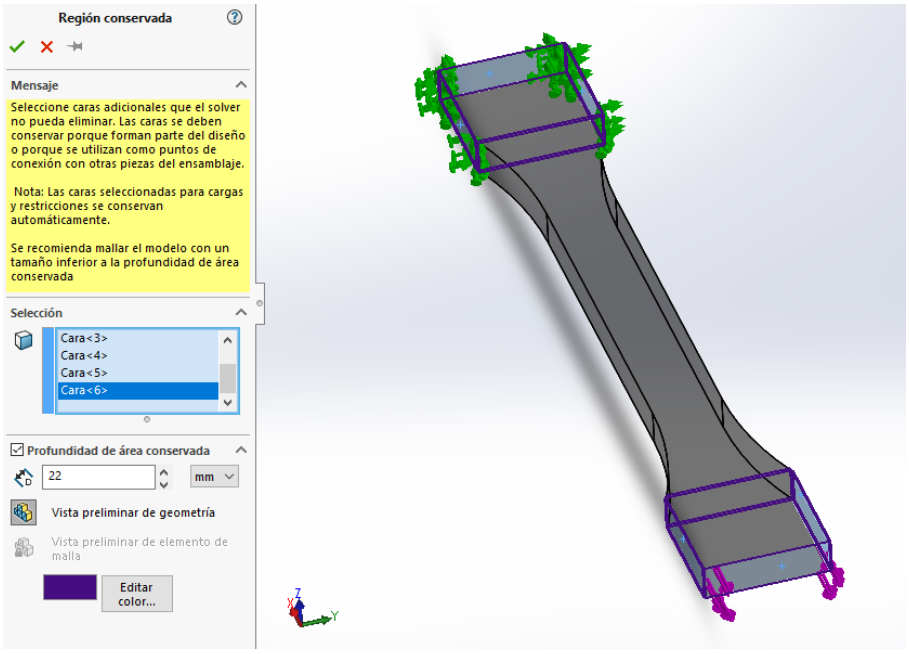

Figure 19. ISO 527-2 topology study preserved areas

While being attached in both extremes, the testing machine only pulls from one of them, meaning the other remains fixed.

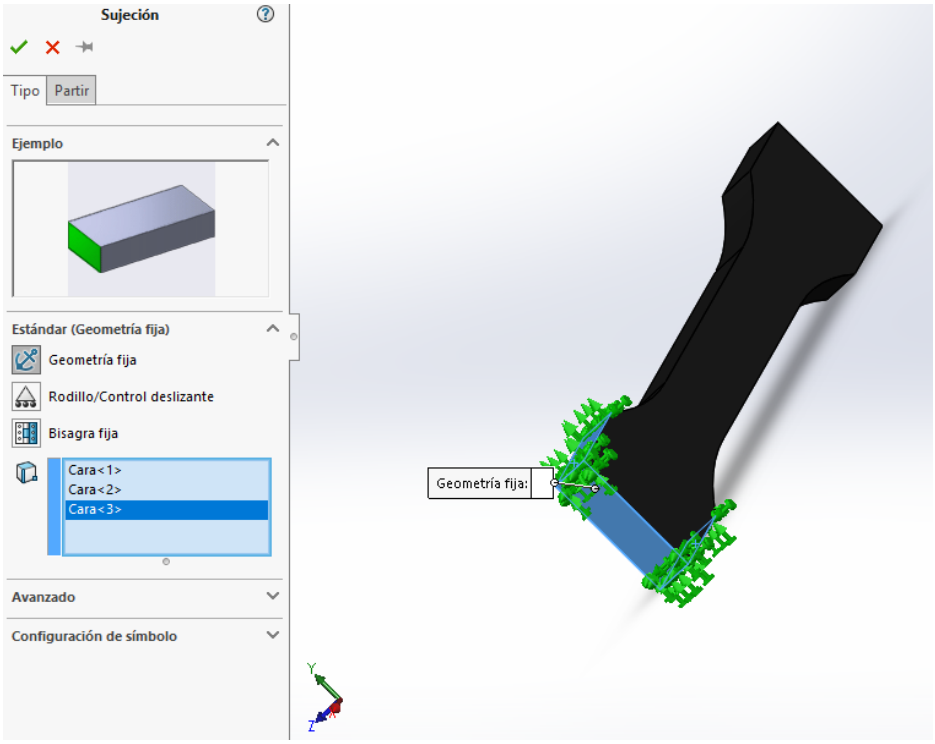

Figure 20. ISO 527-2 topology study fixed areas

The force is applied on the other extreme and is defined only on the outer surface to be aligned on the vertical direction, the stretching direction. It is set to be 3000N as previously computed.

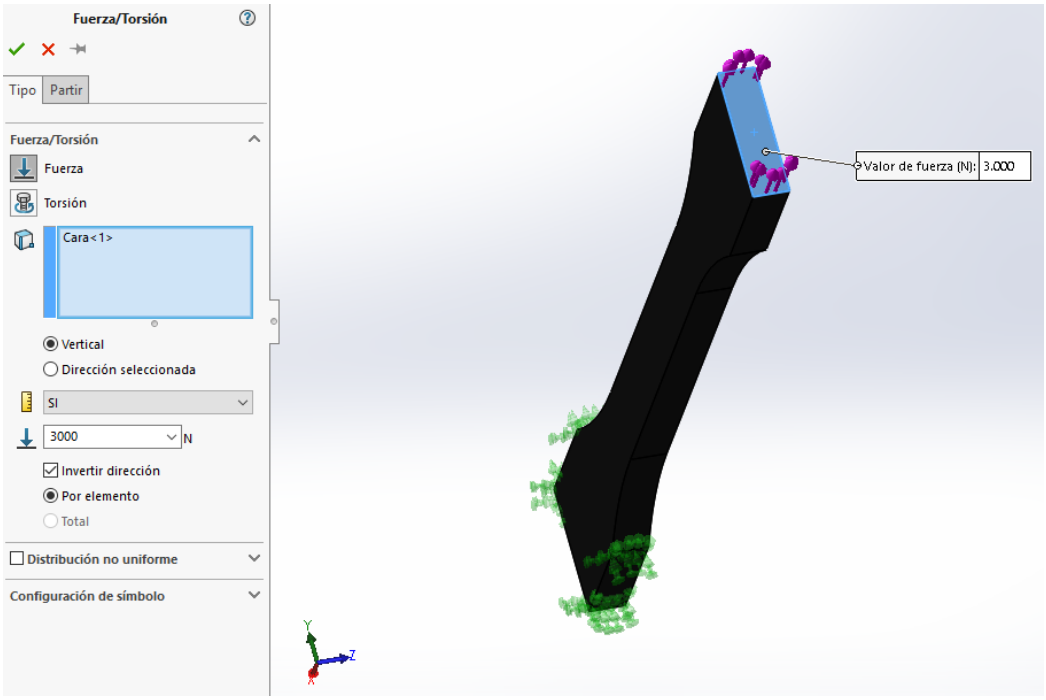

Figure 21. ISO 527-2 topology study 3000N forces

Real percentage of topological optimization

It is of utmost importance to note that the % optimization in the specimens does not refer to the entire piece. This is because both squared corners are designed to be the grip of the tensile test. Hence, the only part of interest to the study is the narrowed part, see figure 24.

Figure 22. ISO 527-2 comparison with the narrow center subjected to TO

This way, in order to compute the % optimization that the software yields, it needs to be computed in base of this central part, not the whole specimen.

The central part has a mass of **6.26 grams** equivalent to a **35.57%** of the total mass. With a simple calculus the real TO % is computed:

$$Real\ TO\ [\%] = \frac{17.6\ [g] - mass\ of\ the\ optimized\ specimen\ [g]}{6.26\ [g]} * 100$$

Once the TO study is conducted satisfactorily, **the result is a specimen with a % reduction in mass which theoretically stands the same force as the one set as a constraint**. The scope of this study aims to demonstrate it.

The "Equivalent specimen" is designed to that end, with the **same shape as the 100% solid specimen and being optimized at the same mass % as the TO % equivalent**. This means the **optimization is not topological**, but a simple reduction in density throughout the whole geometry. In practice, this is achieved by changing the infill density to the 100% solid specimen by:

$$Infill\ density = 100\% - Real\ TO\ [\%]$$

Printing parameters

Manufactured PLA that comes in coils has certain properties, which are the ones that are taken as a reference for its mechanical properties. However, when printed by a 3D printer this material is no longer a single solid, but the geometries printed are a set of fine threads linked together. Therefore, the properties of the material are no longer valid. For this reason, [27] propose some changes in the settings of the 3D printer with the goal to maximize the similarity between solid and extruded PLA.

The settings, see Table 2, are modified in Cura software.

Table 2. Process parameters of 3D printing

Parameter	Value	Unit
Layer thickness	0.3	mm
Layer width	0.4	mm
Print speed	55	mm/s
Initial layer speed	40	mm/s
Print acceleration	4000	mm/s^2
Printing temperature	250	°C
Printing temperature initial layer	255	°C
Final printing temperature	240	°C
Bed temperature	70	°C

Then are the paths the machine follows when printing. The goal of the printer is to minimize time, which does not necessarily mean maximum quality, hence usually some excess travel lines are printed which are inadequate for axial testing. Is important to solve this issue because a failure produced due to such phenomena would not be representative of the material itself. To solve this issue, the article provides the configurations for modified travel shown in Table 3.

Table 3. Standard and modified travel configurations in Cura

Parameter	Standard	Modified
Combining mode	All	Not in Skin
Max comb. distance with no retract	0 mm	100 mm
Avoid printed parts when traveling	✓	✓
Travel avoid distance	3 mm	10 mm
Layer Start X	213.0 mm	200.0 mm
Layer Start Y	198.0 mm	200.0 mm
Z hop when retracted	✓	✓
Z hop only over printed parts	✓	✓
Z hop height	2 mm	5 mm

Procedure

In this first attempt the goal of the study is set to be a 30% reduction in mass weight.

The result obtained is not as expected, see Figure 25, since only a 7% reduction is achieved with a mass of 16.5 grams, see Figure 26. **Bear in mind this 7% reduction refers to the total mass of the specimen**. Applying the formula (*see pg.40),* the real TO percentage is computed:

$$\frac{17.6\,[g] - 16.5[g]}{6.26\,[g]} * 100 = 17.5\%$$

Meaning the narrow part, the part of interest, is topologically optimized at a real **17.5%** in mass.

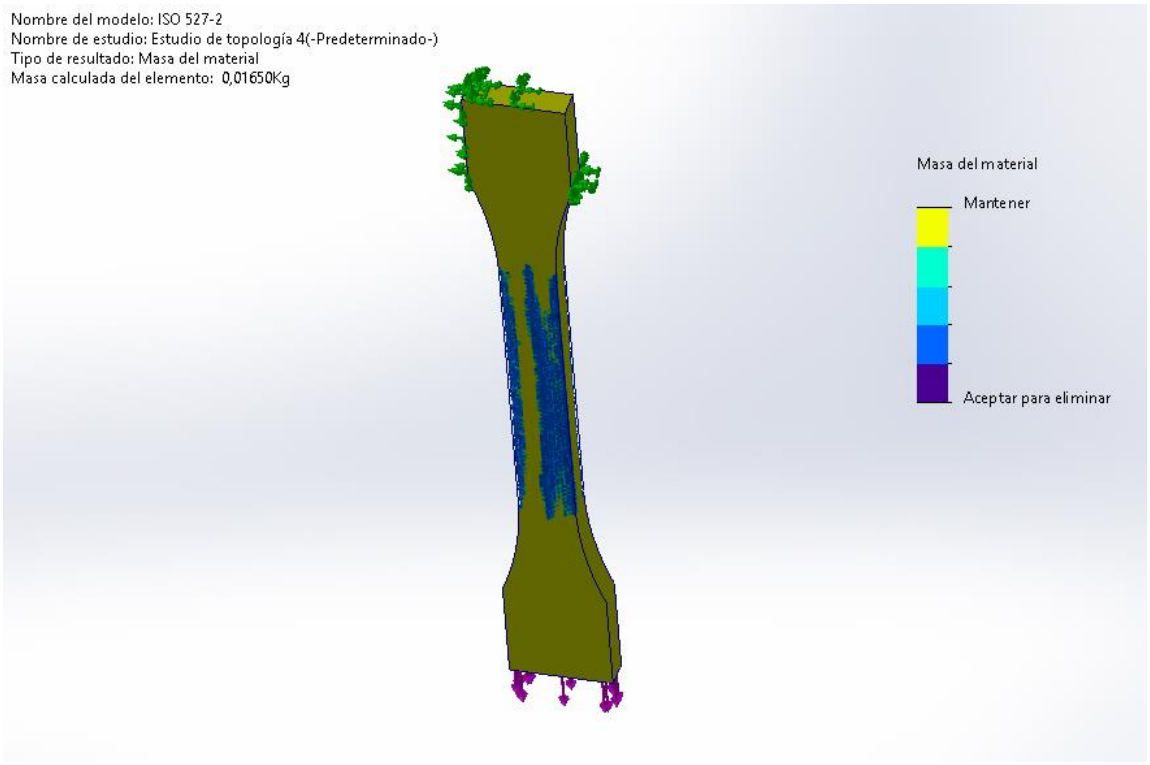

Figure 23. ISO 527-2, 3000N topology study result

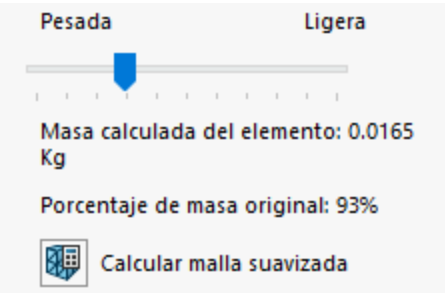

Figure 24. ISO 527-2, 3000N topology study result mass percentage

After optimizing the specimen topologically, the equivalent specimen is computed. In this case of a real 17.5% optimization, it will have an infill density of 82.5%.

Figure 25. Detail of infill density when printing

Bearing in mind the maximum theoretical force the specimen resists until failure, 3240N, this result is analyzed. The force applied in this study has been of 3000N, a quantity quite close to the maximum. Hence it is not surprising not to obtain a very noticeable reduction in weight, since the piece would not be able to stand much more force until failure. To verify the previous statement, a complementary study is carried out applying 4500N, see Figure 28.

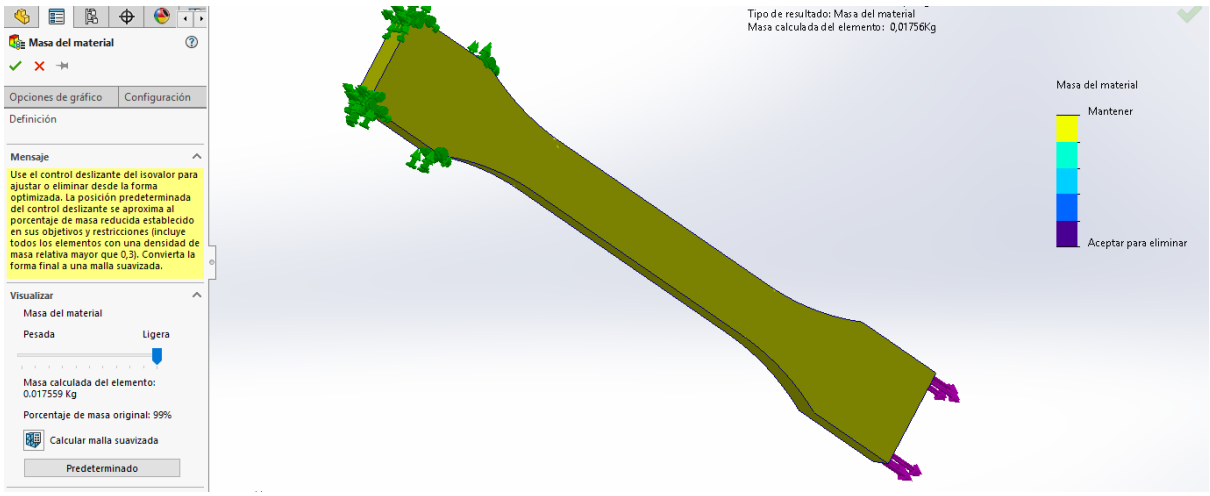

Figure 26. ISO 527-2, 4500N topology study result

As expected, the specimen remains the same since this force goes beyond the maximum stress of the specimen and would break. Hence, the algorithm cannot remove any material from it.

After the results of the first study, a second one is carried out with 1500N. The rest of the constraints stay the same and the goal is set again to a 30% reduction in mass.

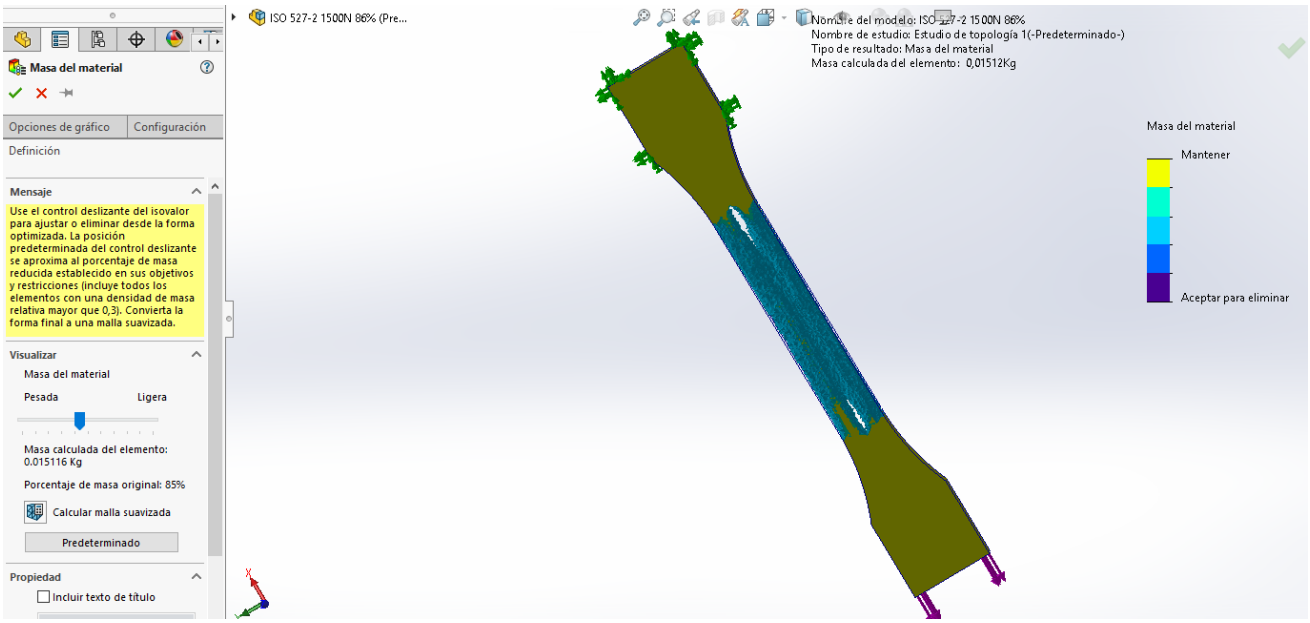

Figure 27. ISO 527-2, 3000N second topology study result

As seen in Figure 29 this time with a smaller force a reduction of 14% is achieved (total mass). This means the optimized specimen should resist the 1500N applied in that direction in the same way as the initial specimen does. The real optimization in this case is:

$$\frac{17.6\,[g] - 15.1[g]}{6.26\,[g]} * 100 = 39.9\%$$

This **second TO specimen achieves a 39.9% real optimization**. The equivalent specimen will have an infill density of 60.1%.

Notice that when a topology study runs successfully in the software, it does not only give a single result. Rather it yields a continuous interval of solutions ranging from the complete initial piece to the maximum allowable reduction in mass, which can easily be modified in the interface, see Figure 30. Material is removed or added yielding different optimizations. However, all along the interval of solutions the constraints are always satisfied.

The result of the second specimen falls somewhere along the center of this interval, meaning the optimization still has room for improvement.

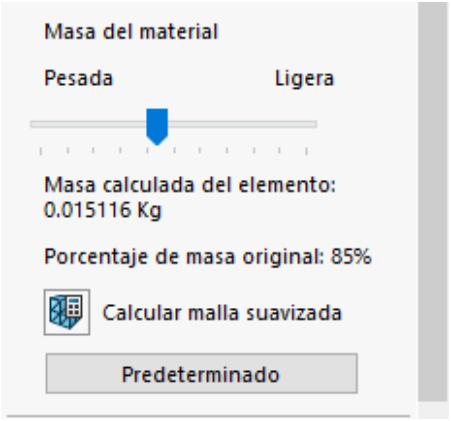

Figure 28. ISO 527-2, 3000N second topology study result mass percentage

A **third TO specimen** is studied by pulling the optimization to the limit, removing all the material possible but still standing the 1500N. A mass of 14.3g is achieved, equal to a 19% reduction (total mass), or **52.7% real optimization**, see Figure 31. The equivalent specimen will have an infill density of 47.3%

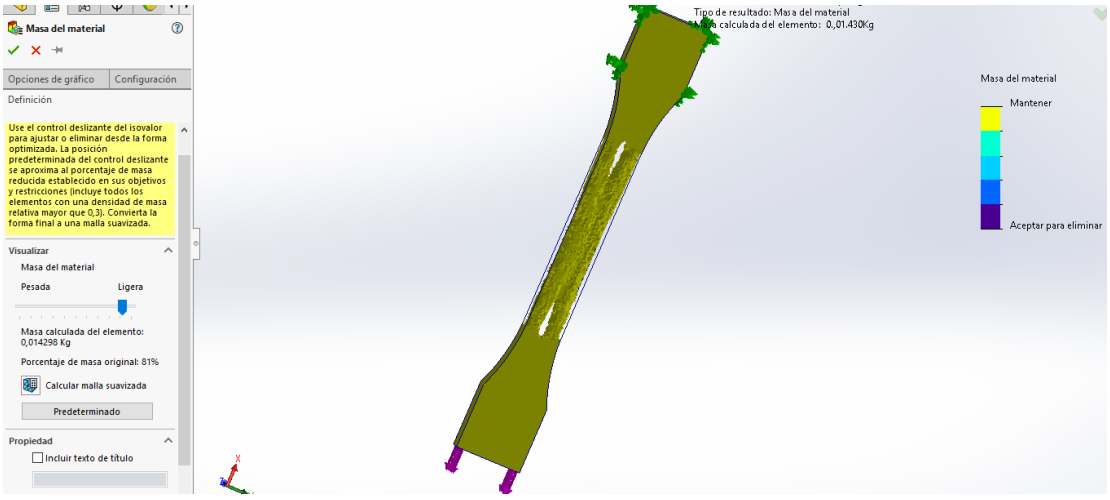

Figure 29. ISO 527-2 third topology study result

The next step before printing the specimen, is to compute the **smoothed mesh**. At this point, the final shape of the piece is visualized and can be modified. This can be necessary in case the software computations yield some error which obviously is not manufacturable, or does not add any mechanical property to the part. To be: protruding tips, voids, unattached pieces… This is a trade-off between a percentage reduction in mass and structural strength which the designer is to decide.

As well the quality of the mesh can be modified to be either finer or coarser, to have rounded corners, which are a very important step to take into account for the quality impression of the printer.

In the 52.7% case the optimized specimen has 2 thin wires on each extreme, see Figure 32. One of the wires in the beginning was not even joined to the extreme. Then the mesh is modified to make these wires thicker, hence, the % mass reduction is reduced. However, this reduction in % mass is negligible.

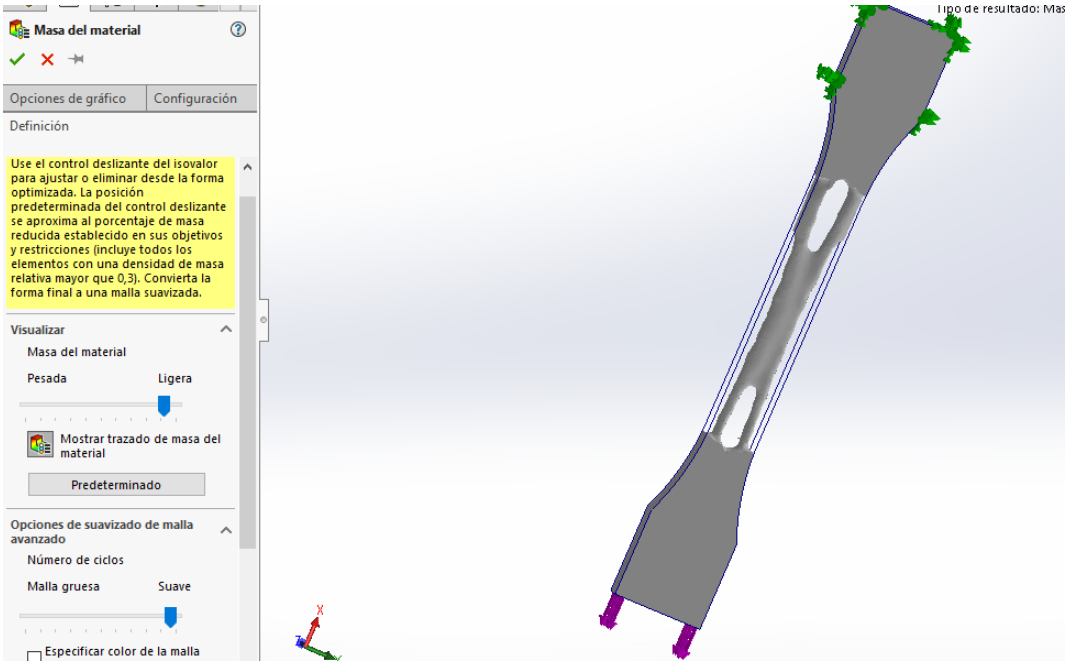

Figure 30. ISO 527-2 third topology study result smoothed mesh

The files are exported in STL format and open in Cura software, where the printing parameters are set up to maximize the quality of the printed specimens, *see 8.2.2 Printing parameters.*

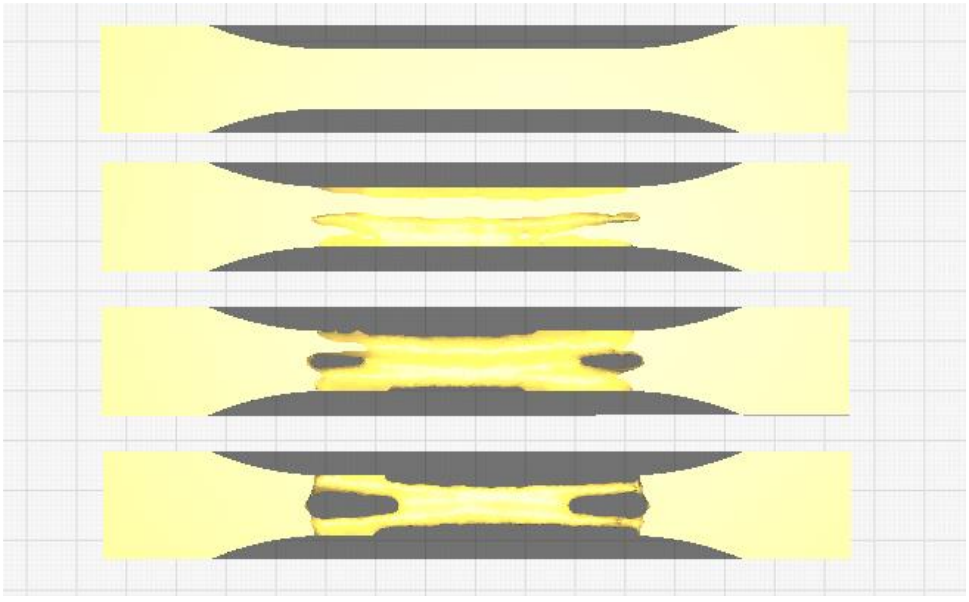

Figure 31. Comparison of ISO 527-2 optimized specimens in Cura

5.2.1 Results

Three different studies have been carried out successfully, achieving 17.5%, 39.9% and a maximum optimization of 52.7%, respectively.

Table 4. Specimen TO studies results

	Force	Mass (g)	% total mass	**Real % TO**	Infill density*
100% solid		17.6	100%	**0%**	
1st study	3000N	16.5	93%	**17,5%**	82.5%
2nd study	1500N	15.1	86%	**39.9%**	61.1%
3rd study	1500N	14.3	81%	**52.7%**	47.3%

*Infill density of the equivalent specimen

The specimens are printed in the OpenSpace facility. The steps can be found in *7.2 Steps of workflow*.

Figure 34 shows the real specimen, altogether with the 3 topologically optimized specimens ordered vertically from lowest to highest optimization achieved.

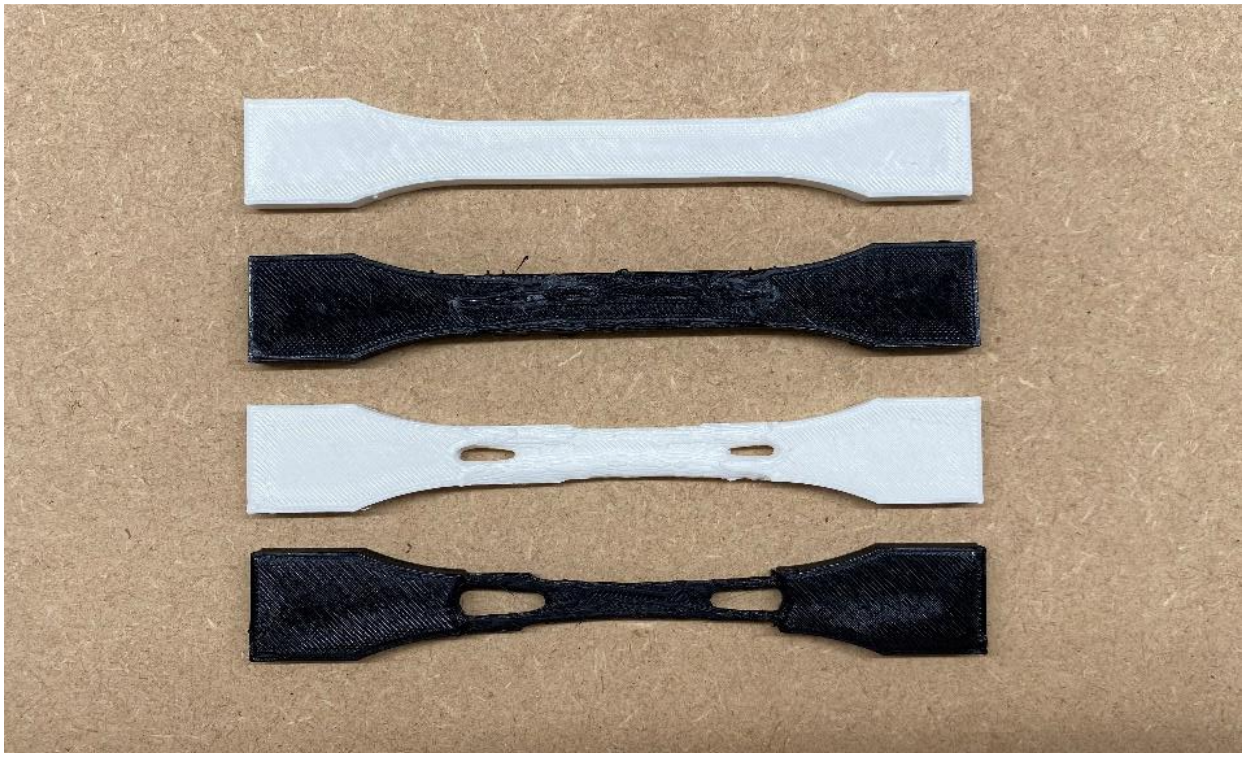

Figure 32. 3D printed specimens top view

Figure 33. 3D printed specimens lateral view

Notice the most optimized specimen (lowest one) is especially thinner than the rest. This can be a problem when printing, but easily solved by adding supports, automatically generated by Cura. They are designed to be easily removed after printing.

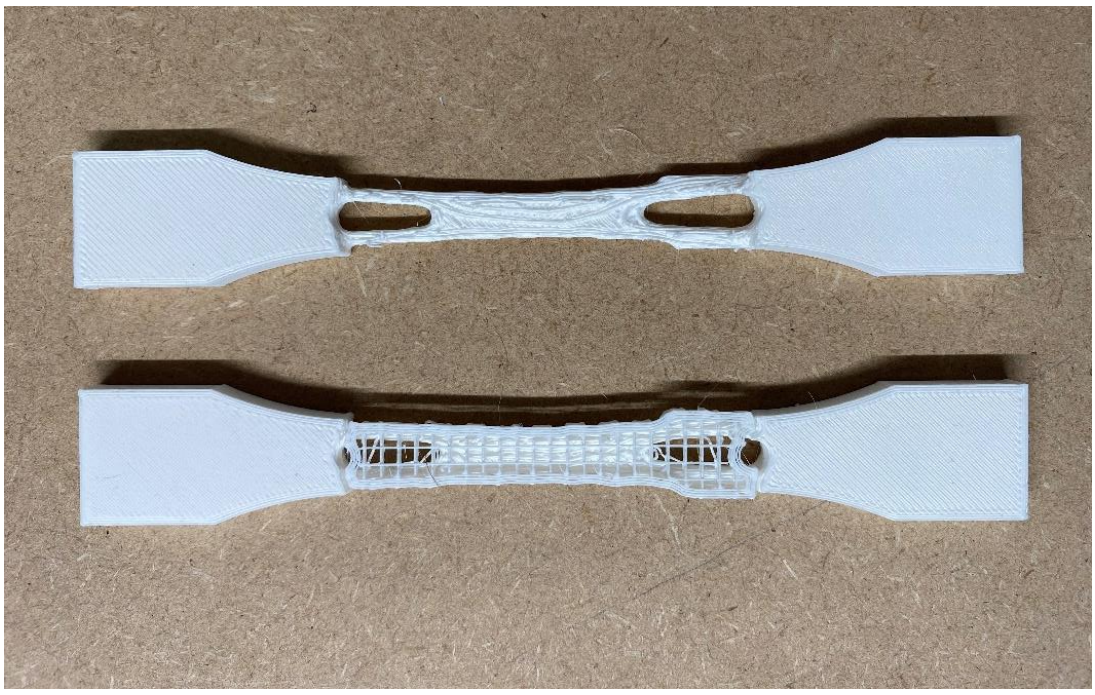

Figure 34. Support generated by Cura

Figure 37 shows all the collection of specimens printed. With the objective of being studied in a traction machine, 3 of each type are printed to take data averages. On the top is found the real 100% solid specimen. The column on the right shows the TO specimens, while the left one shows the equivalent specimens. The latter ones may seem equal to the solid specimen, but their inside is manufactured with the infill densities of Table 4.

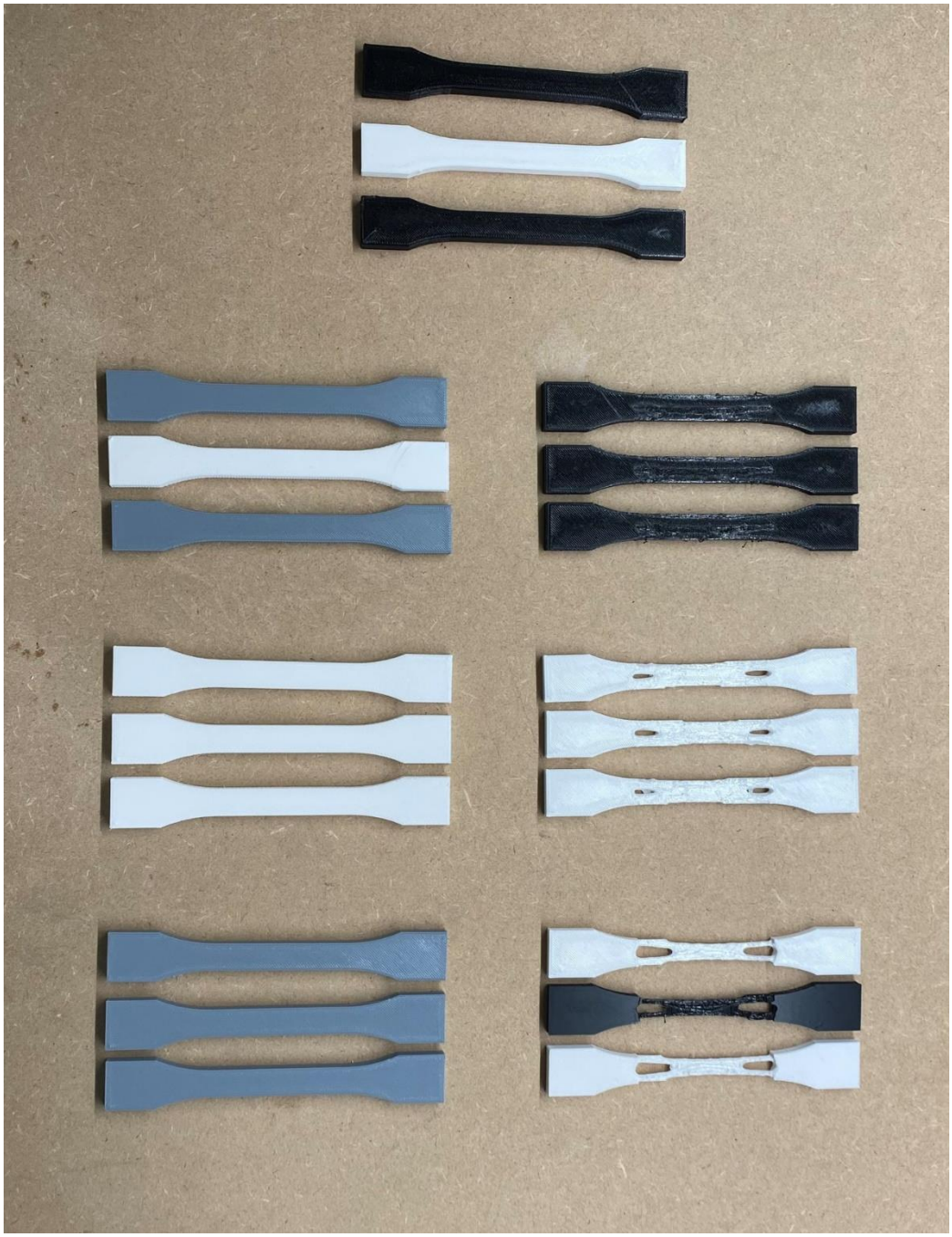

Figure 35. Collection of 3D printed specimens

5.3 Discussion

In this study, the ISO 527-2 specimen was subjected to TO in order to minimize its weight while maintaining mechanical performance when tested in a tensile machine. The designs exhibited significant optimization in terms of mass reduction, achieving improvements of 17.5%, 39.9% and 52.7% in the narrow part where the specimen ultimately fails.

The study highlights the potential of combining TO and 3D printing in engineering design. By selectively redistributing material within the design space, it is possible to minimize material usage while maintaining structural performance.

Further research is warranted to validate the mechanical properties of the optimized specimens through physical testing in a laboratory.

From the results of this study emerge several points for discussion:

- Laboratory Analysis. Comparing the performance of the topologically optimized specimens with the conventionally designed ones under the same test conditions in a testing machine. This task remains for further analysis to verify that indeed the topological studies simulated by computer are validated in real life and support the constraints.
  Furthermore, the comparison of the TO specimen with the equivalent specimen could provide a comprehensive understanding of the benefits of topological optimization in comparison with an ordinary density optimization.
- Optimization parameters. The process involves various parameters such as load conditions, design constraints, and objectives. A deeper exploration of these parameters could reveal additional optimization possibilities, potentially leading to even more significant efficiency gains.
- Material considerations. While PLA has been used in this study, further research could investigate the use of optimized metal specimens, for more demanding applications. This could broaden the potential applications of optimized designs.
- Scaling and practical implementation. The study focused on a specific specimen design. However, the principles explored here have implications for a broader range of components and structures. The next sections of this thesis delve into the TO of two real components, investigating scalability and the challenges associated with applying it to more complex geometries.

6 Gear Mn5 z50

The piece to be studied is a Mn5 z50 gear from the company ENPA. The STP format is provided, there is no need to design it. It is a 50-teeth gear, custom designed, for very high power application.

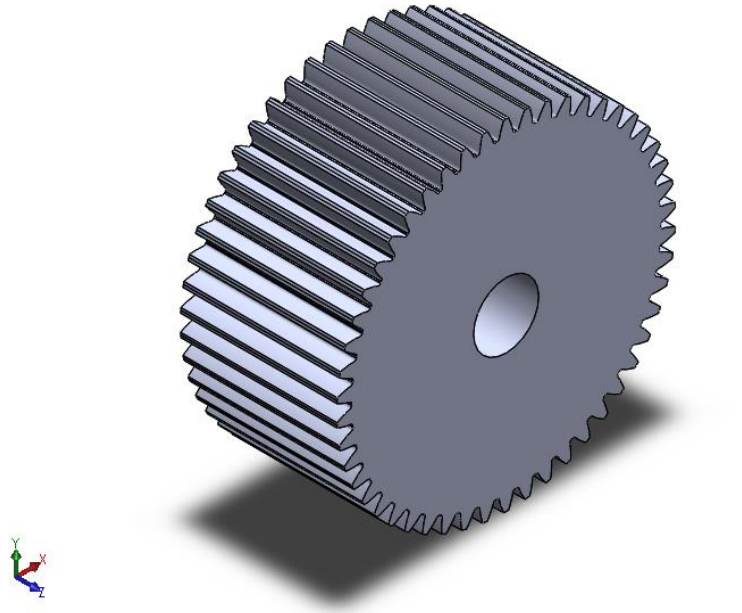

Figure 36. Gear Mn5 z50

The material is 316L stainless steel, which is directly found in SolidWorks library. Gears are normally superficially treated in order to harden the teeth, in order to increase their wear resistance. In this study, the properties of the library are directly used for not having more detailed information available.

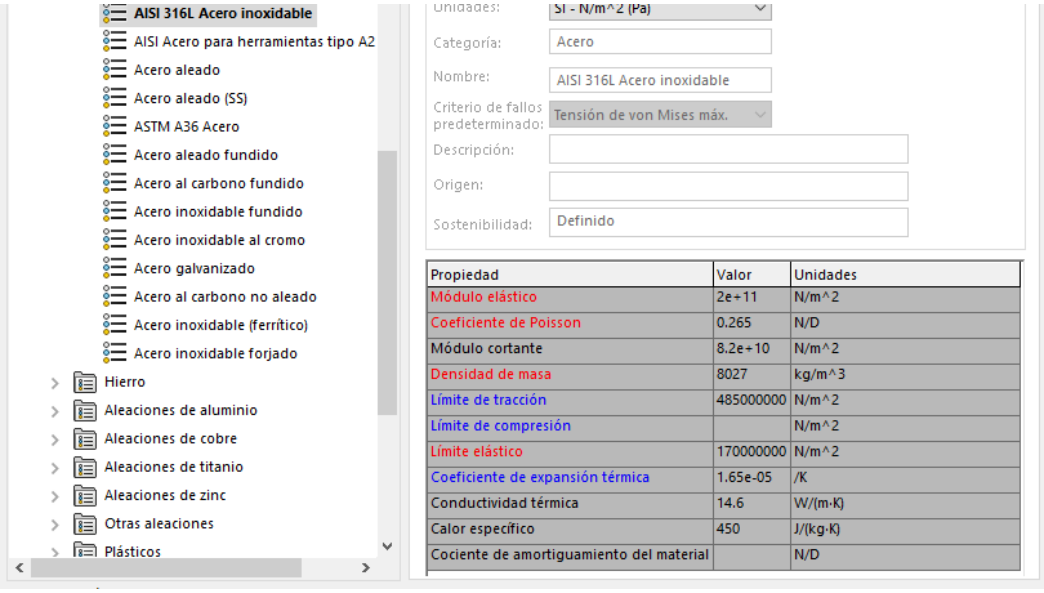

Propiedad	Valor	Unidades
Módulo elástico	2e+11	N/m^2
Coeficiente de Poisson	0.265	N/D
Módulo cortante	8.2e+10	N/m^2
Densidad de masa	8027	kg/m^3
Límite de tracción	485000000	N/m^2
Límite de compresión		N/m^2
Límite elástico	170000000	N/m^2
Coeficiente de expansión térmica	1.65e-05	/K
Conductividad térmica	14.6	W/(m·K)
Calor específico	450	J/(kg·K)
Cociente de amortiguamiento del material		N/D

Figure 37. 316L stainless steel library in SolidWorks

In a first approach to understanding this geometry, a study is carried out with a **quarter gear.** The forces applied are the main one, perpendicular to the teeth, with a modulus of 1000N, and the contact force between gears, with 100N.

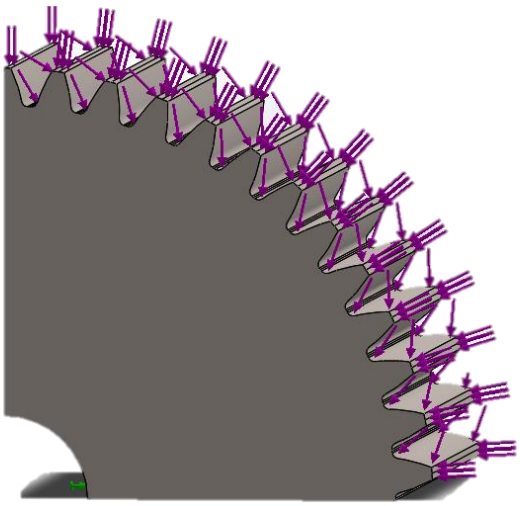

Figure 38. Quarter gear initial constraint of forces

In the first attempts of simulation it is noticed that since it is a big piece, the computer needs a lot of power computation. Power computation is directly related to FEA, which interprets the solid as small elements. The more elements it has, the more computation power is needed. The same applies to external constraints, in this case, the forces.

This first simulation is never carried out completely due to the computation power. This is until the contact forces are removed, see Figure 41. They are much smaller forces in comparison with the perpendicular ones, hence by removing them, computation power is released without altering much the results. Still, the outer surface of gears is an essential part in order to ensure contact with other gears at every moment. Both problems are easily solved by making this region a preserved area.

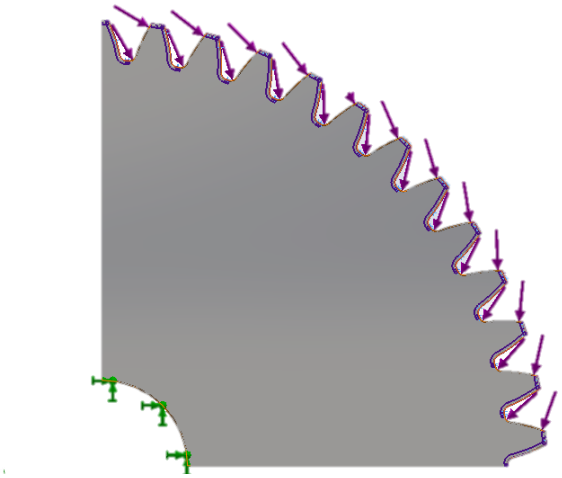

Figure 39. Quarter gear final constraint of forces

The study is performed with 3 different meshes: fine, medium and coarse, in order to analyze one more time the dependence on computation power. Only the study performed with the coarse mesh reaches completion. These studies are also carried out in the cases of one and five teeth and in the case of the whole gear. In every case, the results are the same. The computer does only have the power to compute this gear TO in case the mesh is coarse. To see more details of the definition of coarse mesh see Appendix 5.

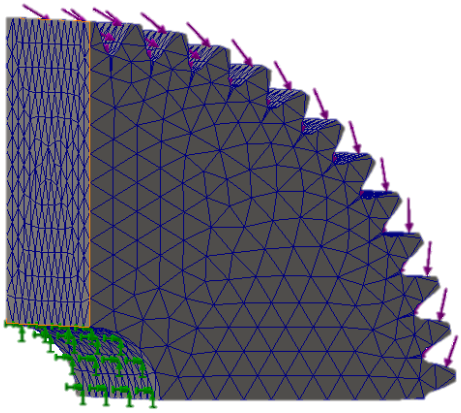

Figure 40. Quarter gear coarse mesh

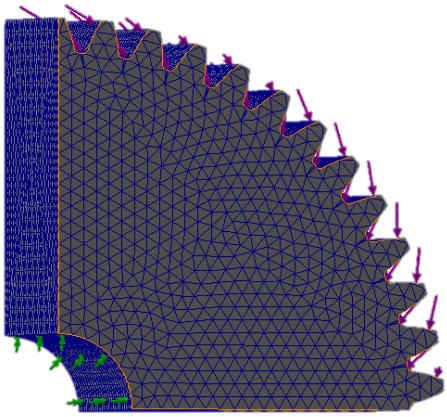

Figure 41. Quarter gear medium mesh

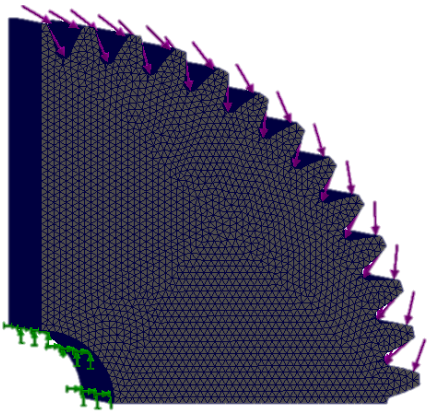

Figure 42. Quarter gear fine mesh

6.1 Topological Optimization

The sequence steps for the study can be found in *7.3.2 TO in SolidWorks.*

Gears are complex objects to study because of their motion and because of the forces they suffer. The instantaneous force is only applied to a single tooth. If this was the case it would be a steady state analysis, however, the motion must be added.

In order to understand better the behaviour of the TO in a gear, different studies are carried out:

- Entire gear
- A quarter section
- Five teeth
- Single tooth

The studies are designed taking into account the geometry. With 7.2º per tooth, the goal is to extrapolate the individual optimizations into the whole gear. Meaning, that with the TO solid in the case of five teeth, it will create a whole gear combining it 10 times.

Entire gear

Gears are in circular motion around its axis. In the study, this inner circle is set as the fixation.

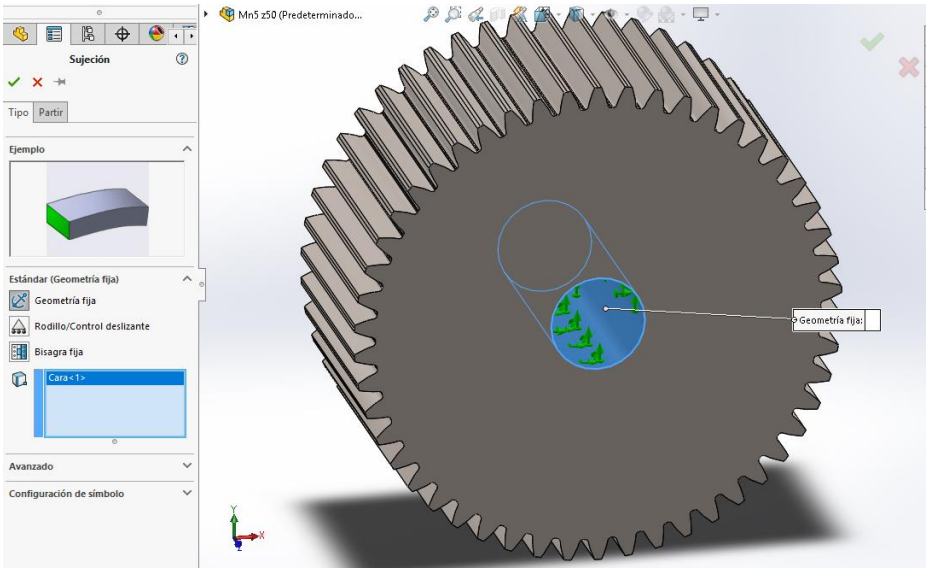

Figure 43. Entire gear fixation

In this case the forces which are set to 1000N, only applied on one face of the teeth as previously explained.

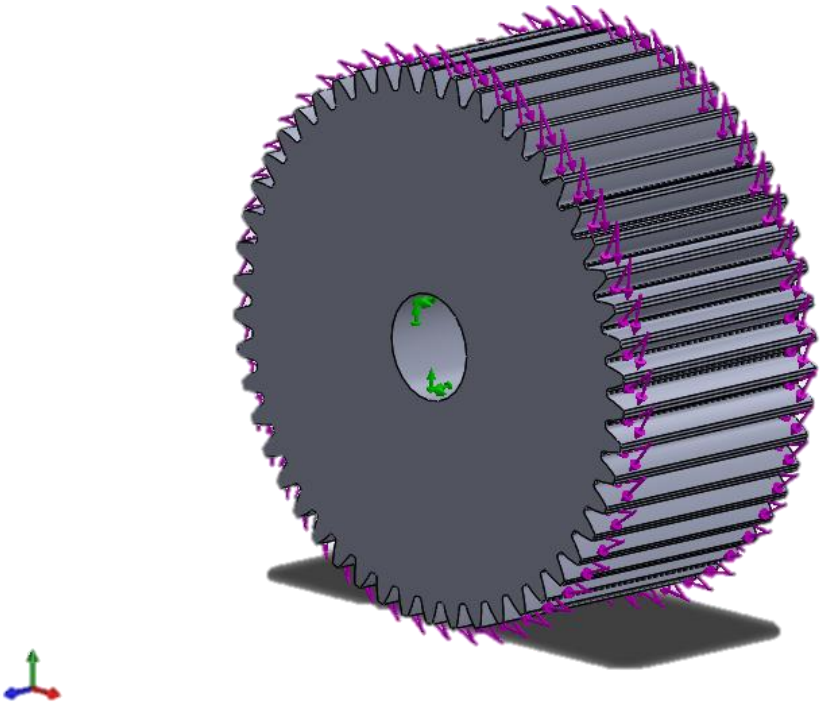

Figure 44. Entire gear 1000N forces

The study of the whole gear arises a new problem regarding the preserved areas and power computation. In the other cases since the geometry is smaller, the computer seems to be able to carry on with the simulation when preserving the outer surfaces as seen in detail in Figure 47. The solution is found in the scheme shown in Figure 48, by only keeping one of the preserved area, hence reducing to half the number of constraints, and increasing its width so that it covers both previous surfaces.

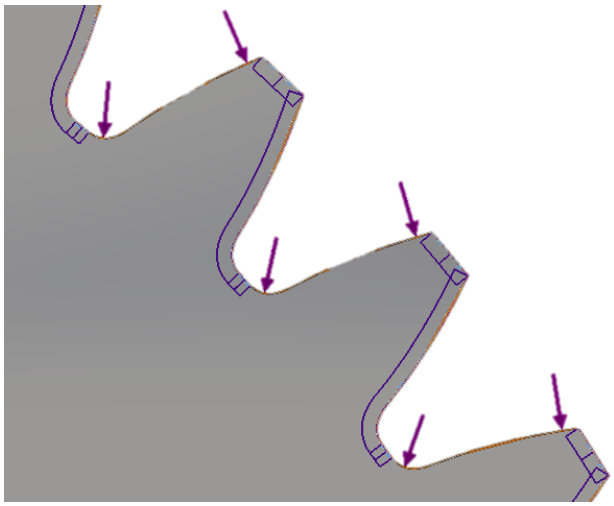

Figure 45. Detail of 2mm outer preserved areas in quarter gear

The width of the preserved area is set to 15mm on the outer surface.

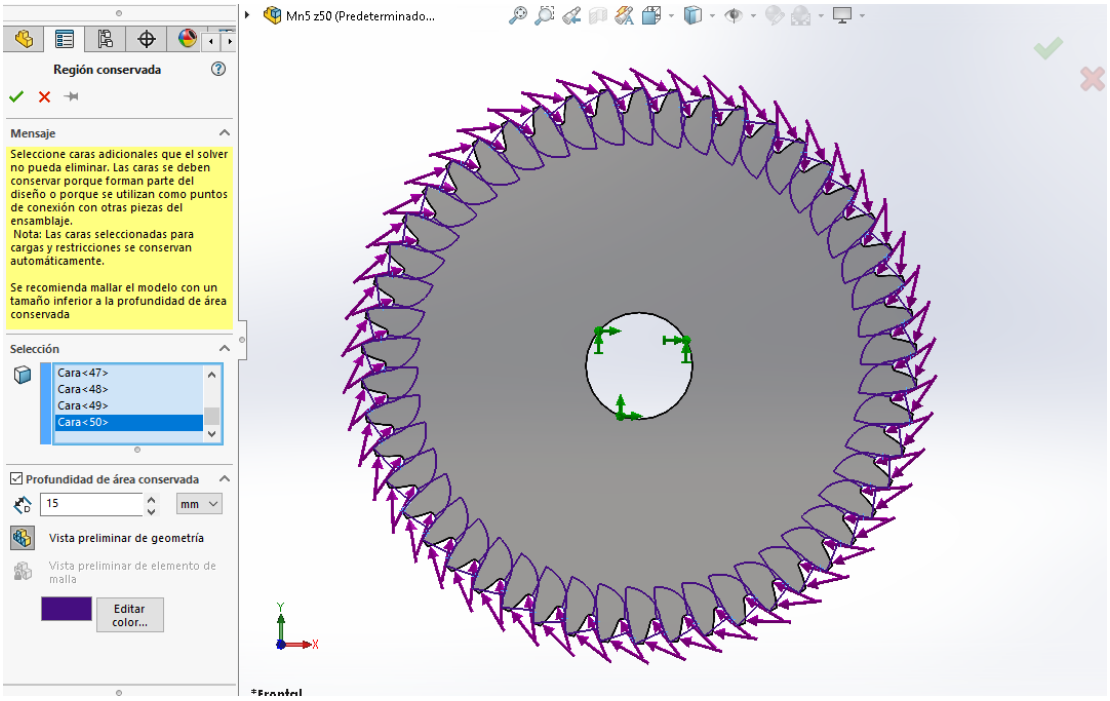

Figure 46. Entire gear 15mm outer preserved areas

The other preserved area is the inner hole. Since it is the axis of rotation, in contact with another component, it is subjected to wearing. It is set to maintain at least 10mm of material.

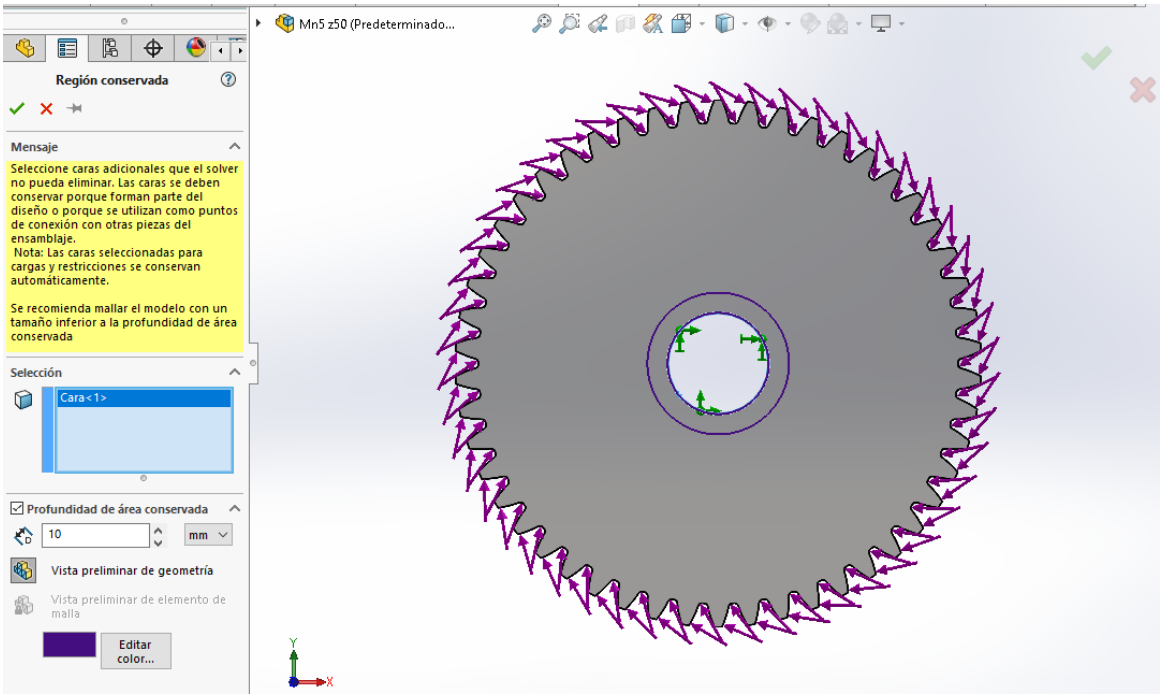

Figure 47. Entire gear 10mm inner preserved area

Once all the constraints are input, the mesh is created. Again, a coarse mesh is set in order to ensure enough power computation so that the study runs satisfactorily.

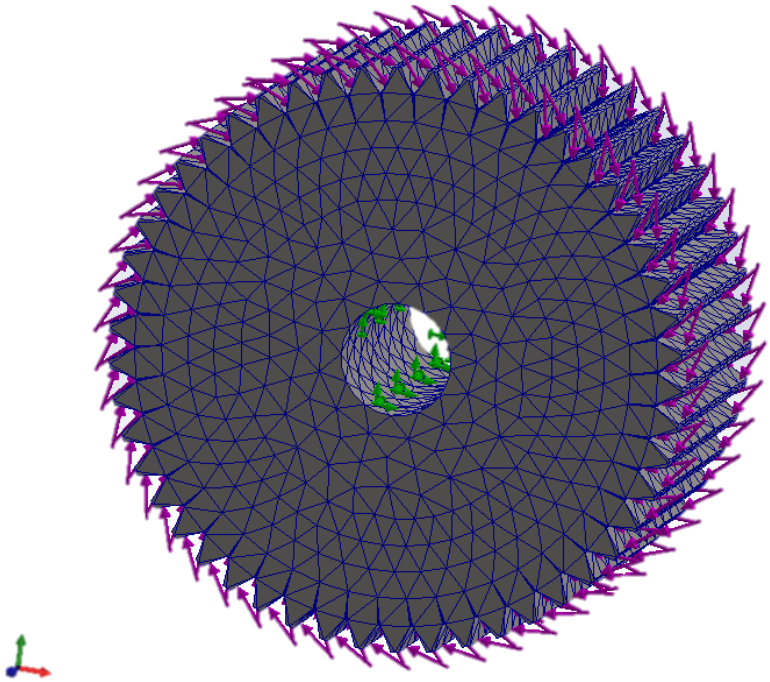

Figure 48. Entire gear coarse mesh

The goal of the study is set to a 50% reduction in mass. The simulation takes 50 minutes to run successfully. The result of the study is shown in Figure 51.

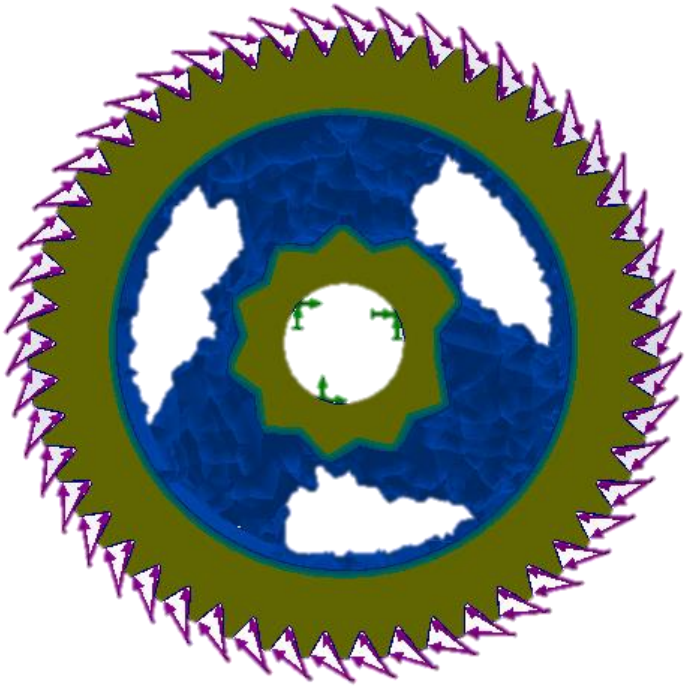

Figure 49. Entire gear 1000N topology study result front view

With a **49% reduction in mass**, the study is considered an absolute success. The optimization seems to be quite logical and feasible, with three radial components that strengthen the structure.

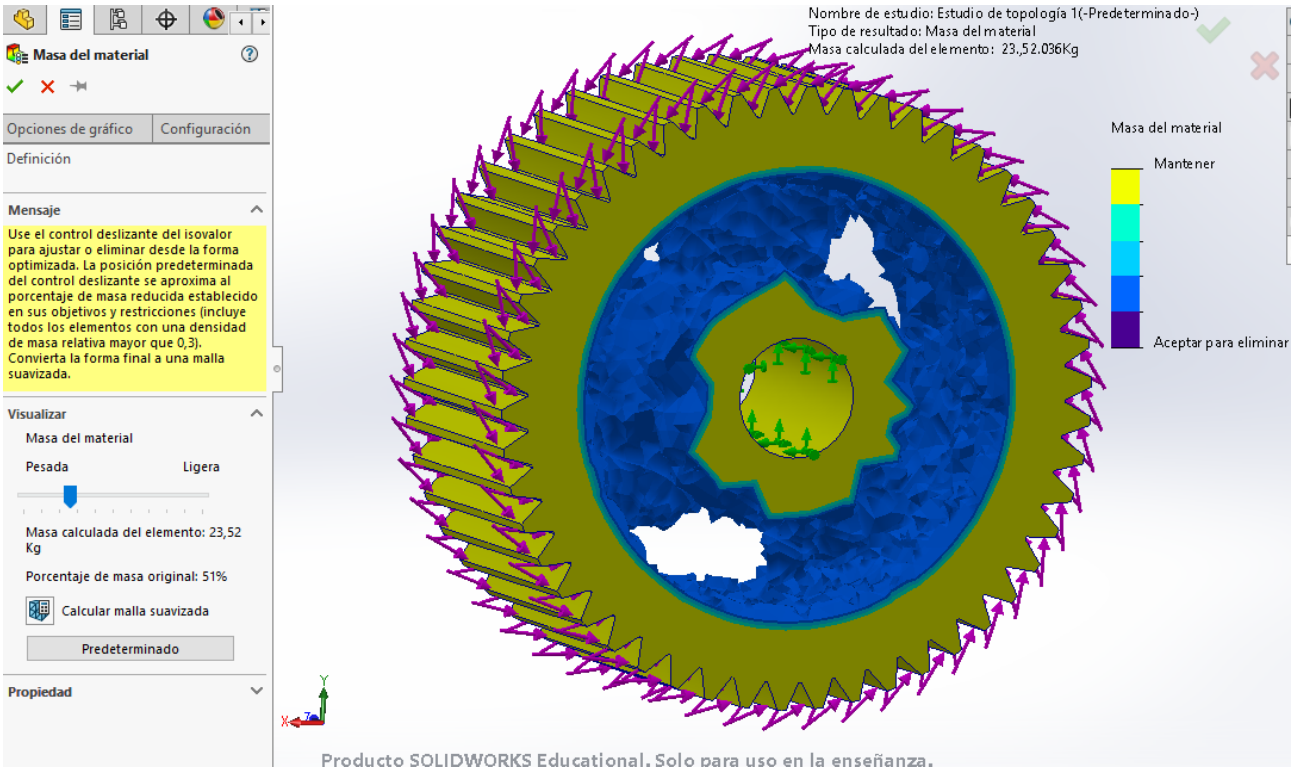

Figure 50. Entire gear 1000N topology study result 3D view

Afterwards, the smoothed mesh is created, yielding an even more uniform design. Notice how the preserved areas remain untouched, reinforcing those areas.

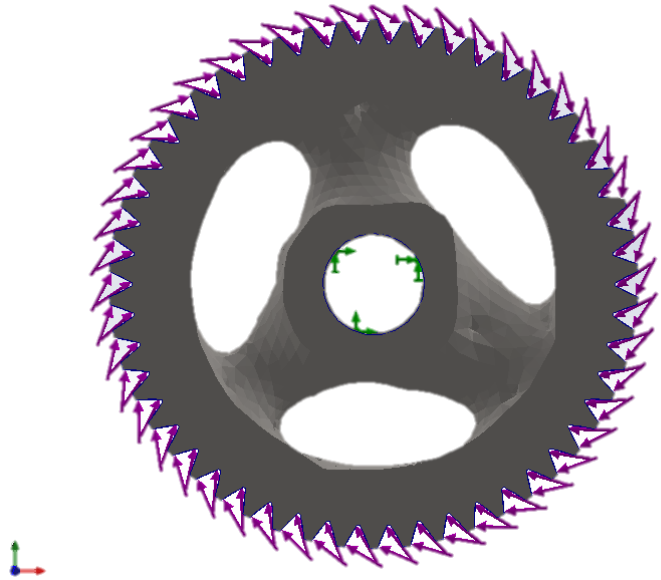

Figure 51. Entire gear 1000N topology study smoothed mesh result front view

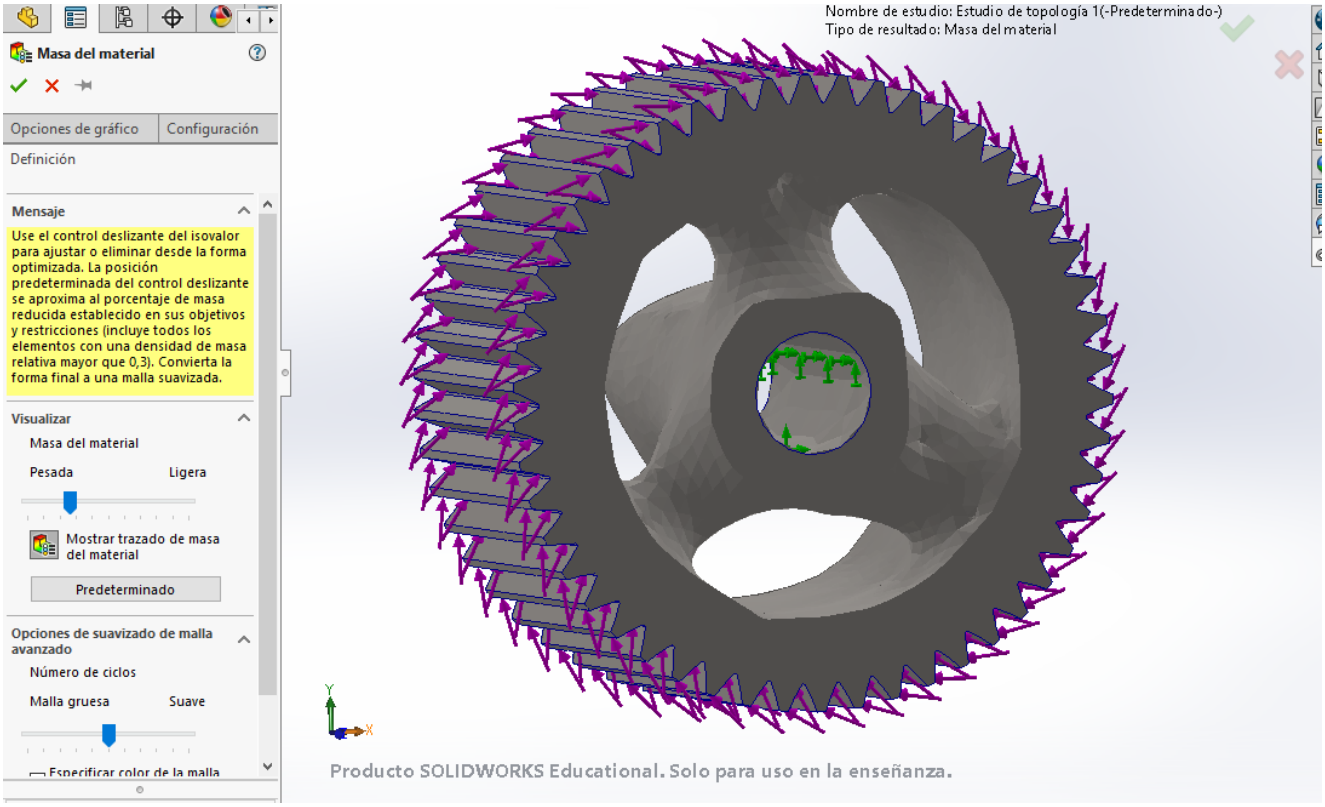

Figure 52. Entire gear 1000N topology study smoothed mesh result 3D view

Observe how the 3 radii are not display evenly with respect to the axis, see Figure 55. Two of them are aligned in the same plane, while the third one stands by itself on another plane. This arrangement possibly contributes more to the strength of the structure than if the 3 were on the same plane.

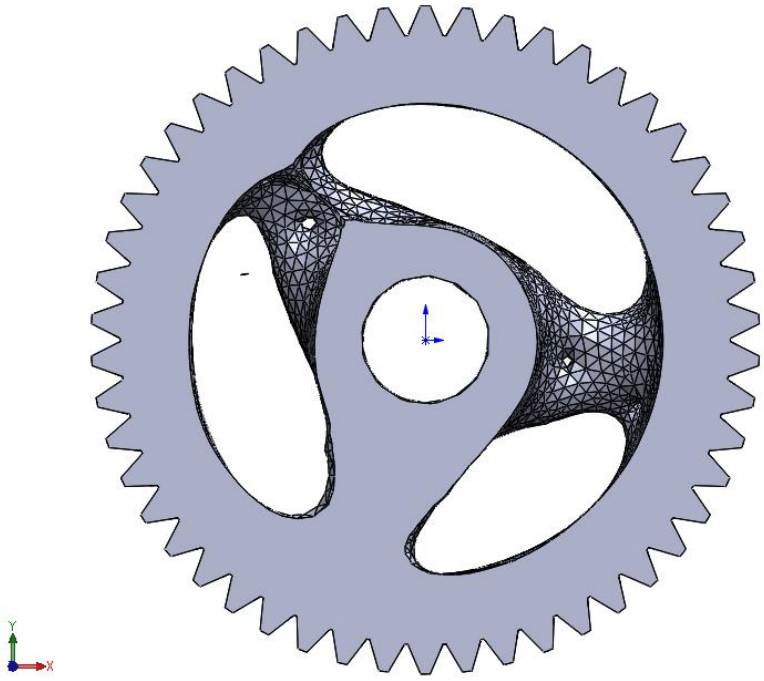

Figure 53. Entire gear 1000N topology study cross-sectional view

Gears are components that must withstand enormous stresses. Although this study with 1000N per tooth yields a satisfactory result, that figure is far from the maximum order of magnitude it could actually reach in working conditions.

A second study is carried out, this time applying 100000N per tooth in order to ensure safety in any case. The rest of the constraints remain equal.

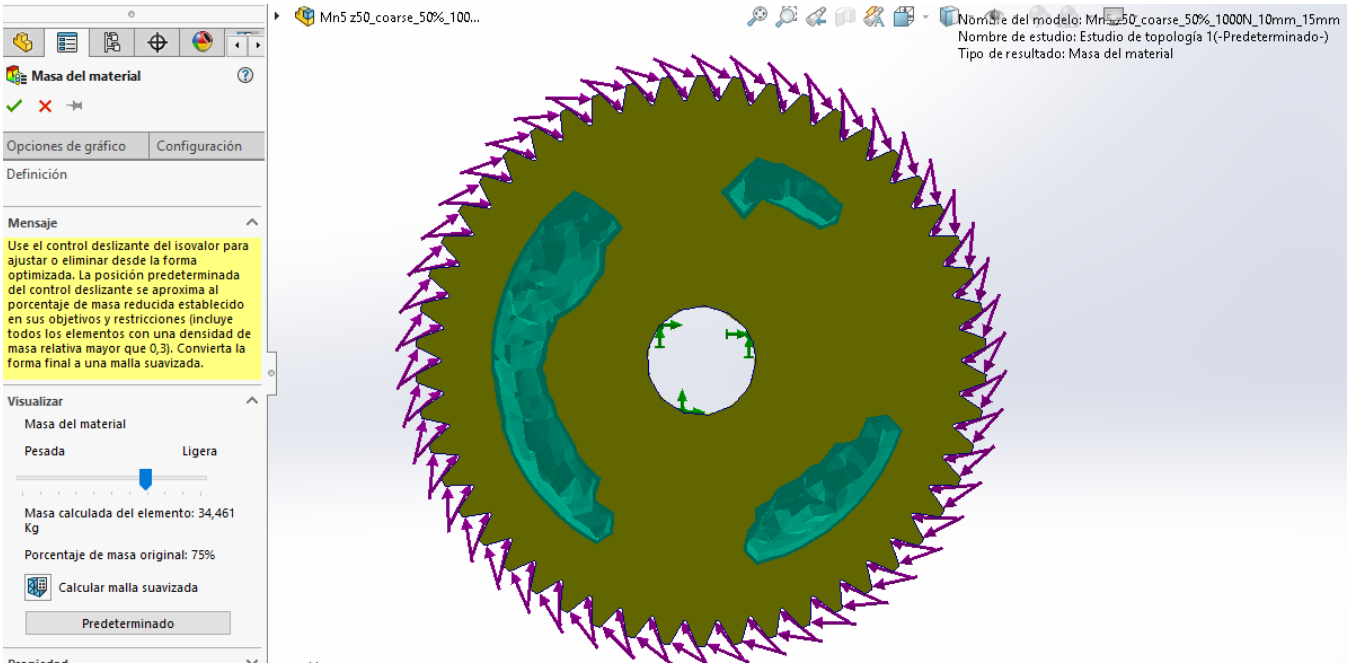

Figure 54. Entire gear 100000N topology study result front view

A **25% reduction in mass** is achieved, which can be considered a great success again, taking into account the applied force is 100 times bigger. Likewise, it can be discerned that the pattern of removing material is similar to the previous study, which reaffirms its validity.

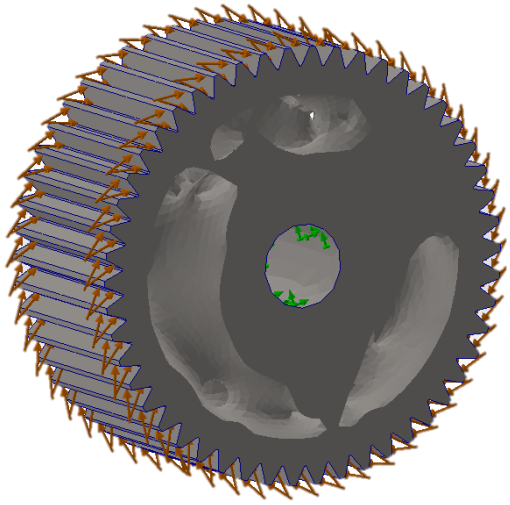

Figure 55. Entire gear 100000N topology study smoothed mesh result 3D view

As it has been verified that the optimization resulting from a study with 1000N or with 1000000N presents a similar pattern, the rest of the studies are carried out with 1000N to show a more visible result.

A quarter section

The whole gear is cut in equal parts in order to achieve different optimization designs. The simplest quartering is possibly a 90º cut in the gear. After being studied it can be recomposed as a set of 4 parts intuitively easy. As stated, the force applied on each tooth face remains at 1000N. In this case, there is no complete inner cylinder as a hole, still, the quarter cylinder remains as the fixation. Finally, the preserved areas, again the opposite face of the teeth where no force is applied are selected, both with the external part of the gear. This is because this quarter of gear is 75% smaller than the whole gear, which frees computing power, enabling going back to the constraints set in the initial stages of this study and setting the preserved areas as seen in Figure 45, with a 2mm thickness. Due to the same reason of power computation, the goal is set to reduce a 70% in mass

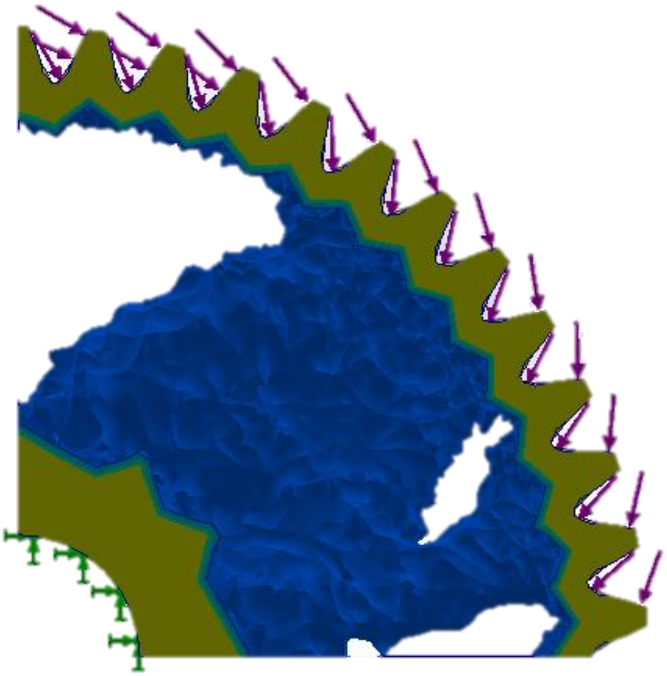

Figure 56. A quarter gear 1000N topology study result front view

The study yields a feasible design that follows the pattern of the previous study with a radii supporting the structure. Not only runs successfully, but the optimization achieves a **75% reduction in mass**, see Figure 59.

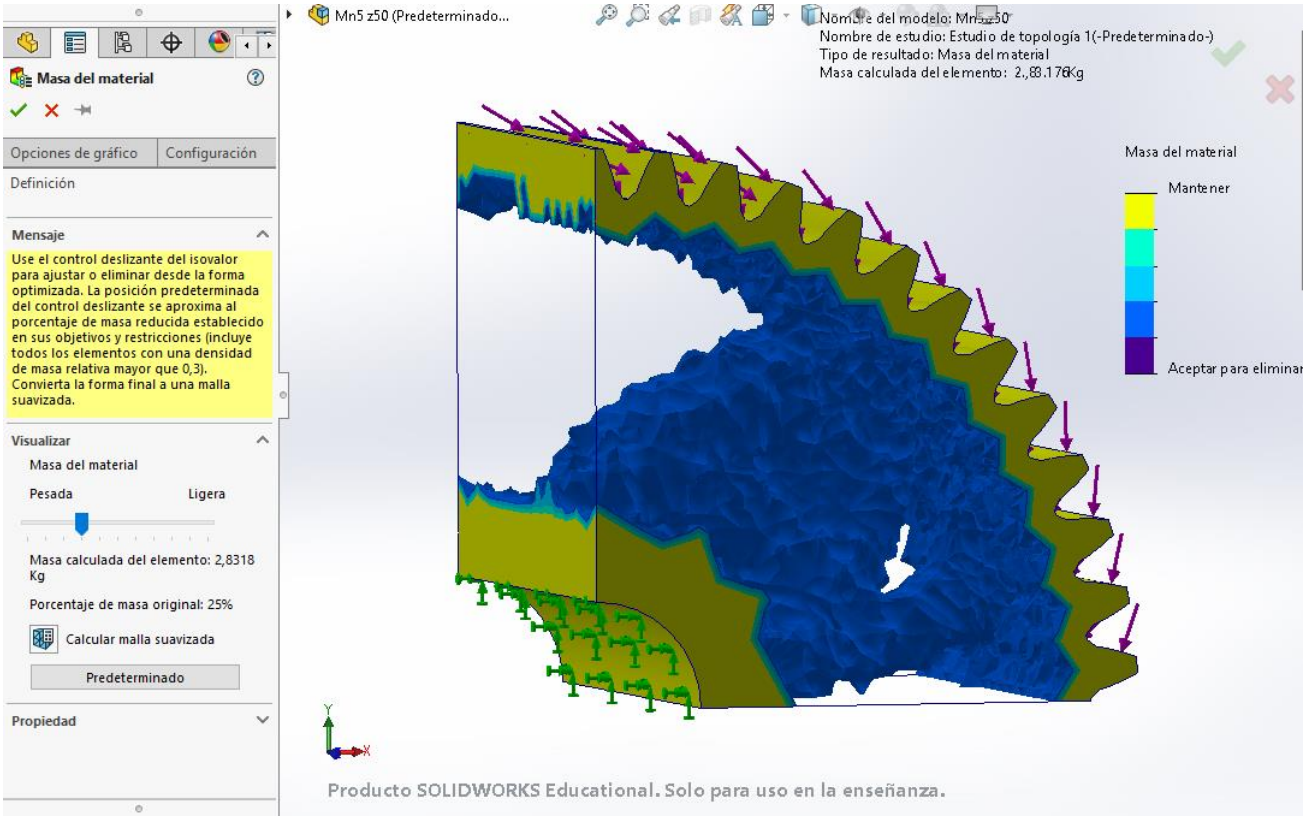

Figure 57. A quarter gear 1000N topology study result 3D view

After the designer decides among the interval of solutions the software yields, the smoothed mesh is created, and the final shape of the quarter gear is set.

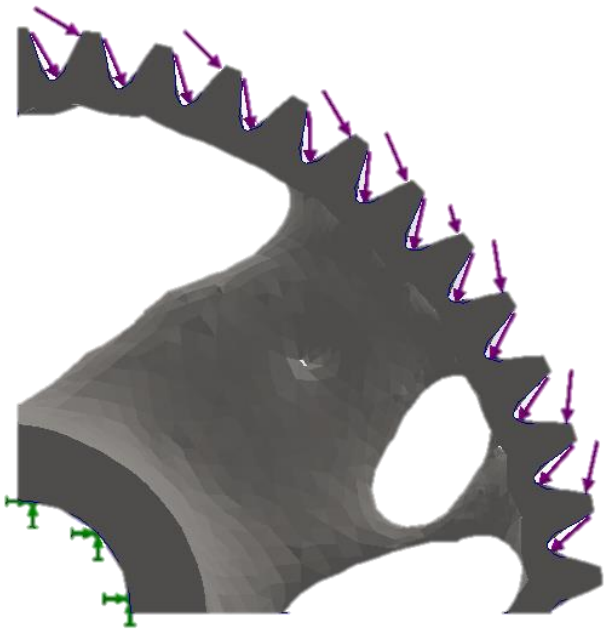

Figure 58. A quarter gear 1000N topology study smoothed mesh result front view

Observe the outer circle, much thinner than in the study of the whole gear even the applied force is the same. This probably results from the new preserved areas defined more in detail.

Figure 61 shows how the 75% optimization is achieved by the reduction in thickness of the support.

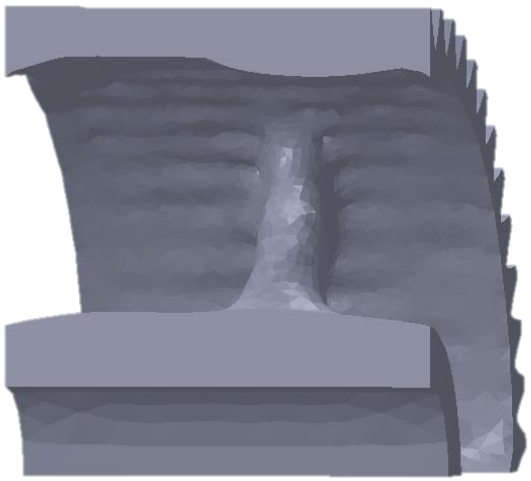

Figure 59. A quarter gear 1000N topology study smoothed mesh result 3D view

The last step in this study is extrapolating the result of a single quarter of the gear to a whole gear. This is done by creating an assembly of 4 parts. But, at this point, another problem arises. The quarter gear, although intuitive, does not cut in a number multiple of the teeth. That is why the joints of the whole assembly do not match perfectly. Nonetheless, the result is a great help by reassuring one more time that the radial geometry is a candidate when TO in gears. Besides, it shows a new possible design case of study and the possibility of making thinner preserved areas.

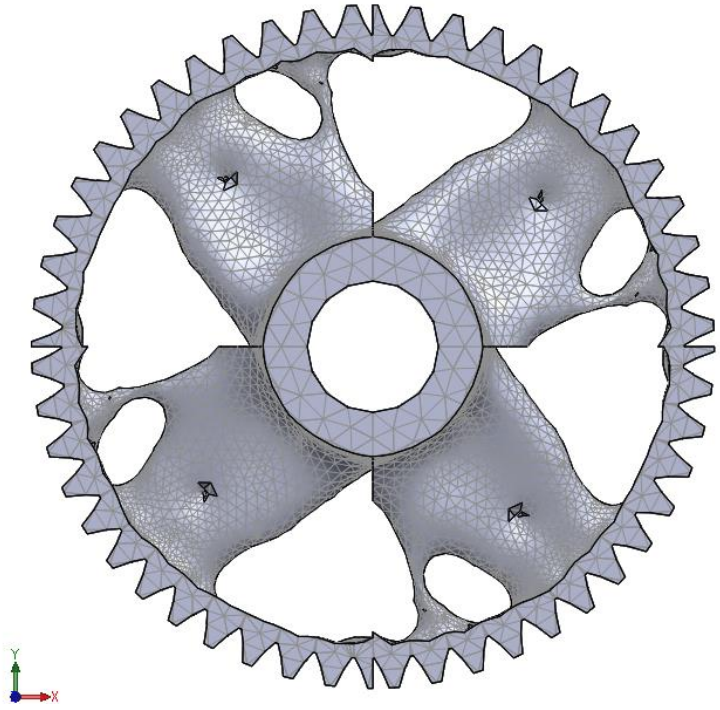

Figure 60. Entire gear composed by the assembly of four quarter optimized gears

Five teeth

Similar to the previous study, the gear can be divided into 10 parts, each composed of 5 teeth. This way, the problem that appear in the quarter gear is solved since this number of teeth is a multiple of the total, hence the final assembly would match perfectly together.

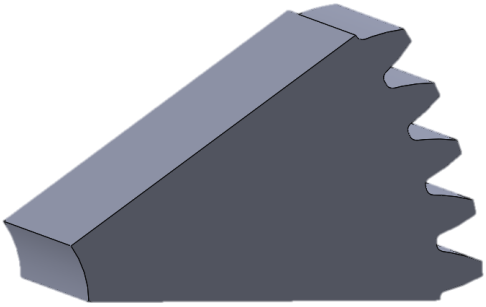

Figure 61. Five teeth of gear

The simulations in this case are run with the exact same constraints as the quarter gear. The results, however, seem to not be manufacturable nor useful. Taking a look at the front and top views, the geometry of the design does not seem to have any pattern or mechanical strength. Several different simulations are carried out with no better results. The simulation with 5 teeth seems not to be applicable to the study.

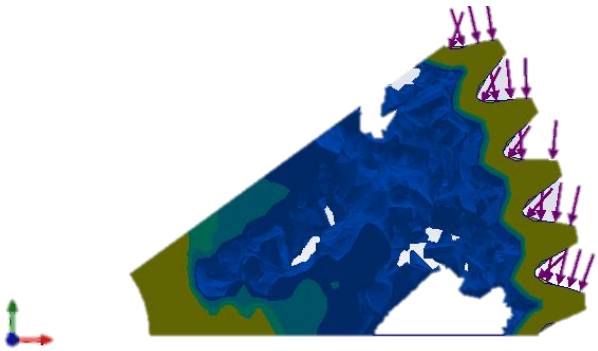

Figure 62. Five teeth of gear 1000N topology study result front view

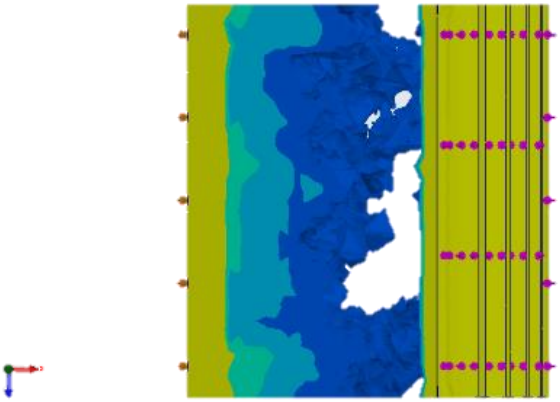

Figure 63. Five teeth of gear 1000N topology study result top view

Single tooth

Divided into 50 different parts, the gear is TO by taking into account just a single tooth at a time. All the constraints are set as usual. In this case, the power computation is not a problem and different sizes of mesh are studied, similar results are obtained though, with big-time differences in the simulations.

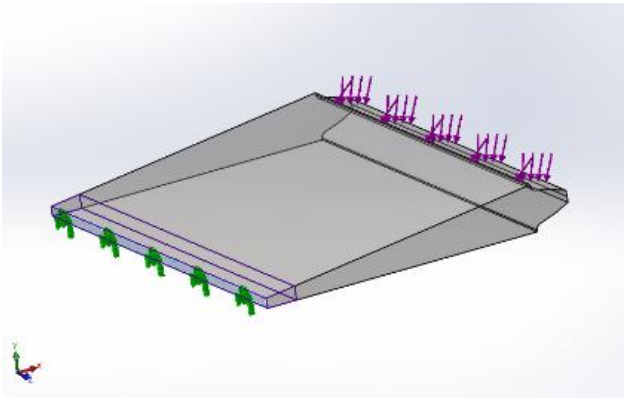

Figure 64. One tooth of gear with topology study constraints

In the light of the five teeth study, it seemed that this one would yield even more non-applicable results. It is true that a whole gear composed of fifty parts of this optimization would probably not be the most efficient TO in terms of mechanical properties and manufacturability. However, very interesting results can be observed.

First of all, a **40% reduction in mass** is very considerable even more if it is taken into account that it is achieved in such a small piece.

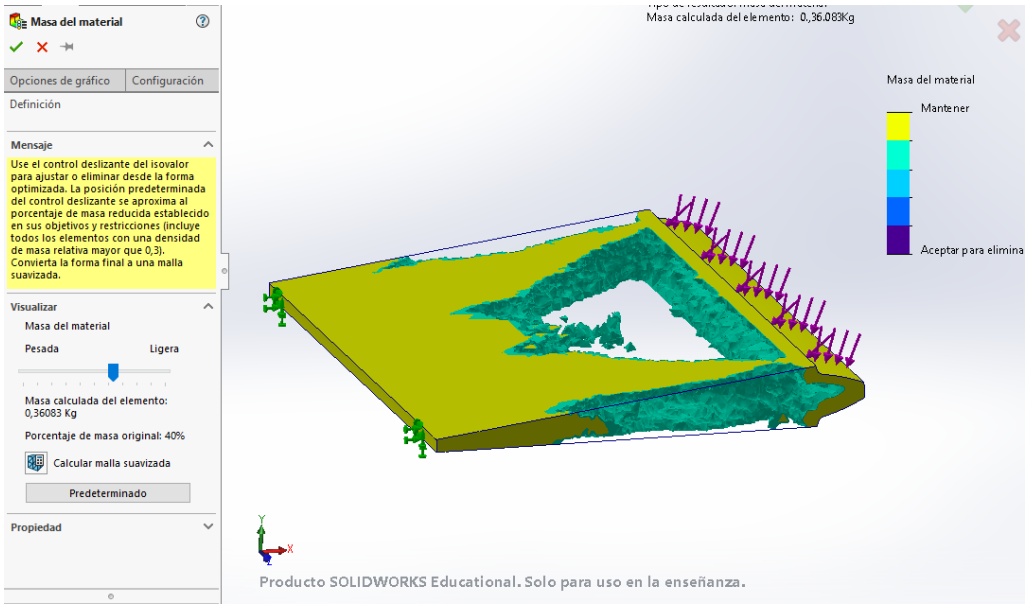

Figure 65. One tooth of gear 1000N topology study result 3D view

The second and more important observation is more visible in the front view of the smoothed mesh. The inside of the tooth itself can also be topologically optimized. Notice the removal of material is substantial, hence, in a whole gear it could make a great difference. Since the force is the same as in previous studies, it is obvious that the preserved areas used before were exaggerated.

Figure 66. One tooth of gear 1000N topology study smoothed mesh result front view

Finally, Figure 69 shows an arrangement of the inner radii not seen previously. In this case, instead of being the only support going from the inner circle to the outer, the support is divided into two axial radii, each of them going outwards to the sides of the gear.

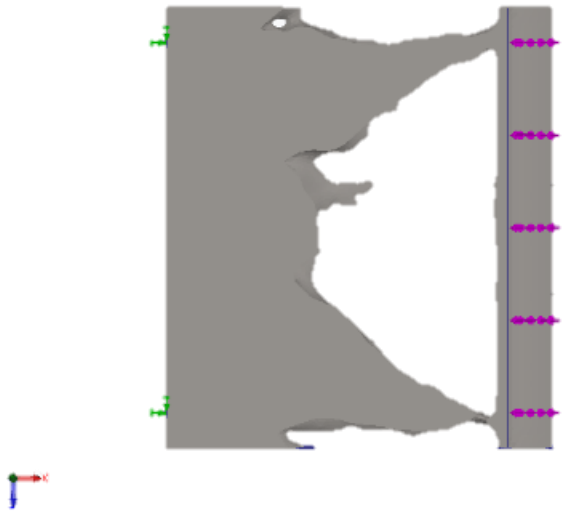

Figure 67. One tooth of gear 1000N topology study result front view

Thanks to this study of a single tooth, where the power computation has allowed to study it in more detail, this conclusion has been reached: the TO of gears is not only applicable to the interior of the gear but also to the teeth themselves. In reality, this application may not be feasible, for reasons of safety factors, however in cutting-edge applications such as the automotive or aerospace industries.

6.1.1 Results

The process of conducting TO simulations on a gear with 50 teeth has provided valuable insights on the design optimization capabilities. A comprehensive analysis was carried out through successive simulations, encompassing the entire gear, a quarter section, five teeth, and ultimately a single tooth.

The results present the optimization of the complete gear as the most promising outcome, with a substantial 49% reduction in mass achieved through a three-radii design. Besides, it is demonstrated the feasibility of manufacturing it via 3D printing. This configuration shows the potential for significant weight reduction while preserving mechanical integrity.

In contrast, the quarter gear simulation, when extrapolated to create the complete assembly, yielded a four-radius configuration, characterized by a surprising 75% reduction in mass.

The five teeth simulation concluded in a series of inconclusive outcomes that further emphasize the need of a feasible component.

The single tooth study brought into focus the intricate optimization opportunities within the interior of individual teeth.

In conclusion, the study has illuminated a wide range of possibilities for gear optimization, with a main pattern on the design composed of a number of radii, which optimal number remains for further study.

Figure 68. Entire gear 1000N topology study result 3D printed front view

6.2 Discussion

The trajectory of this study has been influenced by the computational resources available, a factor that has stimulated introspection into the implications of computation power on the outcomes. The limitation in achieving finer mesh resolutions due to the intricate size of the gear presents a void, as augmenting computational capacity may yield divergent results.

The one tooth study has demonstrated the potential for interior optimization within the teeth. Due to the constraints imposed by computational limitations a prudent preservation of thickness was adopted for the teeth in the initial studies. However, a glimpse into a more detailed optimization has illuminated the capacity for substantially improved designs, thereby showing a fruitful path for future investigations.

The optimization of the complete gear resulted in an unexpected outcome, revealing the disparity in the three radii, located in different planes. The question of whether to design radii in the same or differing planes remains for further study.

All in all, the study culminates in success, emphasizing the achievement of a feasible 49% mass reduction through TO in the Mn5 z50 gear.

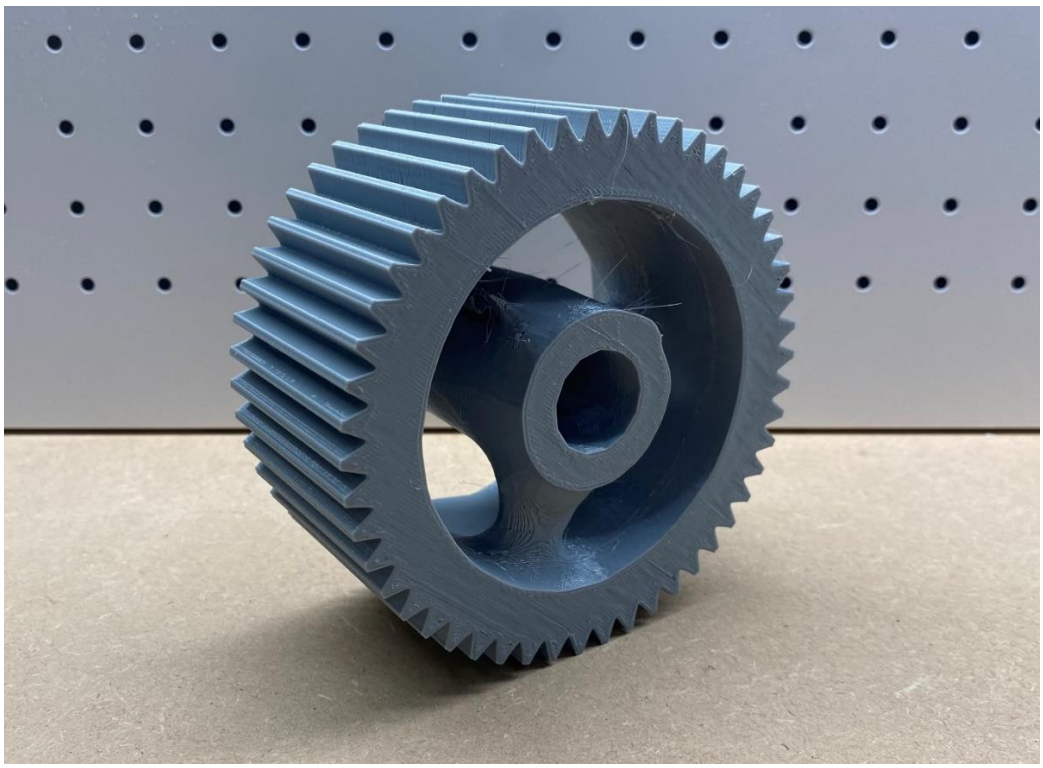

Figure 69.Entire gear 1000N topology study result 3D printed 3D view

7 Mold component (pre-form Motlle ampoule 100ml)

Piece for the study of the set VI23-0100 080023, mold for preform Motlle ampoule 100 ml.

Function inside the mold: This piece positions the plastic pre-form of the bottle inside the mold, once it is closed and prior to the blowing phase. See Appendix 6 for a better understanding of the assembly. The STEP file is provided together with the STL.

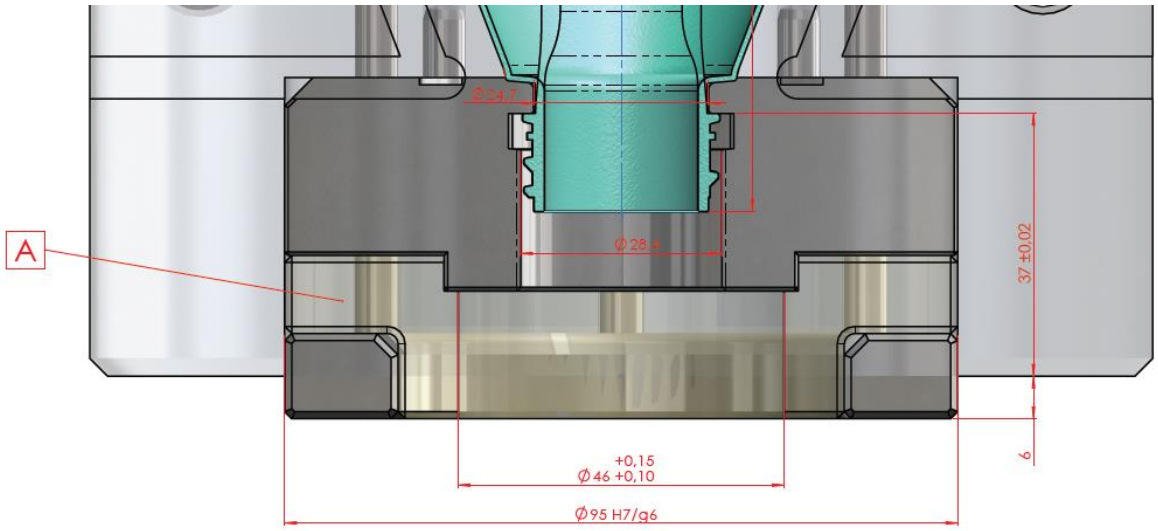

Figure 70. VI23-0100 080023 set cross-section

The part of the mold component of the study is depicted in the darker grey, see Figure 72. It serves as a fixation for the neck of the bottle to be extruded.

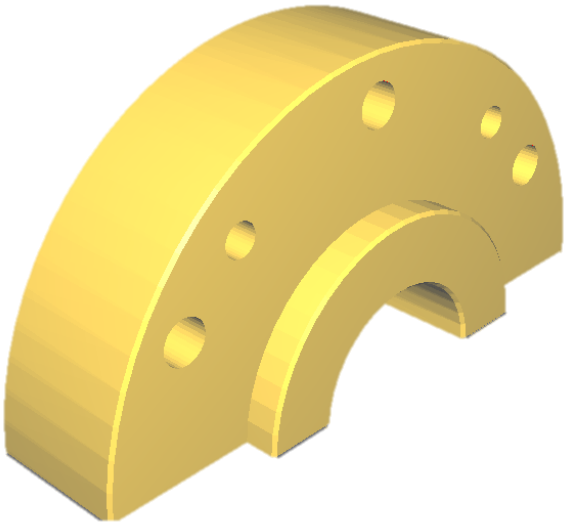

Figure 71. Mold for pre-form STL file 3D view

The material is F-552 steel and it is heat treated to increase its hardness to 54-56HRC. Also known as 1.2824 steel, is a carbon steel alloy with additions of other elements that give it certain specific properties after heat treatment. Not directly found in SolidWorks, it is defined as in Figure 74.

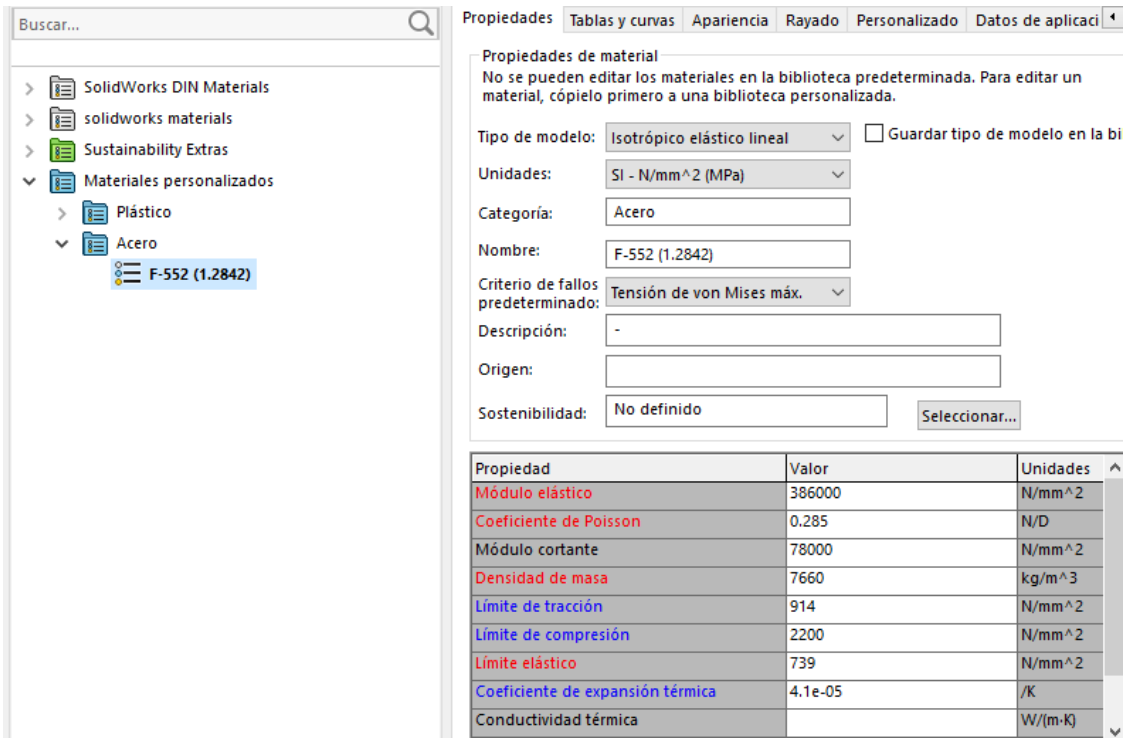

Figure 72. Steel F-552 definition in SolidWorks

7.1 Topological Optimization

The sequence steps for the study can be found in *7.3.2 TO in SolidWorks.*

The fixed parts in the mold are the two holes shown in Figure 75, where bolts are placed. The three holes left not serve for this purpose, but serve as a guide for the assembly.

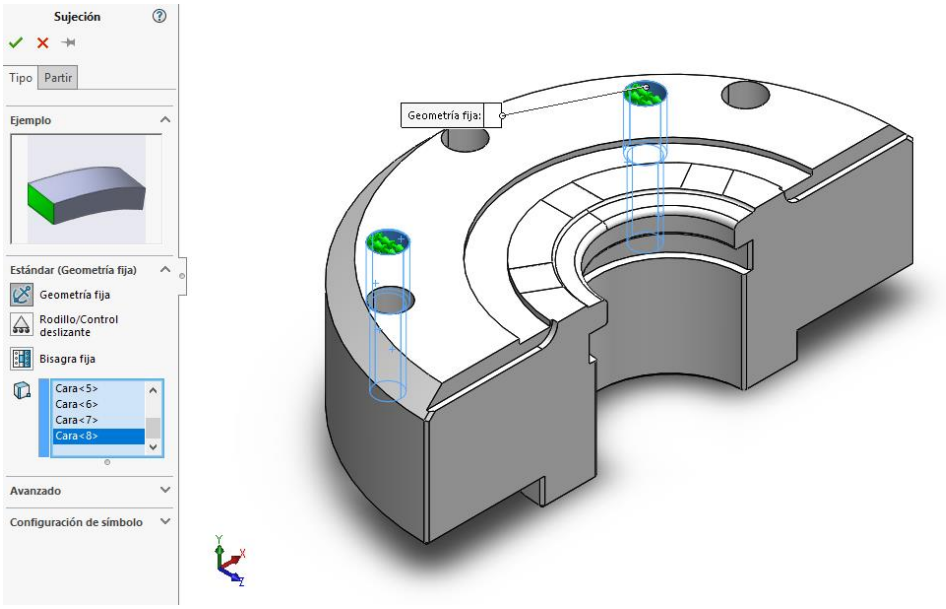

Figure 73. Mold for pre-form fixations

The mold is composed of two halves. They are symmetric, so there is only need to optimize one of them. Afterwards, they are joined by a closing force of 50 tons.

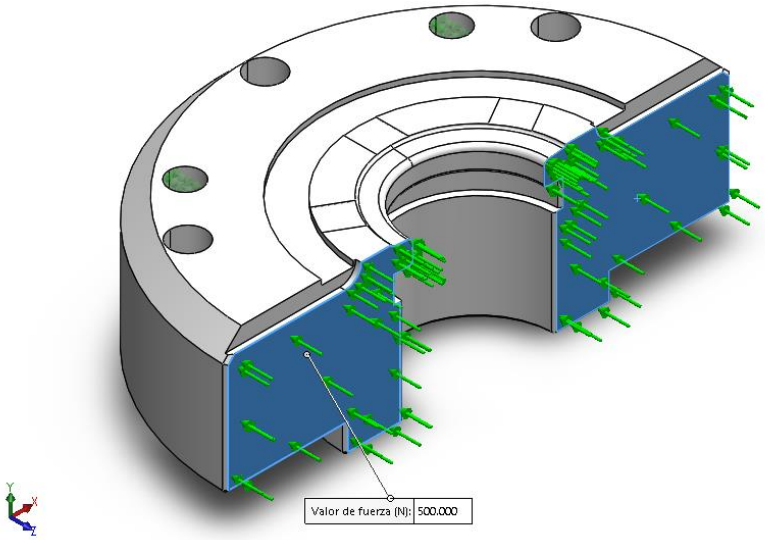

Figure 74. Mold for pre-form 50 tons closing forces

The mold is in contact with other pieces inside the assembly. This applies a force on the up and down faces, much smaller than the closing force. In the scope of this optimization, this vertical force is the variable subject to change in case the resulting design is not satisfactory. Initially, it is set as 10kN.

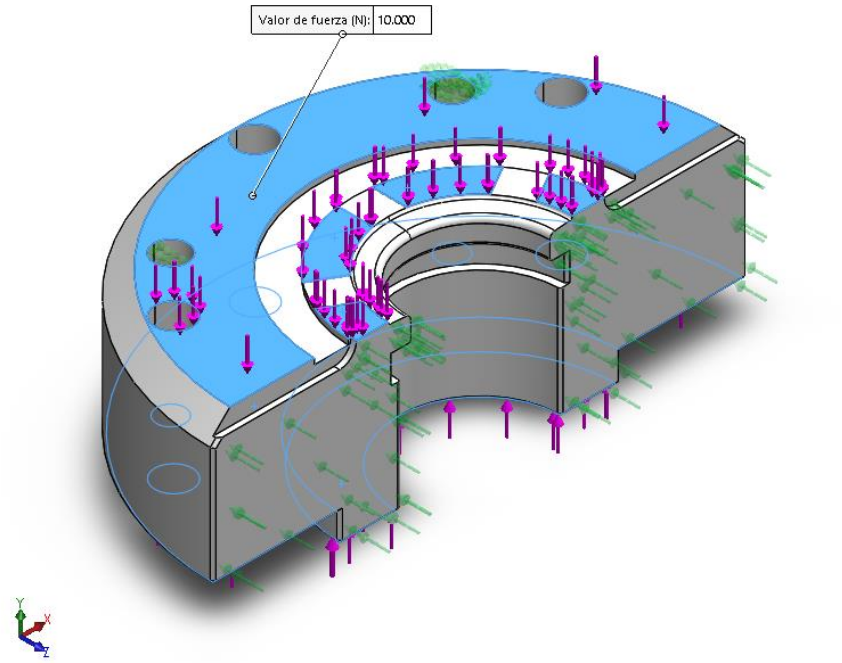

Figure 75. Mold for pre-form vertical forces top view

Notice not all the above surfaces are subjected to this force. This is because they are in different planes located at different heights, so the lowest ones do not see the force.

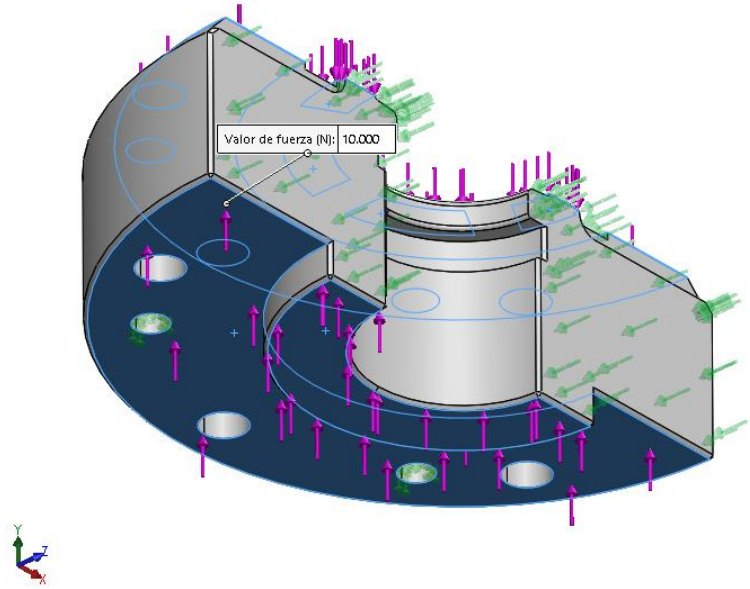

Figure 76. Mold for pre-form vertical forces bottom view

The last force in the component is a pressure, applied where the neck of the bottle is attached. Here, a vertical stroke of air inflates the plastic creating the bottle-shape. The air has a pressure of 40 bar.

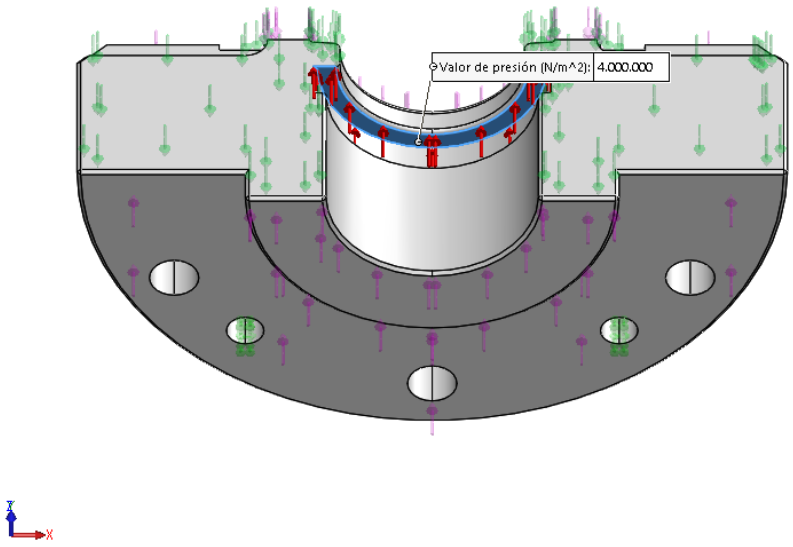

Figure 77. Mold for pre-form 40 bar pressure

The three forces applied to the mold are shown in a cross-sectional view in Figure 80. Color red arrows represent the pressure, the green ones are the closing forces, and the purple ones the vertical forces.

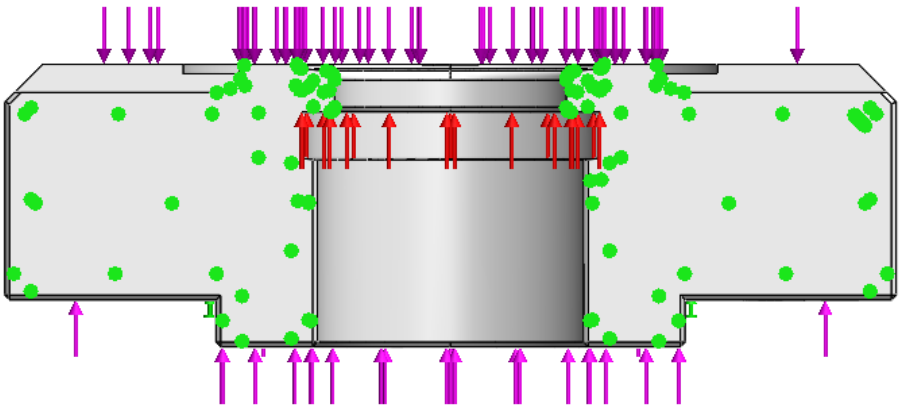

Figure 78. Mold for pre-form forces cross-section view

After defining all the constraints, a fine mesh is created. Unlike in the case of the gear, the computer has enough power to carry out this simulation, probably due to the smaller size of the component. For detailed properties of the mesh see Appendix 6.

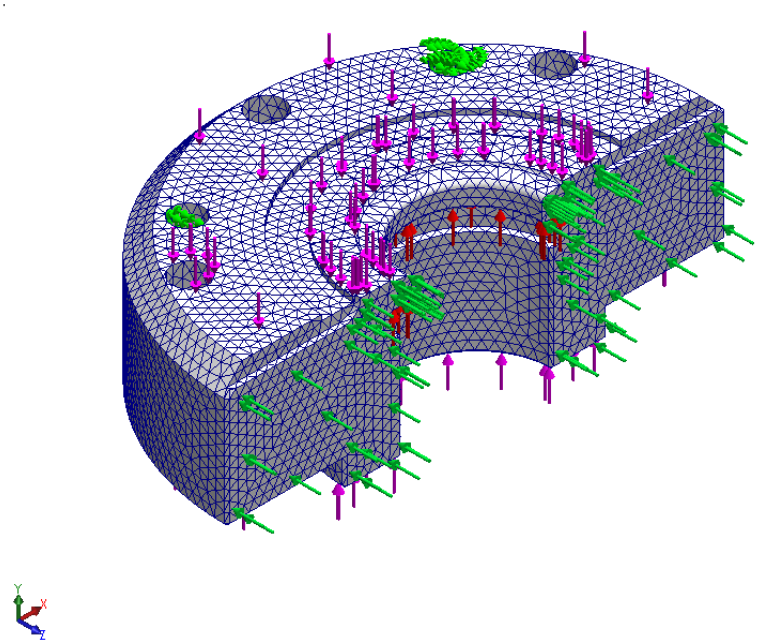

Figure 79. Mold for pre-form topology study mesh

After the simulation runs successfully, an 11% reduction in weight is achieved. However, this result is unwanted since some critical surfaces have been removed, see Figure 82. Still, some conclusions can be drawn. Notice in the cleft of the upper surface, which served no purpose, some little holes of material are removed. This remains listed as a case study for further research.

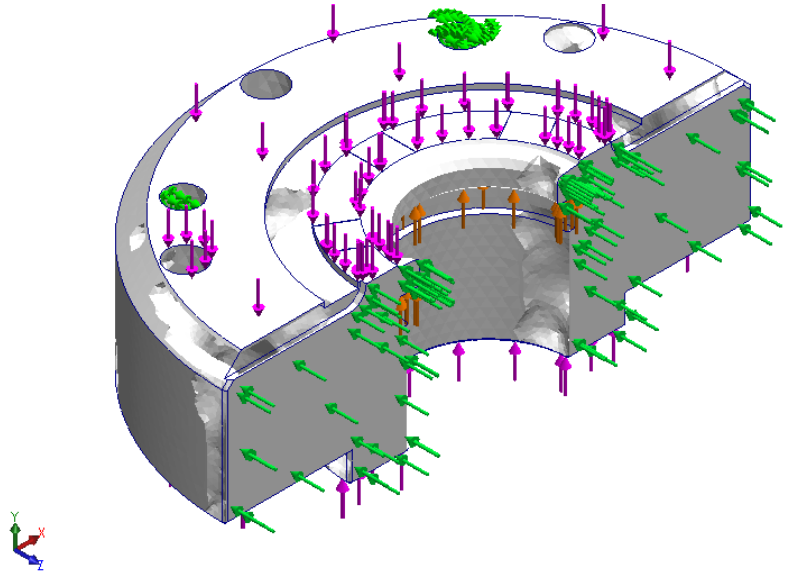

Figure 80. Mold for pre-form topology study result with no preserved regions

In order to solve this preserved areas are added with 2mm thickness. These are the three holes that serve as a guide for the assembly, as well as the interior surfaces where the piece is positioned.

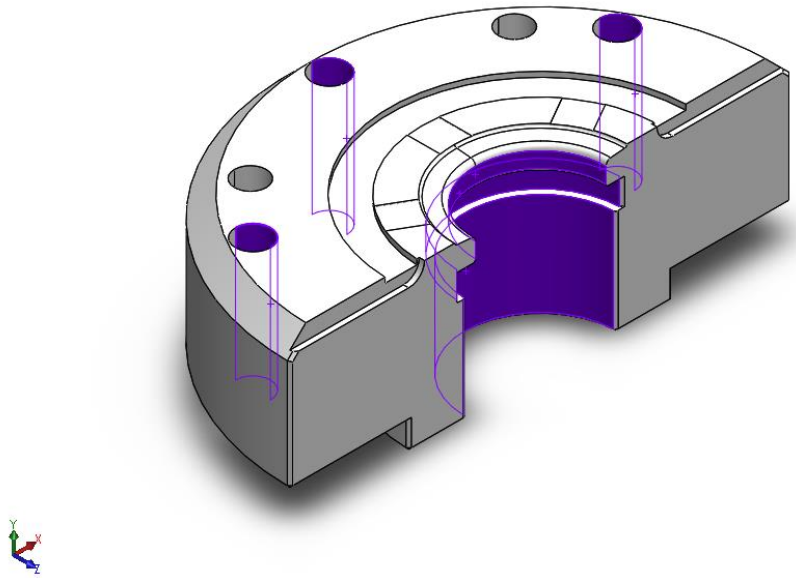

Figure 81. Mold for pre-form preserved regions

The simulation runs successfully again, yielding one more time an optimization of an 11% in mass. However, in this case, the design achieved seems to be feasible and does not interfere with any critical surface, hence seems to be a satisfactory result.

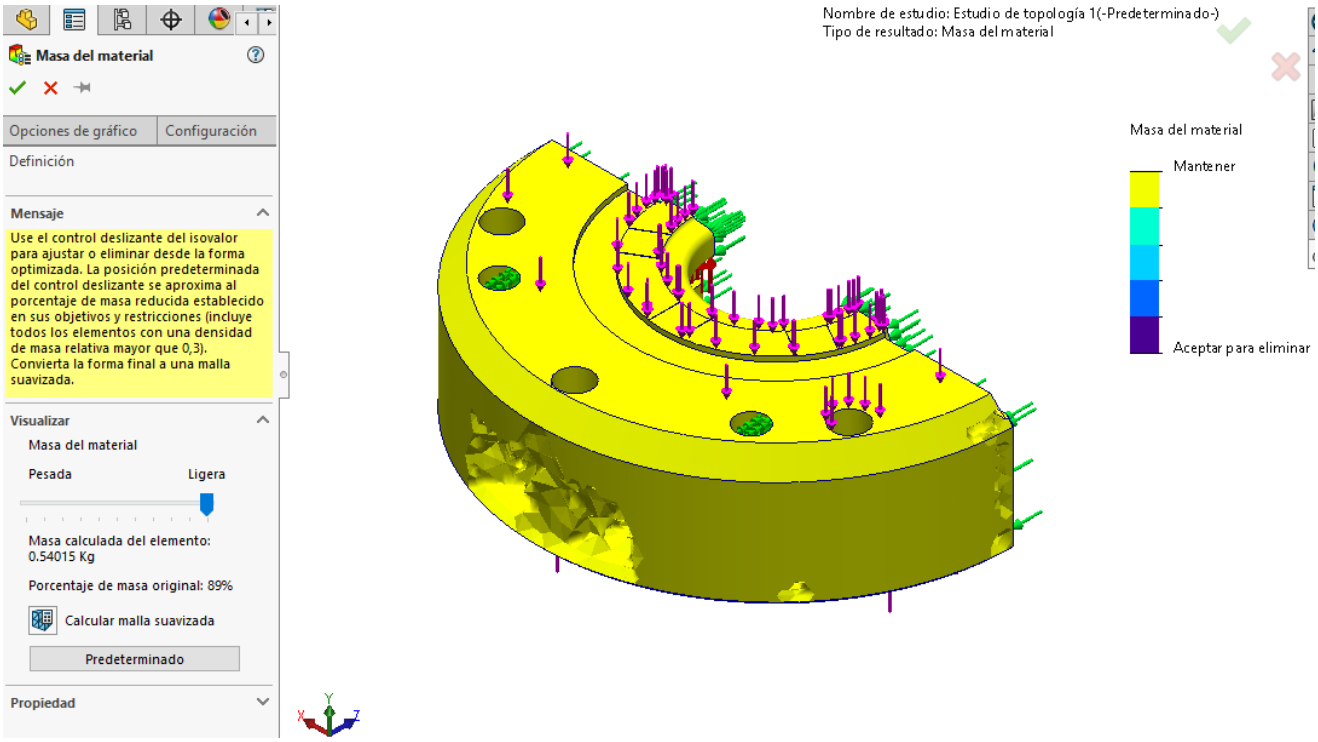

Figure 82. Mold for pre-form 11% optimization

The smoothed mesh is computed in order to see a finer result. As seen in Figure 85, most of the material is removed from the back part of the piece. Notice though, how the algorithm respects the preserved areas by keeping some material around the guide hole, Figure 86.

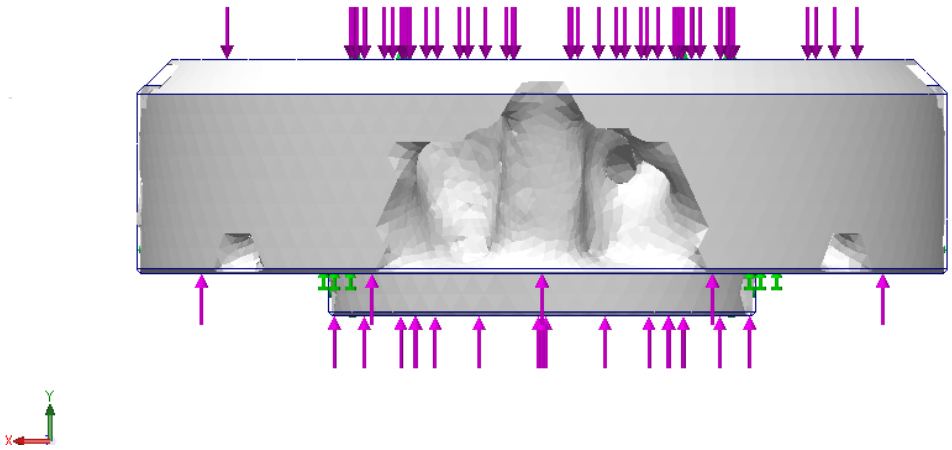

Figure 83. Mold for pre-form 11% optimization smoothed mesh front view

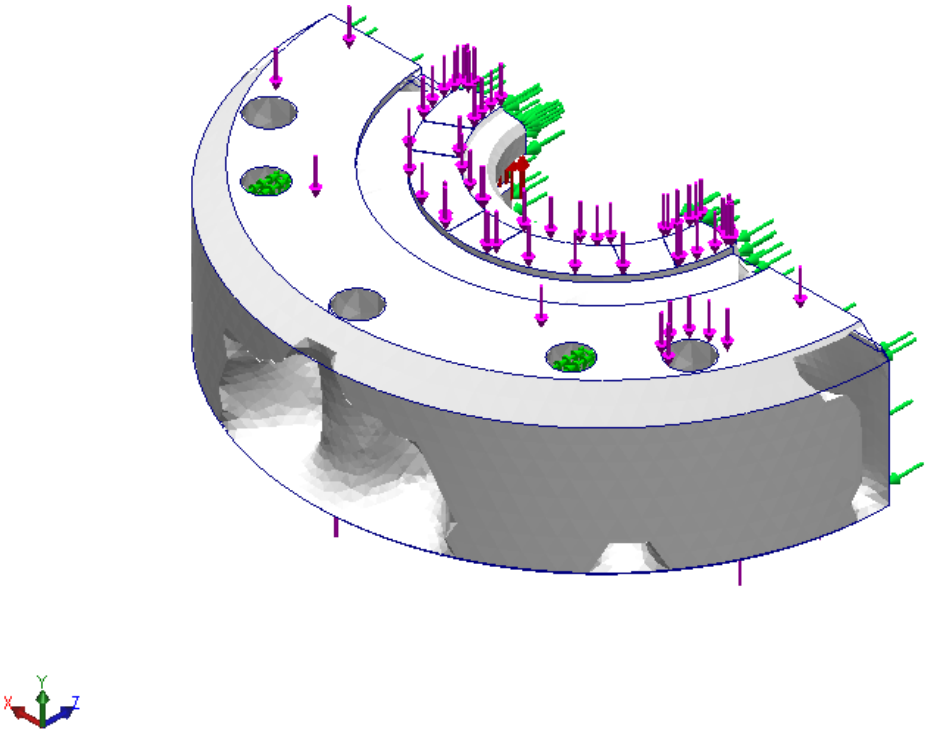

Figure 84. Mold for pre-form 11% optimization smoothed mesh 3D view

Different studies are carried out modifying the vertical force. However, all of them lead to a result where the maximum TO achievable is an 11%. Figure 87 shows the result when removing completely the vertical force.

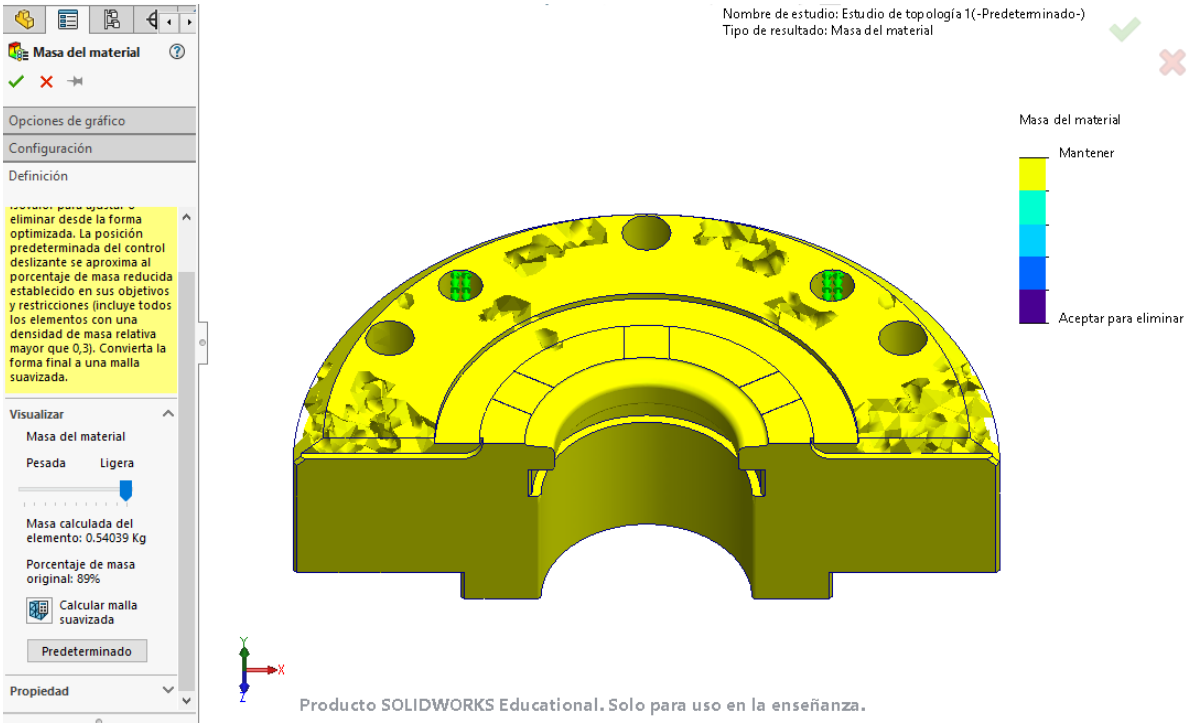

Figure 85. Mold for pre-form topology study results with no vertical forces

The result of the study with no vertical forces yields one more time an 11% optimization. It can be reached to the conclusion that no further optimization is possible with the constraints this component must deal with in working conditions, which are the 40 bars pressure and the closing force of 50 tons.

The geometry of this last simulation is not valid though, since the upper surface has some voids. For further studies this surface should be set as a preserved area, since it makes contact with other pieces.

7.1.1 Results

The TO of the mold component has been a success, representing a significant achievement in engineering innovation. With a notable 11% optimization, this study highlights the efficacy of TO in enhancing the design of complex components critical to manufacturing processes.

It has been essential the preserve of areas in direct contact with other components within the assembly. This preservation of critical features ensures the components' structural integrity and compatibility within the larger assembly context.

It is pertinent to acknowledge that rigorous exploration was undertaken to surpass the attained 11% optimization mark. However, the trajectory encountered limitations, potentially attributed to the formidable 50 ton closing force. This constraint influences the optimization potential beyond the established threshold

Finally, the subsequent 3D printing of the optimized design serves as a testament to the feasibility and manufacturability of the achieved outcome.

Figure 86. Mold component topologically optimized design 3D printed with PLA

7.2 Discussion

The research surrounding the TO of the mold component designed for bottle prefabrication offers valuable insights into the engineering challenges and potential solutions encountered. The intrinsic constraint imposed by the 50 ton closing force influences the extent of attainable optimization. This formidable force limits the boundary of material removal to an 11%, even though several optimization attempts were carried out with the aim of exceeding that threshold. Certain designs proved unfeasible, however, it is noteworthy that this optimization was consistently achieved, what highlights the inherent optimization capability of this particular component.

Exploring potential feasible designs for an optimized solution can lead to the following conclusion. A pattern can be observed in the removal of material used by the algorithm. It either subtracted material from the top surface cleft or from the rear part of the piece. Combining both material removal strategies could potentially yield a more comprehensive solution. The study of leveraging the strengths of both strategies remains for further investigation.

Finally, the feasibility of this mold part was demonstrated by a successful 3D printing with PLA. Still, there exists space for future investigation, evaluating the manufacturability of it within the context of metal 3D printing.

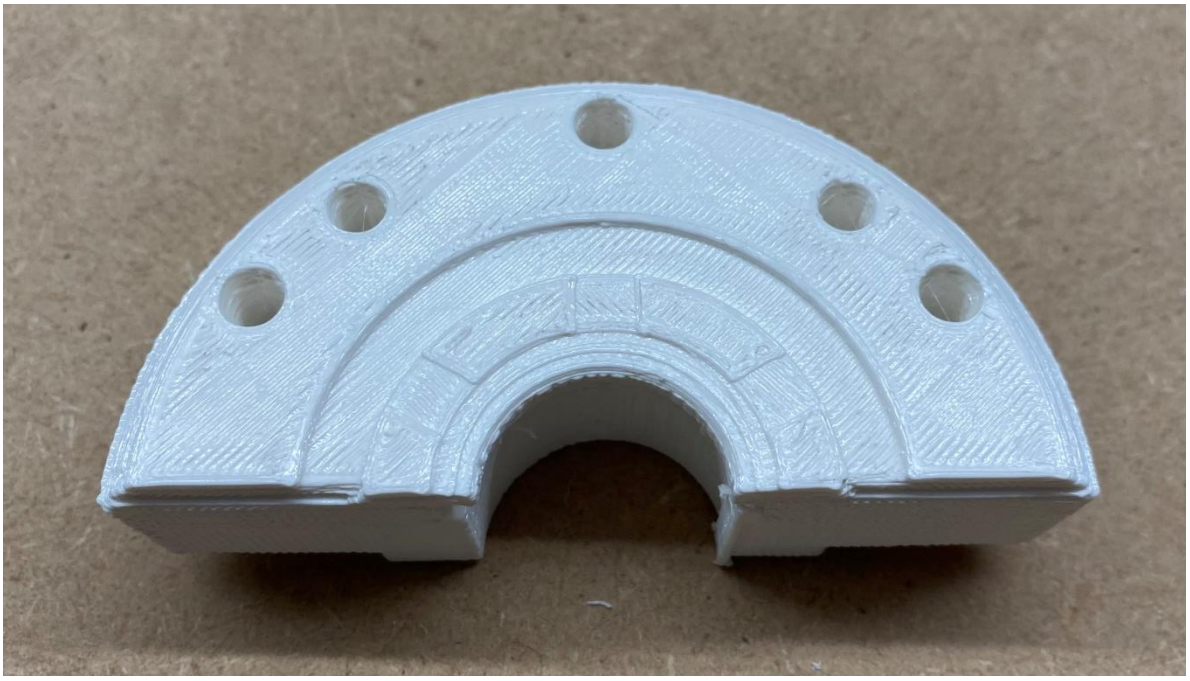

Figure 87. Mold component 3D printed with PLA

8 Conclusions

The present Thesis constitutes a comprehensive exploration into the symbiotic relationship between topology optimization (TO) and 3D printing when applied to metal components. Within this study, three distinct yet interconnected branches unfold, each aiming the efforts to the objective of achieving maximum mass reduction while preserving the structural integrity of the optimized components.

The first branch of investigation concerns the meticulous design and subsequent topological optimization of tensile traction test specimens, concluding with their 3D printing. A remarkable degree of optimization, reaching up to 52.7% is achieved. This resounding success underscores the profound capability of TO to effectuate significant improvements in component efficiency. As this branch of research progresses, the upcoming phase involves the experimental validation of these optimized designs through tensile testing.

The second branch of study ventured into the realm of gear optimization, focusing on a component from the distinguished ENPA company. Despite encountering computational limitations, this exploration yielded notable insights and results. An impressive 49% optimization was realized through the implementation of a three-radius design. Besides, this outcome looks enriched by the proven feasibility of the design, achieved through 3D printing. Moreover, an alternative design emerges incorporating a four-radii design, with an astonishing 75% mass optimization. This sheds light on the intriguing dynamics of radius count and their arrangement within gear designs, which remains for further investigation. Another quest for further advancements involves the use of advanced computation programs with more computational power to unveil divergent results.

The third and final branch of research unfolds through the optimization of a mold component belonging to the pharmaceutical sector. Achieving a noticeable 11% optimization, this highlights the intricate balance required between TO efficacy and the tangible constraints imposed by real-world operating conditions. Despite intensive efforts to surpass this threshold, the study reveals the complexities stated by the external forces and pressures experienced by the component. As the investigation unfolds, the next phase involves the transition to metal 3D printing.

Collectively, this thesis stands as evidence of the progressive evolution of engineering innovation, where TO and 3D printing converge to redefine conventional paradigms. As engineering boundaries continue to expand, this study shows the potential to be found in component redesign through TO.

9 References

[1] T. D. Ngo, A. Kashani, G. Imbalzano, K. T. Q. Nguyen, y D. Hui, «Additive manufacturing (3D printing): A review of materials, methods, applications and challenges», *Composites Part B: Engineering*, vol. 143, pp. 172-196, jun. 2018, doi: 10.1016/j.compositesb.2018.02.012.

[2] X. Wang, M. Jiang, Z. Zhou, J. Gou, y D. Hui, «3D printing of polymer matrix composites: A review and prospective», *Composites Part B: Engineering*, vol. 110, pp. 442-458, feb. 2017, doi: 10.1016/j.compositesb.2016.11.034.

[3] D. D. Gu, W. Meiners, K. Wissenbach, y R. Poprawe, «Laser additive manufacturing of metallic components: materials, processes and mechanisms», *International Materials Reviews*, vol. 57, n.º 3, pp. 133-164, may 2012, doi: 10.1179/1743280411Y.0000000014.

[4] L. Thijs, F. Verhaeghe, T. Craeghs, J. V. Humbeeck, y J.-P. Kruth, «A study of the microstructural evolution during selective laser melting of Ti–6Al–4V», *Acta Materialia*, vol. 58, n.º 9, pp. 3303-3312, may 2010, doi: 10.1016/j.actamat.2010.02.004.

[5] L. E. Murr *et al.*, «Metal Fabrication by Additive Manufacturing Using Laser and Electron Beam Melting Technologies», *Journal of Materials Science & Technology*, vol. 28, n.º 1, pp. 1-14, ene. 2012, doi: 10.1016/S1005-0302(12)60016-4.

[6] F. P. W. Melchels, J. Feijen, y D. W. Grijpma, «A review on stereolithography and its applications in biomedical engineering», *Biomaterials*, vol. 31, n.º 24, pp. 6121-6130, ago. 2010, doi: 10.1016/j.biomaterials.2010.04.050.

[7] D.-G. Ahn, «Directed Energy Deposition (DED) Process: State of the Art», *Int. J. of Precis. Eng. and Manuf.-Green Tech.*, vol. 8, n.º 2, pp. 703-742, mar. 2021, doi: 10.1007/s40684-020-00302-7.

[8] M. Ziaee y N. B. Crane, «Binder jetting: A review of process, materials, and methods», *Additive Manufacturing*, vol. 28, pp. 781-801, ago. 2019, doi: 10.1016/j.addma.2019.05.031.

[9] E. Atzeni y A. Salmi, «Economics of additive manufacturing for end-usable metal parts», *Int J Adv Manuf Technol*, vol. 62, n.º 9, pp. 1147-1155, oct. 2012, doi: 10.1007/s00170-011-3878-1.

[10] J. Nandy, H. Sarangi, y S. Sahoo, «A Review on Direct Metal Laser Sintering: Process Features and Microstructure Modeling», *Lasers Manuf. Mater. Process.*, vol. 6, n.º 3, pp. 280-316, sep. 2019, doi: 10.1007/s40516-019-00094-y.

[11] A. Mohammadhosseini, S. H. Masood, D. Fraser, y M. Jahedi, «Dynamic compressive behaviour of Ti-6Al-4V alloy processed by electron beam melting under high strain rate loading», *Adv. Manuf.*, vol. 3, n.º 3, pp. 232-243, sep. 2015, doi: 10.1007/s40436-015-0119-0.

[12] Osezua Ibhadode, Zhidong Zhang, Jeffrey Sixt, Ken M. Nsiempba, Joseph Orakwe, Alexander Martinez-Marchese, Osazee Ero, Shahriar Imani Shahabad, Ali Bonakdar & Ehsan Toyserkani (2023) «Topology optimization for metal additive manufacturing: current trends, challenges, and future outlook, Virtual and Physical Prototyping », 18:1, e2181192, doi: 10.1080/17452759.2023.2181192

[13] T. P. Ribeiro, L. F. A. Bernardo, y J. M. A. Andrade, «Topology Optimization in Structural Steel Design for Additive Manufacturing», *Applied Sciences*, vol. 11, n.º 5, Art. n.º 5, ene. 2021, doi: 10.3390/app11052112.

[14] X. Wang *et al.*, «Topological design and additive manufacturing of porous metals for bone scaffolds and orthopaedic implants: A review», *Biomaterials*, vol. 83, pp. 127-141, 2016, doi: 10.1016/j.biomaterials.2016.01.012.

[15] G. Wang *et al.*, «Design and Compressive Behavior of Controllable Irregular Porous Scaffolds: Based on Voronoi-Tessellation and for Additive Manufacturing», *ACS Biomaterials Science and Engineering*, vol. 4, n.º 2, pp. 719-727, 2018, doi: 10.1021/acsbiomaterials.7b00916.

[16] J. Robbins, S. J. Owen, B. W. Clark, y T. E. Voth, «An efficient and scalable approach for generating topologically optimized cellular structures for additive manufacturing», *Additive Manufacturing*, vol. 12, pp. 296-304, 2016, doi: 10.1016/j.addma.2016.06.013.

[17] A. M. Mirzendehdel y K. Suresh, «Support structure constrained topology optimization for additive manufacturing», *CAD Computer Aided Design*, vol. 81, pp. 1-13, 2016, doi: 10.1016/j.cad.2016.08.006.

[18] S. M. Giannitelli, D. Accoto, M. Trombetta, y A. Rainer, «Current trends in the design of scaffolds for computer-aided tissue engineering», *Acta Biomaterialia*, vol. 10, n.º 2, pp. 580-594, 2014, doi: 10.1016/j.actbio.2013.10.024.

[19] N. Gardan y A. Schneider, «Topological optimization of internal patterns and support in additive manufacturing», *Journal of Manufacturing Systems*, vol. 37, pp. 417-425, 2015, doi: 10.1016/j.jmsy.2014.07.003.

[20] J. Gardan, «Additive manufacturing technologies: State of the art and trends», *International Journal of Production Research*, vol. 54, n.º 10, pp. 3118-3132, 2016, doi: 10.1080/00207543.2015.1115909.

[21] H. Chen, Q. Han, C. Wang, Y. Liu, B. Chen, y J. Wang, «Porous Scaffold Design for Additive Manufacturing in Orthopedics: A Review», *Frontiers in Bioengineering and Biotechnology*, vol. 8, 2020, doi: 10.3389/fbioe.2020.00609.

[22] A. M. Aliyi y H. G. Lemu, «Case study on topology optimized design for additive manufacturing», *IOP Conf. Ser.: Mater. Sci. Eng.*, vol. 659, n.º 1, p. 012020, oct. 2019, doi: 10.1088/1757-899X/659/1/012020.

[23] «Topology Optimization - an overview | ScienceDirect Topics». https://www.sciencedirect.com/topics/computer-science/topology-optimization (accedido 23 de agosto de 2023).

[24] P. Keane, «Performing Topology Optimization: A Step-by-Step Guide», *Engineers Rule*, 29 de enero de 2018. https://www.engineersrule.com/performing-topology-optimization-step-step-guide/ (accedido 23 de agosto de 2023).

[25] Y. Wang, F. Chen, y M. Y. Wang, «Concurrent design with connectable graded microstructures», *Computer Methods in Applied Mechanics and Engineering*, vol. 317, pp. 84-101, 2017, doi: 10.1016/j.cma.2016.12.007.

[26] «Filamento 3D PLA - Diámetro 1.75mm - Bobina 1kg - Negro», *EcoPrinter*. https://ecoprinter.es/bobina-filamento-3d/4304-filamento-3d-pla-diametro-175mm-bobina-1kg-negro-8435490624061.html (accedido 23 de agosto de 2023).

[27] A. Özen, D. Auhl, C. Völlmecke, J. Kiendl, y B. E. Abali, «Optimization of Manufacturing Parameters and Tensile Specimen Geometry for Fused Deposition Modeling (FDM) 3D-Printed PETG», *Materials*, vol. 14, n.º 10, Art. n.º 10, ene. 2021, doi: 10.3390/ma14102556.

[28] A. A. Zadpoor, «Additively manufactured porous metallic biomaterials», *Journal of Materials Chemistry B*, vol. 7, n.º 26, pp. 4088-4117, 2019, doi: 10.1039/c9tb00420c.

10 Appendices

10.1 Figures appendix

10.2 Tables appendix

10.3 Planification (Gantt Diagram)

In the pursuit of effective project management, the Gantt diagram emerges as a fundamental tool. It visually represents the tasks and timelines, providing a clear roadmap for the completion of the project. The Gant diagram for the current project was drafted to date June 15, 2023. See Figure 88.

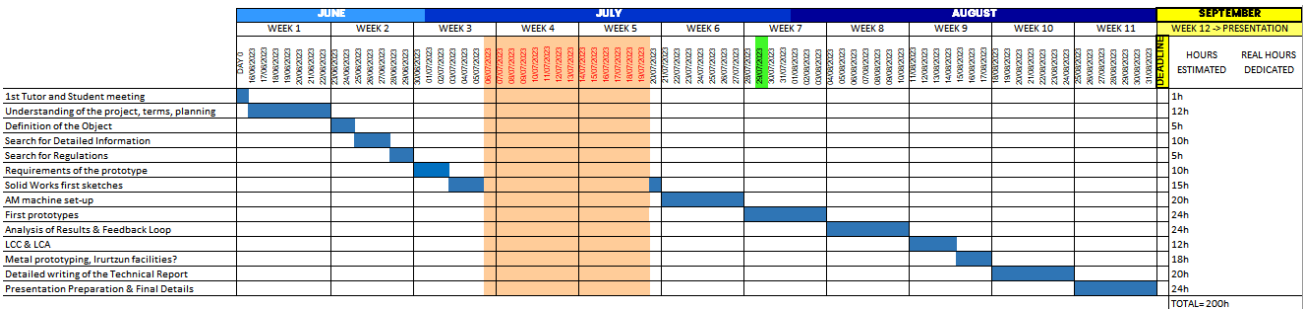

Figure 88. Gantt Diagram first draft

This tool guides the project progression. However, it is of utmost importance to periodically make adjustments and adaptations if there are delays or changes. With that goal it is stated two columns: Hours estimated and Real hours dedicated. In the first draft of this Gantt diagram a number was assigned to each of the tasks to be completed, expecting it would be the duration in hours of the same. Along the development of the project real duration of each task was registered to study the deviation. See Table 5

Table 5. Planification of tasks, hour deviations

TASK	HOURS ESTIMATED	REAL HOURS DEDICATED
1st Tutor and Student meeting	1h	1h
Understanding of the project, terms, planning	12h	10h
Definition of the Object	5h	6h
Search for Detailed Information	10h	12h
Search for Regulations	5h	2h
Requirements of the prototype	10h	10h
Solid Works first sketches	15h	20h
AM machine set-up	20h	4h
First prototypes	24h	30h
Analysis of Results & Feedback Loop	24h	20h
LCC & LCA	12h	x
Metal prototyping, Irurtzun facilities?	18h	x

Detailed writing of the Technical Report	20h	60h
Presentation Preparation & Final Details	24h	20h
	TOTAL= 200h	195h

Overall the research took as long as expected (around 200h), however, in a daily basis considerable adjustments can be seen. Probably the most noticeable one is the writing of the Thesis document itself, which took 3 more times than planned. On the contrary, plenty of time was won on the set up of the 3D printer. This is because initially a personal printer was going to be used, but the facilities of Upna ended being much more convenient.

Starting printing the first specimens was probably one of the most time demanding tasks, since each took around one hour of printing.

The tasks of LCC & LCA remain for further analysis. Due to time constraints it was not possible to assess these two topics on the research.

In the beginning of the project it was proposed to conclude the project with the topologically optimized gear and mold being printed in metal. Due to the summer season and with a tight schedule in many companies, it was not possible. However, they were successfully printed with PLA, ensuring its manufacturability.

Several lessons can be drawn from this time-management tool in order to apply them in further research. Firstly, if 3rd parties may be needed to involucrate in the project, it should be a priority to contact them as soon as possible in order to arrange possible future meetings. Secondly, a small margin should always be left in all tasks for possible setbacks. At the end of the day, as has been seen, the advances of some are offset by the delays of others and the general time is usually similar. Finally, carrying out the experimental part is obviously necessary, but without a report which includes the details of the whole study from the initial idea to the conclusions, the experiment would just vanish, not useful for further investigations nor comparison. Hence, it is of utmost importance to write on a daily basis all the steps taken.

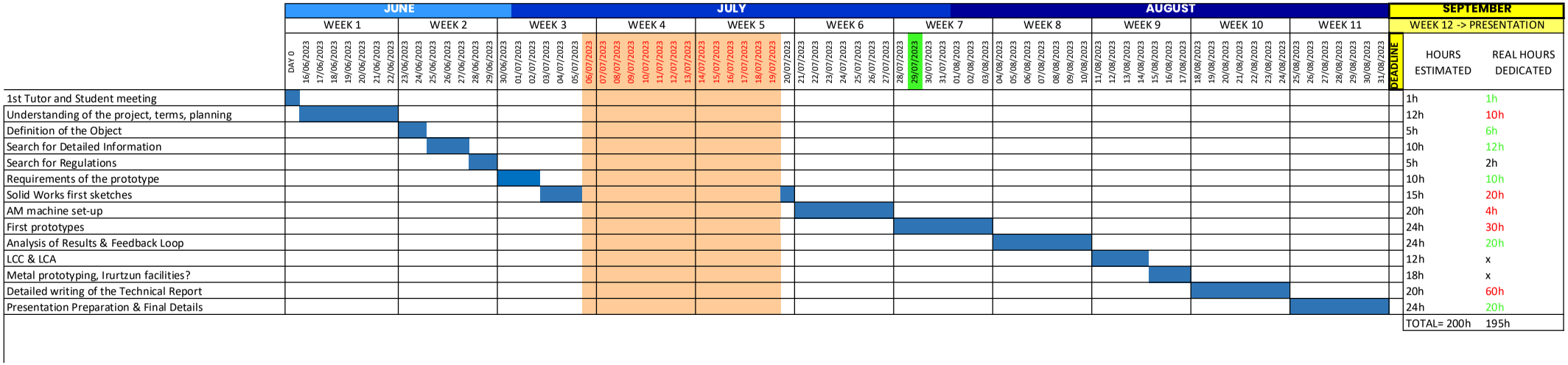

	HOURS ESTIMATED	REAL HOURS DEDICATED
1st Tutor and Student meeting	1h	1h
Understanding of the project, terms, planning	12h	10h
Definition of the Object	5h	6h
Search for Detailed Information	10h	12h
Search for Regulations	5h	2h
Requirements of the prototype	10h	10h
Solid Works first sketches	15h	20h
AM machine set-up	20h	4h
First prototypes	24h	30h
Analysis of Results & Feedback Loop	24h	20h
LCC & LCA	12h	x
Metal prototyping, Irurtzun facilities?	18h	x
Detailed writing of the Technical Report	20h	60h
Presentation Preparation & Final Details	24h	20h
	TOTAL= 200h	195h

Propiedades de masa de ISO 527-2
Configuración: Predeterminado
Sistema de coordenadas: -- predeterminado --

Densidad = 0.00 gramos por milímetro cúbico

Masa = 17.60 gramos

Volumen = 14192.07 milímetros cúbicos

Área de superficie = 6806.55 milímetros cuadrados

Centro de masa: (milímetros)
X = 18.52
Y = 0.51
Z = 3.00

Ejes principales de inercia y momentos principales de inercia: (gramos * milímetros cuadrados)
Medido desde el centro de masa.
Ix = (1.00, 0.00, 0.00) Px = 502.60
Iy = (0.00, 1.00, 0.00) Py = 40604.82
Iz = (0.00, 0.00, 1.00) Pz = 41001.83

Momentos de inercia: (gramos * milímetros cuadrados)
Obtenidos en el centro de masa y alineados con el sistema de coordenadas de resultados. (Usando notación tensorial positiva
Lxx = 502.60 Lxy = -0.03 Lxz = 0.00
Lyx = -0.03 Lyy = 40604.82 Lyz = 0.00
Lzx = 0.00 Lzy = 0.00 Lzz = 41001.83

Momentos de inercia: (gramos * milímetros cuadrados)
Medido desde el sistema de coordenadas de salida. (Usando notación tensorial positiva.)
Ixx = 665.60 Ixy = 166.99 Ixz = 977.67
Iyx = 166.99 Iyy = 46798.14 Iyz = 27.06
Izx = 977.67 Izy = 27.06 Izz = 47041.39

Detalles de malla:
Nombre de estudio: Estudio de topología 1* (-Predeterminado-)
Tipo de malla: Malla sólida
Mallador utilizado: Malla basada en curvatura de combinado
Puntos jacobianos para malla de alta calidad: 16 puntos
Tamaño máx. de elemento: 12,3041 mm
Tamaño mín. de elemento: 7,81212 mm
Calidad de malla: Elementos lineales de bajo orden
Número total de nodos: 13093
Número total de elementos: 63582
Cociente máximo de aspecto : 19,088
Porcentaje de elementos\con cociente de aspecto < 3 : 78,5
Porcentaje de elementos\con cociente de aspecto > 10 : 6,01
Tiempo para completar la malla (hh;mm;ss): 00:00:08
Nombre de computadora: A01308W

Detalles de asignación de tamaño:
1. <Sólido 1(Mn5 z50.stp<1>)> : [7.81212mm : 12.3041mm]

Detalles de malla:
Nombre de estudio: Estudio de topología 1 (-Predeterminado-)
Tipo de malla: Malla sólida
Mallador utilizado: Malla basada en curvatura de combinado
Puntos jacobianos para malla de alta calidad: 16 puntos
Tamaño máx. de elemento: 2,77673 mm
Tamaño mín. de elemento: 1,88253 mm
Calidad de malla: Elementos cuadráticos de alto orden
Número total de nodos: 55968
Número total de elementos: 37791
Cociente máximo de aspecto : 556,21
Porcentaje de elementos\con cociente de aspecto < 3 : 98
Porcentaje de elementos\con cociente de aspecto > 10 : 0,148
Porcentaje de elementos distorsionados: 0
Número de elementos distorsionados:0
Tiempo para completar la malla (hh;mm;ss): 00:00:07
Nombre de computadora: A3021W

Detalles de asignación de tamaño:
1. <Sólido 1(VI23-0104_v2022.STEP<1>)> : [1.88253mm : 2.77673mm]

SECCIÓN B-B

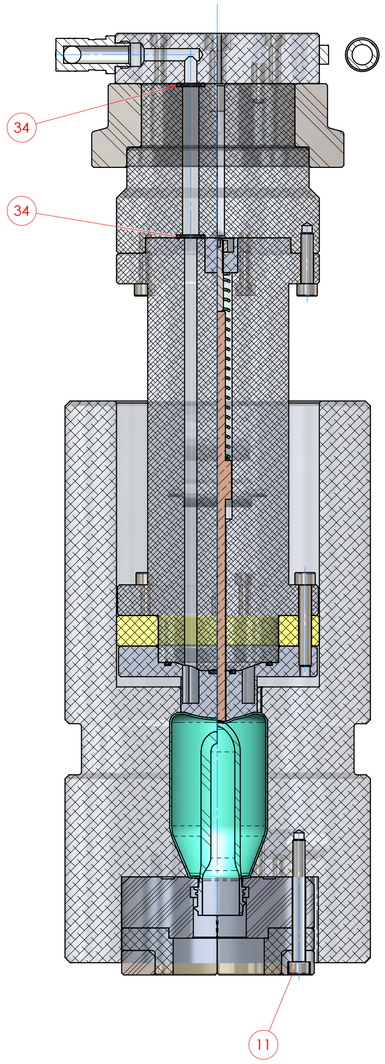

SECCIÓN A-A

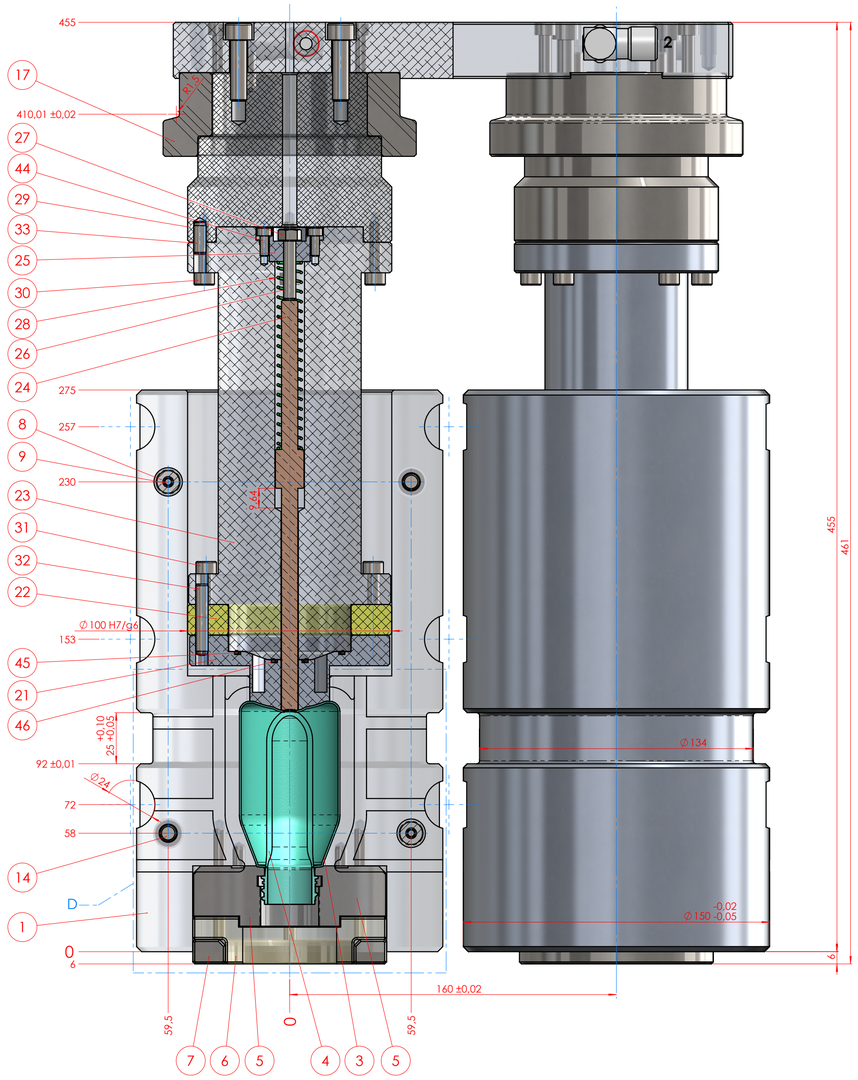

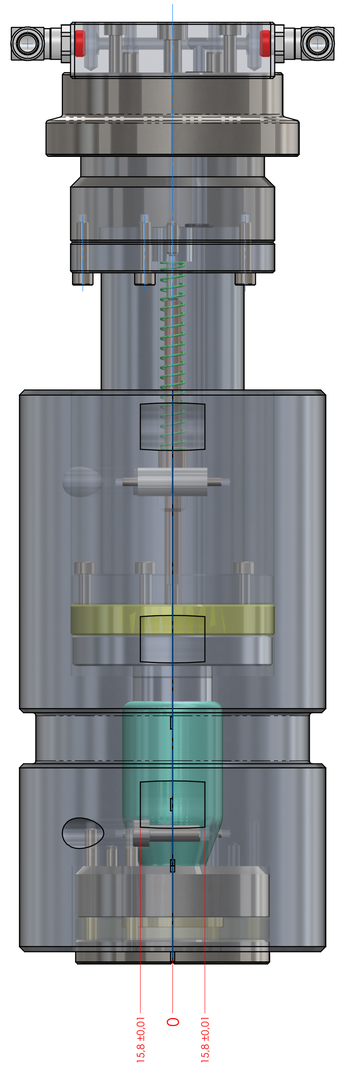

DETALLE D
ESCALA 1.5 : 1

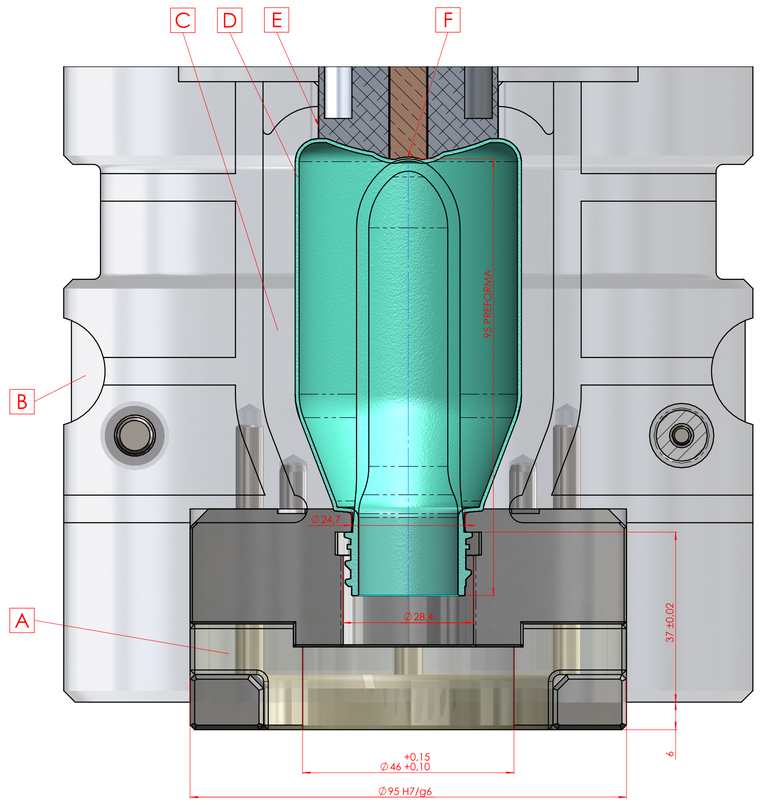

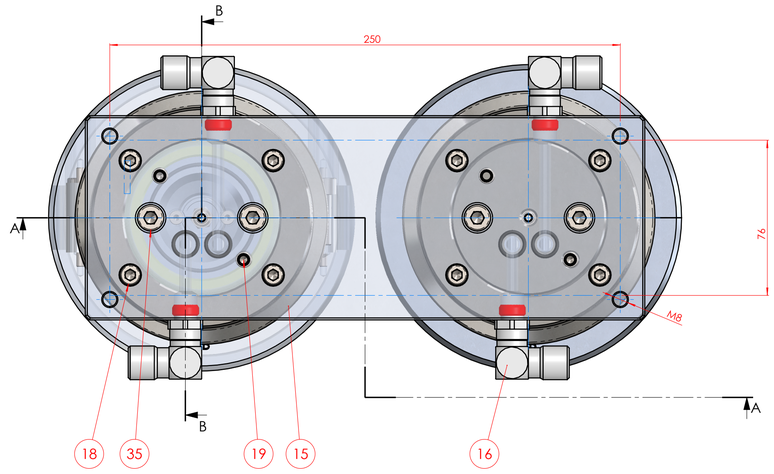

ITEM NO.	PART NUMBER	QTY.
1	Bloc figura cos	2
2	Bloc figura cos	2
3	VI23-0101	2
4	VI23-0101	2
5	VI23-0104	1
6	VI23-0105	4
7	VI23-0106	1
8	E 13102_14	4
9	DIN 912 M4 x 25 --- 25N	4
10	DIN EN ISO 8735-6x26-A-St	4
11	DIN 912 M6 x 60 --- 24N	6
12	E 13101_14	4
13	DIN 912 M4 x 12 --- 12N	4
14	DIN 912 M8 x 25 --- 25N	4
15	VI23-0115	1
16	E 7405_10_1_4	4
17	VI23-0114	1
18	DIN 912 M6 x 30 --- 30N	8
19	DIN EN ISO 8735-8x20-A-St	4
20	VI23-0104	1
21	VI23-0107	1
22	VI23-0108	2
23	VI23-0109	1
24	VI23-0110	2
25	VI23-0111	2
26	DIN 913 - M6 x 35-C	2
27	Hexagon Nut ISO 4033 - M6 - W - C	2
28	VI23-0112	2
29	VI23-0113	1
30	DIN 912 M6 x 25 --- 25N	10
31	DIN 912 M6 x 40 --- 24N	10
32	DIN EN ISO 8735-6x35-A-St	2
33	DIN EN ISO 8735-6x16-A-St	2
34	Tórica 10x2	8
35	DIN 912 M8 x 30 --- 30N	4
36	VI23-0106	1
37	VI23-0106	2
38	VI23-0109	1
39	VI23-0107	1
40	VI23-0113	1
41	VI23-0104	1
42	VI23-0114	1
43	VI23-0104	1
44	DIN 912 M4 x 10 --- 10N	4
45	Tórica 50x2	1
46	Tórica 14x2	1

Modificaciones	Fecha	Nombre	Concepto

Escala	1:1.5	Denominación	Motlle ampolla 100ml		Nº plano
DIN A1		Nombre	Fecha	VICO TRANSFORMADOS EN INYECCIÓN	Tolerancia general ISO2768-mK
Dibujado		F.Povedano	08/03/23		Sustituye a
Comprobado		F. Povedano	08/03/23		Sustituido por
Material				Tratamiento/Acabado	
Volumen			Peso	Gama molde	

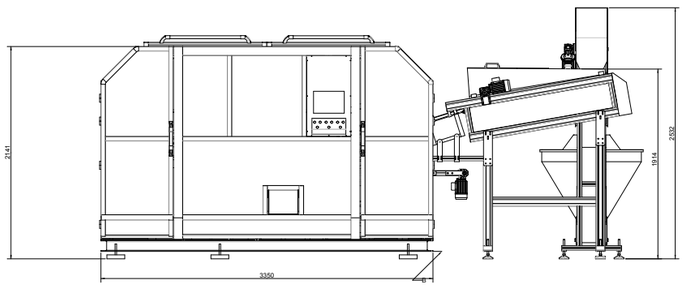

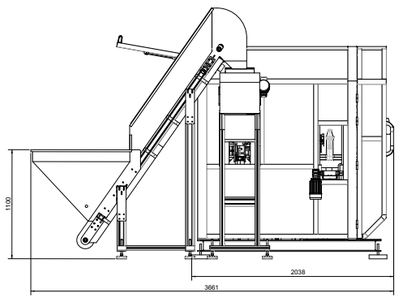

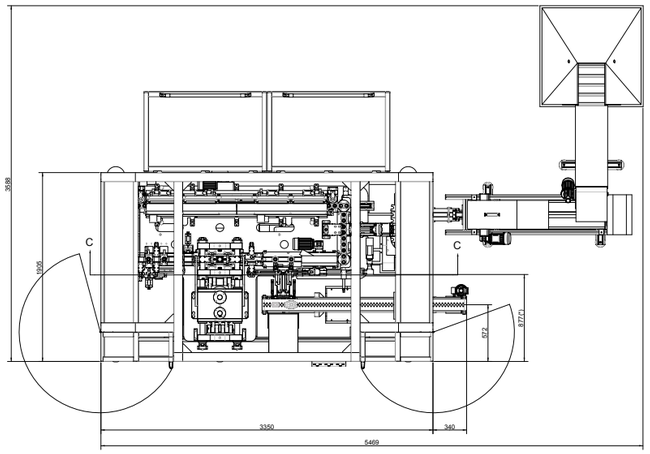

MIPET 2P

PET preform
Stretch **B**low **M**oulders

MECCANOPLASTICA GROUP

MECCANOPLASTICA IBERICA PET DIVISION SL
Calle Alemania n°9, Nave E Pol.Ind.Pla de Llerona
08520 Les Franqueses del Vallés - Barcelona - ESPANA
Tel. (+34) 93 8615482
www.meccanoplastica-group.com

MECCANOPLASTICA srl
Via Albert Einstein, 35/51 - 50013 Campi Bisenzio (Firenze) - ITALY
Tel. (+39) 055 898187
info@meccanoplastica-group.com
www.meccanoplastica-group.com

MECCANOPLASTICA GROUP

THE STRETCH BLOW MOULDING.

PET preform Stretch Blow moulders

Soffiatrice di provette **PET**
Souffleuse de préformes **PET**
Sopladora de preformas **PET**

Scan me

MIPET 2P

Realizzazione: 4ideas - www.forfideas.it

2


3


4


5

6


7

PET preform **S**tretch **B**low **M**oulders


1

1 Fully electric machine
Macchina totalmente elettrica | Machine entierement electrique | Máquina totalmente eléctrica

2 High production performances
Elevate prestazioni produttive | Productivité tres élevé | Alto rendimiento de producción

3 High product quality and process repetiveness
Ottima qualità del prodotto e ripetitività del processo | Qualité du produit très élevé et répétitive du procès | Óptima calidad del producto y repetividad del proceso

4 Low Energy consumption. Optimized heating system
Basso consumo energetico. Ottimizzazione del sistema di riscaldamento | Consommation d'energie contenue. Optimisation du systeme de chauffage
Bajo consumo de energia. Optimización del sistema de calentamiento

5 Especially made for non conventional bottles. Optional preferential heating
Specialmente pensata per contenitori di forma complessa. Possibilità di installare forno differenziale | Ideale pour bouteilles speciales. Possibilité d'installer le four differential | Especialmente pensada para envases de formas complejas. Opcion de instalar horno preferencial

6 Easy and quick mould / preforms change
Facile e rapido cambio del formato | Changement du format tres facile et rapide | Fácil y rápido cambio de molde/preformas

7 Ergonomically made for operators and maintenance
Studiata ergonomia per l'operatore e la manutenzione | Ergonomique pour l'operateur et pour les operations de maintenance | Estudiada ergonomia tanto para el operador como para funciones de mantenimiento

MIPET 2P

MAINS | RETE ELETTRICA | RESEAU ELECTRIQUE | RED ELECTRICA		
Main tension supply (triphase+ground+neutral) | Tensione alimentazione (trifase+terra+neutro) | Tension d'alimentation (triphasé+terre+neutre) | Ténsion de entrada (trifasica+tierra+neutro)		400
Permissible voltage range ± 10% Volt | Caduta tensione ammissibile | Chute de tension admissible | Caidas tensiòn admisible	Volt	±10%
Frequency | Frequenza | Fréquence | Frecuencia	Hertz	50/60
Permissible frequency variation | Variazione frequenza ammissibile | Variation de fréquence admissible | Variaciòn de frecuencia admisible	Hertz	±5%
Installed or Nominal Power | Potenza Totale installata | Puissance Totale installée | Potencia Total instalada	kW	48
Average power consumed | Potenza media consumata | Consommation moyenne en production | Potencia media consumida	kW	18
HIGH PRESSURE AIR | ARIA ALTA PRESSIONE | AIR A HAUTE PRESSION | AIRE ALTA PRESION		
Air pressure | Pressione aria | Pression d'air | Presiòn aire		40
Air flow (*) | Portata aria (*) | Flux d'air demandé (*) | Consumo aire (*)		320 (*)
Air quality requirement | Qualità dell'aria | Qualité de l'air | Calidad del aire	dry, cool, oilfree (food grade) | secca, fredda, senza olio (qualità alimentare) sec, froide, sans huile (qualité alimentaire) | seco, frìo, libre de aceite (calidad alimenticia)	
LOW PRESSURE AIR | ARIA BASSA PRESSIONE | AIR A BASSE PRESSION | AIRE DE BAJA PRESION		
Air pressure | Pressione aria | Pression d'air | Presiòn aire	bar	6 ÷ 10
Air flow (*) | Portata aria (*) | Flux d'air demandé (*) | Consumo aire (*)	m^3 / h	30 (*)
Air quality requirement | Qualità dell'aria | Qualité de l'air | Calidad del aire		dry | secca | sec | seco
COOLING WATER | ACQUA RAFFREDDAMENTO | EAU DE REFROIDISSEMENT | AGUA DE REFRIGERACION		
Water pressure | Pressione acqua | Pression de l'eau | Presiòn agua	bar	3 ÷ 5
Temperature | Temperatura | Température | Temperatura agua	°C	8 ÷ 16
Cooling power (*) | Potenza raffreddamento (*) | Puissance de refroidissement (*) | Potencia de refrigeraciòn (*)	Kcal / h	12.000 (*)
WORK AMBIENCE | AMBIENTE DI LAVORO | ENVIRONNEMENT DE TRAVAIL | INFORMACION GENERAL		
Room work temperature | Temperatura ambiente di lavoro | Température ambiente acceptable | Temperatura ambiente de trabajo	°C	15 ÷ 45
Placement | Posizionamento | Lieu | Emplazamiento	closed area | luogo chiuso | fermé | lugar cerrado	
Relative humidity | Umidità relativa | Humidité relative acceptable | Humededad relativa	%	25 ÷ 70
HEATING OVEN | FORNO DI RISCALDAMENTO | FOUR DE CHAUFFAGE | HORNO		
Nominal power | Potenza totale | Puissance totale | Potencia total instalada	kW	36
Average power consumed (*) | Potenza consumata (*) | Puissance consommée (*) | Potencia consumida real (*)	kW	16 (*)
Number of heating modules | Numero moduli riscaldamento | Numéro de modules de chauffage | Numero de mòdulos calefactores		4
Number of heating zones | Numero zone riscaldamento | Numéro de zones de chauffage | Numero de zonas de calefacciòn		8
Number of lamps per module | Numero lampade per modulo | Numéro de lampes pour chaque module | Numero de lamparas por mòdulo		8
Setting tension range | Regolazione della tensione | Débit variation voltage des lampes | Rango de ajuste de voltaje	Volt	0 ÷ 220
CLAMPING UNIT | GRUPPO DI CHIUSURA | MOULE | GRUPO DE PRENSA		
Number of cavities | Numero di cavità | Numéro de cavités | Nùmero de cavidades	mm	2
Minimum distance between plates (closed) | Distanza minima tra le piastre (stampo chiuso) | Distance minimale entre les plaques (fermées) | Distancia mìnima entre platos (molde cerrado)		210
Maximum distance between plates (open) | Distanza massima tra le piastre (stampo aperto) | Distance maximale entre les plaques (ouvertes) | Distancia màxima entre platos (molde abierto)		350
Opening stroke | Corsa di apertura | Course d'ouverture | Carrera de apertura total	mm	140
TRANSPORT UNIT | SISTEMA DI TRASPORTO | SISTEME DE TRANSPORT | SISTEMA DE TRANSPORTE		
Number of carriers units | Numero unità di trasporto | Numéro de supports-préformes | Nùmero de unidad de transporte		60
Dimensions | Dimensioni | Dimensions | Tamano	mm	60X60
STRETCH ROD UNIT | GRUPPO DI STIRO SOFFIAGGIO | GRUPPE D'ETIRAGE-SOUFFLAGE | GRUPO DE ESTIRO SOPLADO		
Stretch stroke | Corsa di stiro | Course d'étirage | Carrera de estirado	mm	500
Stretch force | Forza di stiro | Force d'étirage | Fuerza de estirado	Kg	280
Air tight force (at 10 bar) | Forza di tenuta (a 10 bar) | Force de tenue (a 10 bar) | Fuerza de estanqueidad (a 10 bar)	Kg	450
Preblow regulation range | Regolazione pressione presoffiaggio | Pression de présoufflage (gamme de régulation) | Rango de ajuste de presiòn de presoplado	bar	0 ÷ 15
BOTTLE DIMENSIONS | DIMENSIONE BOTTIGLIA | DIMENSIONS BOUTEILLE | DIMENSIONES BOTELLA		
Minimum volume | Volume minimo | Volume minimale | Volumen minimo	ml	100
Maximum volume | Volume massimo | Volume maximale | Volumen màximo	ml	2.500
Maximum diameter | Diametro massimo | Diamètre maximale | Diàmetro màximo	mm	120
Maximum height | Altezza massima | Hauteur maximale | Altura maxima	mm	350
Maximum neck diameter | Diametro collo massimo | Diamètre Max. goulot préforme | Diàmetro cuello maximo	mm	40
BLOWER DATA | DATI MACCHINA | DONNEES SOUFFLEUSE | DATOS DE LA MAQUINA		
Mecanical output (blank cycle) | Velocità meccanica (ciclo a vuoto) | Vélocité mécanique (cycle a vide) | Velocidad mecanica (ciclo en vacio)	cycles / h	2.000
Heihgt | Altezza | Hauteur | Altura màquina	mm	2.100
Width | Larghezza | Largeur | Anchura	mm	1.905
Length | Lunghezza | Longueur | Largura longitud	mm	3.350
Weight | Peso | Poids | Peso	Kg	3.500

(*) These data can change according to the final product | Dato dipendente dal tipo di produzione | Cette donée peut changer selon le type de production | Datos dependientes del tipo de produccion